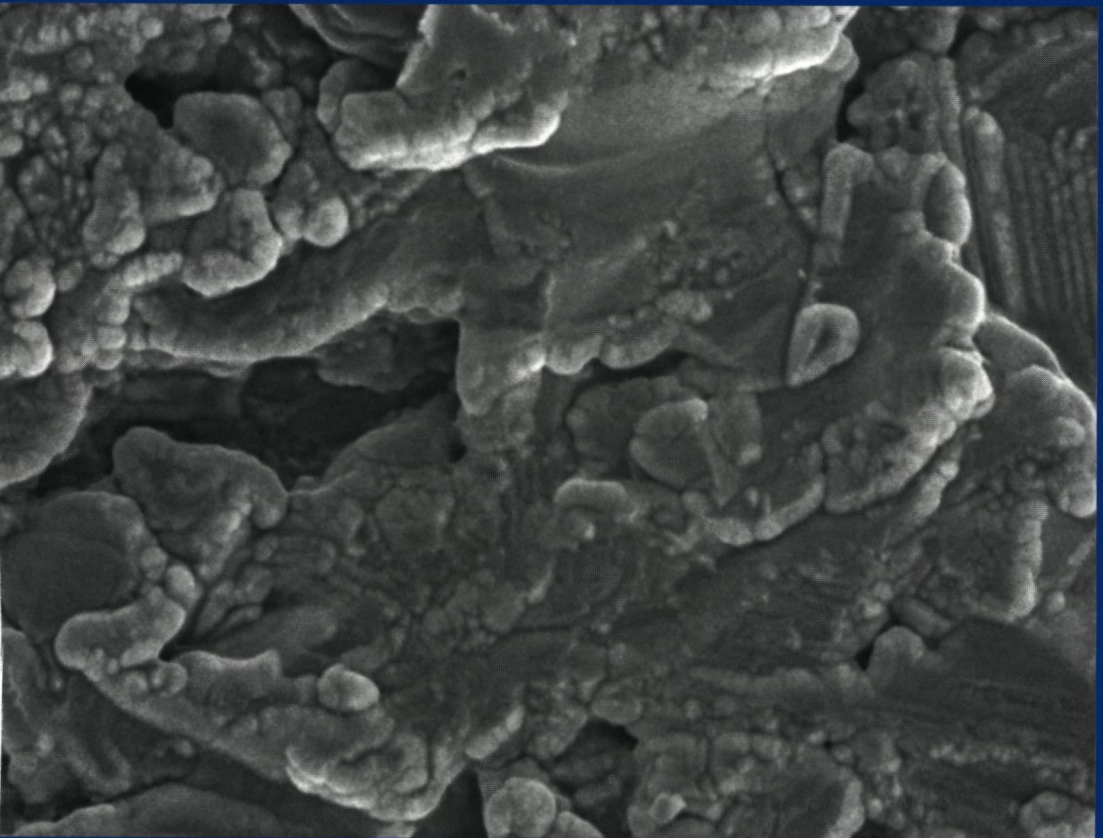


# **RF magnetron sputtered pyrophosphate coatings: Physicochemical and biological characteristics**



**Yan Yonggang**



# **RF magnetron sputtered pyrophosphate coatings:**

Physicochemical and biological characteristics.

**Paranimfen:** J J J P van den Beucken  
W J E M Habraken

RF magnetron sputtered pyrophosphate coatings Physicochemical and biological characteristics / Yan Yonggang  
Thesis Radboud Universiteit Nijmegen – With ref - With Summary in English

Subject headings biomaterials / pyrophosphate / magnetron sputtering / biologic response



# **RF magnetron sputtered pyrophosphate coatings:**

Physicochemical and biological characteristics.

een wetenschappelijke proeve op het gebied van de Medische Wetenschappen

## **Proefschrift**

ter verkrijging van de graad van doctor  
aan de Radboud Universiteit Nijmegen  
op gezag van de Rector Magnificus prof. dr. C. W. P. M. Blom,  
volgens besluit van het College van Decanen  
in het openbaar te verdedigen op dinsdag 24 januari 2006  
des namiddags om 1.30 uur precies  
door

**Yan Yonggang**

geboren op 22 december 1967  
te Shaanxi

**Promotores:**

Prof. dr. JA. Jansen

Prof. dr. L. Yubao (University of Sichuan, Chengdu, China)

**Co-promotor:**

Dr. J.G.C. Wolke

**Manuscript committee:**

Prof. dr. N. Creugers

Prof. dr. K. de Groot

Dr. B. Feddes

The research, which is described in this thesis, was supported financially by the KNAW.



## Contents

### Chapter 1

Bone, Calcium phosphate, Coatings, Heat treatment, Surface characteristic and biocompatibility	9
--	---

### Chapter 2

Preparation and characterization of RF magnetron sputtered Calcium pyrophosphate coatings <i>Yan Yonggang, J G C Wolke, Li Yubao, J A Jansen</i> <i>In press J Biomed Mat Res Part A, 2005</i>	33
--	----

### Chapter 3

The influence of discharge power and heat treatment on calcium phosphate coatings prepared by RF magnetron sputtering <i>Yan Yonggang, J G C Wolke, Li Yubao, J A Jansen</i> <i>Submitted Biomaterials, 2005</i>	51
--	----

### Chapter 4

In vitro evaluation of different heat-treated RF magnetron sputtered calcium phosphate coatings <i>Yan Yonggang, J G C Wolke, Li Yubao, J A Jansen</i> <i>Submitted Clin Oral Impl Res, 2005</i>	67
--	----

### Chapter 5

Growth behaviour of Rat Bone Marrow (RBM) cells on RF magnetron sputtered hydroxyapatite and dicalcium pyrophosphate coatings <i>Yan Yonggang, J G C Wolke, A de Ruijter, Li Yubao, J A Jansen</i> <i>In press J Biomed Mat Res Part A, 2005</i>	87
--	----

### Chapter 6

Subcutaneous evaluation of RF magnetron sputtered calcium pyrophosphate and hydroxylapatite coated Ti implant <i>Yan Yonggang, J G C Wolke, Li Yubao, J A Jansen</i> <i>Submitted Biomaterials, 2005</i>	103
--	-----

### Chapter 7

Thin hydroxyapatite film formation on the surface of polyamide-6 and nano-HA/ polyamide-6 composite by RF magnetron sputtering deposition

*Yan Yonggang, J. G.C. Wolke, Li Yubao, J.A. Jansen*

*Submitted: J Mat. Sc: Mat. Med, 2005*

119

### Chapter 8

Summary and final remarks

133

### Chapter 9

Nederlandse samenvatting

141

Acknowledgement

146

Curriculum Vitae

147



## **Chapter 1**

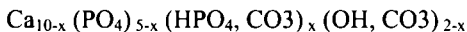
### **General introduction**

## Introduction

Many different kinds of the materials have been used as biomaterial in bone repair, bone disease healing and as replacement of damaged bone. These materials differ in characteristics such as composition, surface energy and surface roughness. On the other hand, they have all one common function, i.e. to provide a temporary or permanent support during the bone regeneration process. Therefore, a successful biomaterial should induce a fast and initially enhanced bone healing response and provide life long stability to the bone defect. Compared with other materials and methods, the use of calcium phosphate based compounds provides a more rapid fixation and stronger bonding with the host bone as well as increased uniform bone ingrowth and/or on-growth.

### 1.1. Bone

Bone is one of the most important biological structures [1]. Its major component is bone mineral, which is a nano-meter-sized, poorly crystalline calcium phosphate, called hydroxyapatite (HA). This HA has a highly hierarchical structure and is found in and along the collagen fibers [2-6]. Hydroxyapatite occurs in the form of complex microcrystals, which have a periodic repetition of the basic structural pattern of the constituent ions known as the unit cell. The unit cell has the formula  $\text{Ca}_{10}(\text{PO}_4)_6(\text{OH})_2$ , which is a right rhombic prism when stacked and forms a hexagonal lattice as well as analogical structures [7-10]. However, the ideal stoichiometric crystalline hydroxyapatite with atomic Ca/P ratio of 1.67 is different from the composition of bone mineral, which may be represented by the following formula:



The Ca/P ratio of bone mineral may vary from 1.50 to 1.90, depending on the age and bone site. The non-stoichiometry is primarily due to the presence of divalent ions, such as  $\text{CO}_3^{2-}$  and  $\text{HPO}_4^{2-}$ , which are substituted for the trivalent  $\text{PO}_4^{3-}$  ions, meanwhile  $\text{Ca}^{2+}$  could be substituted for  $\text{Na}^+$ ,  $\text{K}^+$ , and  $\text{Mg}^{2+}$  [11-15]. Generally, the Ca/P ratio increases during aging of bone, suggesting that the amount of carbonate species increases for older bones. It is supposed that the Ca/P ratio in conjunction with nanocrystalline size and the poorly crystalline nature yields specific solubility property of the bone minerals. The solubility behavior of minerals is important in maintaining a delicate metabolic balance between these cells activities [16-20].

#### 1.1.1. Bone disease, damage and healing

Congenital, hereditary and other acquired diseases, such as achondroplasia, osteogenesis imperfecta (Brittle Bones, Fragilitas Ossium), osteopetrosis (Marble Bone Disease, Osteosclerosis), hereditary multiple exotosis (Osteochondromatosis) and enchondromatosis (Ollier's Disease), can result in bone damage. Also, unexpected events and traffic accidents can lead to bone damage and injury. In view of this, synthetic calcium phosphate materials



have been prepared and studied extensively *in vitro* and *in vivo* to repair bone or to be used as bone substitutes [21-23]. An ideal synthetic materials for bone repair should possess the following characteristics: (1) it should be biologically compatible, like hydroxyapatite or bone-like calcium phosphate based substances; (2) it should allow good fixation or structural integrity to keep the graft in place and intact until the bone healing process is completed; (3) it should be partly soluble to permit resorption during the bone remodeling phase; and, (4) the surface composition and morphology should mimic natural bone and the preparation method should be simple, repeatable and at lower temperature to be beneficial to allow the inclusion of biomolecules, such as bone growth stimulating proteins that can favor the differentiation and proliferation of bone-forming cells.

## 1.2. Calcium phosphate materials

Because their chemical composition and crystal structure are similar to the calcium phosphate as occurs in bone mineral, synthetic calcium phosphate compounds have widely been studied as biomaterials for orthopedic and oral applications [23-25]. There are a number of different calcium phosphates (Table 1).

**Table 1** Calcium phosphate compounds

Compound	Name	Abbreviation	Ca/P ratio
$\text{Ca}(\text{PO}_3)_2 \cdot \text{Ca}_2\text{P}_2\text{O}_6$	Calcium metaphosphate	CMP	0.5
$\text{Ca}(\text{H}_2\text{PO}_4)_2$	Monocalcium phosphate	MCP	0.5
$\text{CaHPO}_3$	Calcium phosphite	CPI	1
$\text{Ca}_2\text{P}_2\text{O}_7$	Calcium pyrophosphate	CPP	1
$\text{CaHPO}_4 \cdot 2\text{H}_2\text{O}$	Hydrated dicalcium phosphate	DCP	1
$\text{CaHPO}_4$	Dicalcium phosphate	ADCP	1
$\text{Ca}_8\text{H}_2(\text{PO}_4)_6 \cdot 5\text{H}_2\text{O}$	Octa calcium phosphate	OCP	1.33
$\text{Ca}_3(\text{PO}_4)_2$	Tricalcium phosphate	TCP	1.5
$\text{Ca}_{10}(\text{PO}_4)_6(\text{OH})_2$	Hydroxy apatite	HA	1.67
$\text{Ca}_{10}(\text{PO}_4)_6\text{F}_2$	Fluoroapatite	FA	1.67
$\text{Ca}_{10}(\text{PO}_4)_6\text{O}$	Oxyapatite	OXA	1.67
$\text{CaO} \cdot \text{Ca}_3(\text{PO}_4)_2$	Tetra calcium phosphate	TTCP	2.0

**1.2.1. Calcium phosphite ( $\text{CaHPO}_3$ , CPI):** In this compound, phosphor is in the oxidation state P (III), which is different from the other calcium phosphate materials as listed in Table 1, where phosphor is in the oxidation state P (V). Phosphite is widely used as inorganic or organic compound, but is only rarely used as biomaterial even although it also can be used to prepare hydroxyapatite [26, 27].

**1.2.2. Calcium metaphosphate ( $\text{Ca}(\text{PO}_3)_2$ , CMP):** This compound is used as component for bioglass and has recently been found biocompatible [28-30].

**1.2.3. Monocalcium phosphate monohydrate (MCPM;  $\text{Ca}(\text{H}_2\text{PO}_4)_2 \cdot \text{H}_2\text{O}$ ):** This is the most acidic CaP compounds, which dissolves easily in water solution at almost all pH values. It can transform into calcium metaphosphate ( $\text{Ca}(\text{PO}_3)_2$ ) after losing water by heating. Although this kind of calcium phosphate is not biocompatible, it can be used as component in CaP based bone cements (CPC) [31-33].

**1.2.4. Dicalcium phosphate:** This includes  $\text{CaHPO}_4$  (DCP) as well as dicalcium phosphate dihydrate  $\text{CaHPO}_4 \cdot 2\text{H}_2\text{O}$  (DCPD) and is one of the biocompatible and biodegradable CaP compounds [34]. DCP results normally from the recrystallization of DCPD and is the most stable CaP compound at low pH. The conversion is faster in water at higher temperature and acidity [35]. This kind of CaP compound is widely used as ingredients of CPCs, such as, Bone Source® and Calcibon®, and Biofill® [36]. The aqueous solution contains a cohesion promoter (e.g. soluble starch, hyaluronic acid) and a setting accelerator (e.g.:  $\text{Na}_2\text{HPO}_4$ ,  $\text{K}_2\text{HPO}_4$ ) [36-38].

**1.2.5. Tetracalcium phosphate (TetCP;  $\text{Ca}_4(\text{PO}_4)_2\text{O}$ ):** It has been reported that this material is biocompatible when used as a bone substitute [39]. Mixing equimolar quantities of DCP and  $\text{CaCO}_3$  and milling them to fine powder, TTCP can be obtained by a solid state-reaction at high temperatures (typically  $1400^\circ\text{C}$ )[40]. When TTCP is mixed with DCP or DCPA in solution, HA is gradually formed. This CaP compound is also widely used in CPC's [41-43].

**1.2.6. Octocalcium phosphate (OCP;  $\text{Ca}_8\text{H}_2(\text{PO}_4)_6 \cdot 5\text{H}_2\text{O}$ ):** This is an intermediate reaction product of the bone mineral because it is a precursor for HAp formation *in vivo* and hence can enhance bone healing [44, 45]. OCP can be prepared by hydrolysis of  $\alpha$ -TCP, [46]. It can be used as coating on a metallic implant surface [45, 47] and as cement component [48].

**1.2.7. Hydroxyapatite: (HA;  $\text{Ca}_5(\text{PO}_4)_3\text{OH}$ ):** HA is the main inorganic bone mineral. It is a very biocompatible and bioactive CaP compound and is considered to be osteoconductive [49-52]. HA is the most stable CaP compound in neutral and basic aqueous solution. Several methods to prepare HAP crystals have been reported, including solid-state reactions, plasma techniques, crystal growth under hydrothermal conditions, layer hydrolysis of other calcium phosphate salts, and sol-gel crystallization. Essentially the synthesis of HAP crystals from supersaturated aqueous solutions is advantageous due to low cost and simplicity. For example, HA can be prepared by using Ca and P containing compounds such as  $\text{Ca}_2\text{Cl}$ ,  $\text{Ca}(\text{NO}_3)_2$ ,

$\text{Ca}_2\text{CO}_3$ ,  $\text{CaO}$ ,  $\text{Ca}(\text{OH})_2$ ,  $\text{CaSO}_4$ ,  $\text{H}_3\text{PO}_4$ ,  $\text{NH}_4\text{H}_2\text{PO}_4$ ,  $\text{NaH}_2\text{PO}_4$ ,  $\text{KH}_2\text{PO}_4$ ,  $\text{Na}_2\text{HPO}_4$ , etc [53-58] Usually synthetic HA contains anions ( $\text{HCO}_3^-$ ,  $\text{HPO}_4^{2-}$ ), and cations ( $\text{Na}^+$ ,  $\text{K}^+$ ), which make the apatite deviate from the stoichiometry of HAP [59, 60] There are mainly three kinds of HAs, including amorphous HA, precipitated HA and the high temperature form of a stoichiometric HA HA is widely used as coating, bone filler and bone cement [61-65]

**1.2.8. TCP: Tricalcium phosphate:** TCP has depending on the temperature, three polymorphs, including  $\alpha$ -TCP ( $\alpha\text{-Ca}_3(\text{PO}_4)_2$ ),  $\beta$ -TCP ( $\beta\text{-Ca}_3(\text{PO}_4)_2$ ) and  $\alpha$ -TCP ( $\alpha\text{-Ca}_3(\text{PO}_4)_2$ ) A-TCP exists only at a very high temperature (above 1450°C)

A-TCP,  $\beta$ -TCP and  $\alpha$ -TCP have exactly the same chemical composition but differ in crystallographic structure TCP can be easily prepared by chemical reaction between calcium salt and soluble phosphate salts [66, 67, 68] A-TCP and  $\beta$ -TCP can be obtained by sintering Usually  $\beta$ -TCP is obtained by thermal heating above 650°C, but  $\alpha$ -TCP needs a much higher temperature, i.e. 1125°C [67, 69] It is also possible to prepare TCP by solid reaction, such as by mixture of MCP and  $\text{CaCO}_3$  and subsequent calcination [70]  $\beta$ -TCP has extensively been used as a bone substitute, which is degradable by osteoclastic activity [71] A-TCP is widely used as the main component of CPC [72]

**1.2.9. Biphasic calcium phosphate (BCP)** Composites with different ratios of HA/ $\beta$ -TCP have been developed in order to control the resorbability of the material and at the same time to maintain its osteoconductive properties [73] This kind of CaP composites shows good biocompatibility and osteoconductivity [74] It is obtained either by chemical reaction in solution or by calcining PHA (precipitated Hydroxylapatite) (with a molar ratio Ca/P between 1.5-1.67) above  $\approx 700^\circ\text{C}$  [75] BCP is more degradable than HA and the degradation rate increases with an increase of the  $\beta$ -TCP content It is extensively used as scaffold material in tissue engineering and as component of CPC [76, 77]

**1.2.10. Oxyapatite (OXA;  $\text{Ca}_{10}(\text{PO}_4)_6\text{O}$ )** This is a highly reactive material, which undergoes at temperatures lower than 800°C, even under vacuum, a small rehydration to give rise to an oxy-hydroxy apatite, which is stable in air at ordinary temperatures It exists only under a vacuum ( $10^{-4}$  to  $10^{-6}$  torr) or in sufficiently water-free gases ( $\text{He}$ ,  $\text{N}_2$ ), in the temperature range 850–1050°C [78] It can be prepared by the partial decomposition of HA OXA is poorly understood due to the difficulties of detecting this phase [79]

**1.2.11. Fluoroapatite (FA,  $\text{Ca}_{10}(\text{PO}_4)_6\text{F}_2$ )** This is “HA”, where F substitutes the OH Pure fluoroapatite (FA) is probably not suited as bone replacement material because it is too stable and seems not to give osteoconduction [81] When combined to composites with hydroxyapatite (HA), it can improve the stability of the HA composite [82] It can be

prepared through solid solution by a sol-gel method but also other methods can be applied [83, 84]

**1.2.12. Calcium pyrophosphate (DCPP,  $\text{Ca}_2\text{P}_2\text{O}_7$ )** Dicalcium pyrophosphate (DCPP), with a formula of  $\text{Ca}_2\text{P}_2\text{O}_7$ , is one of the intermediate products of biological mineralization, while HA is usually considered as the end products of this process [85] Extracellular inorganic pyrophosphate is important for the regulation of the mineralization of bone, and in the pathogenesis of chondrocalcinosis, an arthritic disease in which calcium pyrophosphate dihydrate crystals form in articular cartilage [86] Although many studies suggest that crystalline dicalcium pyrophosphate is biocompatible, it is very complex to understand the role of this CaP materials in the bone formation process, because it is not only involved in bone formation but it is also present at the bone disease site [87-90] Therefore, more research to DCPP has to be done, including the amorphous properties of DCPP *in vitro* and *in vivo*, and the process during which the amorphous DCPP changes into crystalline or other structures Usually DCPP can be obtained by calcining DCP ( $\text{CaHPO}_4$ ) at  $1000^\circ\text{C}$  for 3 h by reaction in solution [91, 92] Recently, DCPP has been developed as bioceramic for biomedical applications [93-95]

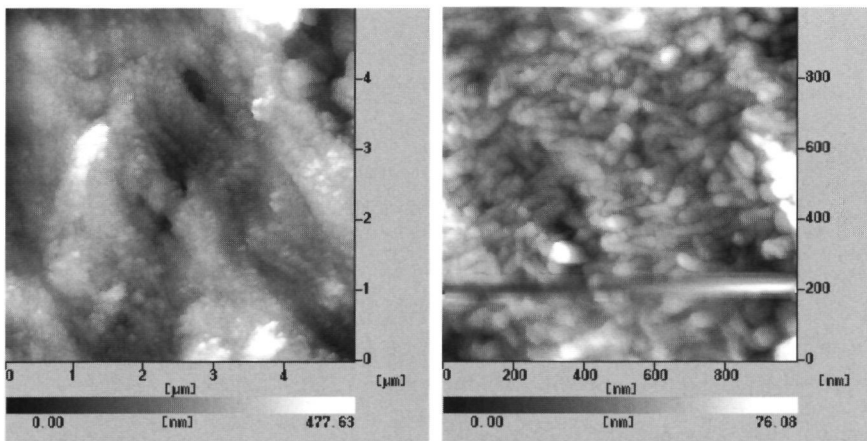
Generally, the term CaP materials is used to describe a number of different materials that vary in composition, crystallinity and method of manufacturing as discussed above Their properties are determined not only by their chemical composition, crystal structure but also by the process with which they are produced For instance, the Ca/P ratio of both CMP ( $\text{Ca}(\text{PO}_3)_2$ ) and MCP ( $\text{Ca}(\text{H}_2\text{PO}_4)_2 \cdot \text{H}_2\text{O}$ ) is 1.5, but the former is biocompatible and the later not It is very important to provide detailed information whenever the term CaP is used

### 1.3. Calcium phosphate coatings and techniques

There are a lot of calcium phosphate compounds that can be used for the manufacturing of dental and orthopedic implants Unfortunately, calcium phosphate ceramics are brittle and fragile, which hampers their use as load-bearing implants To avoid this disadvantage, calcium phosphate ceramics are applied as coating on mechanical strong metallic substrates in order to obtain implants which possess the bioactivity and biocompatibility of calcium phosphates as well as the strength of metals [96-98]

There are various deposition techniques available to prepare calcium phosphate coatings Among them plasma-spray deposition is the most popular and applicable method, because of its many advantages, such as the potential of plasma-sprayed coatings to enhance the long-term stability of the bond between metallic implants and the surrounding bone structure, to promote superior bone apposition, and to reduce healing time [99-103] However, the bond between a plasma-sprayed HA coating and underlying metallic substrate is mainly due to a mechanical interlocking mechanism [104,105] Defects as cracking, flaking and scratching

that are often found in plasma-sprayed HA coatings might eventually lead to delamination of the coating. The delamination of the coating not only enhances the release of metal ions, but it can also lead to loosening of the implant [106-109]. Another disadvantage of plasma spray deposition is that the chemical composition and crystal structure of the deposited coatings is different compared with the original HA. For example, plasma spray deposited HA coatings contain impurities, such as  $\beta$ -tricalcium, tetracalcium phosphates, and calcium oxide, which can result in a biological adverse reaction [110, 111]. To enhance the bond strength and some other properties, a number of other coating techniques have been developed to apply calcium phosphate coatings (See Table 21) [112]. Among these coating techniques is radio frequency (RF) magnetron sputtering the most promising to obtain dense, thin CaP films that are strongly coherent to metal. Furthermore, the substrate temperature of the RF magnetron sputtering system can be controlled so that even polymer substrates are not destroyed or degraded during the sputtering process [113]. Another advantage of this technique is that two or more different targets can be used at the same time during the sputtering process. In this way the coating composition can be further controlled. Generally, the properties of calcium phosphate coatings are determined not only by the starting materials, but also by the production method. For instance, magnetron sputtering generates a homogeneous CaP layer consisted of nano-meter grade particles (Figure 1), whereas a layer produced by plasma spraying consists of mixed amorphous and crystalline phases depending on the parameters used. Most CaP coatings, irrespective of the used coating technique, need post heat-treatment to improve the crystal structure and to get a more preferable morphological surface from the biocompatibility and bioactivity point of view. Such a post heat-treatment procedure is one of the most important factors affecting the final CaP coating properties.



as-sputtered HA coating

heat-treated HA coating

**Figure 1:** AFM macrographs of the RF magnetron sputtering HA coatings

**Table 2** Techniques applied to deposit CaP coatings

Technique	Thickness	Advantages	Disadvantages
Plasma spray deposition	~5 mm	High speed, stronger fixation to substrate,	Impurity, mechanical bonding to substrate, uneven coating surface
RF magnetron sputtering [114-117]	0.5-3 $\mu$ m	Uniform coating thickness on flat substrates; dense coating	Line of sight technique; expensive time consuming; produces amorphous coatings
Thermal spraying [118,119]	30–200 $\mu$ m	High deposition rates; low cost	Line of sight technique; high temperatures induce decomposition; rapid cooling produces amorphous coatings
Pulsed laser deposition [120,121]	0.05-5 $\mu$ m	Coating with crystalline and amorphous; coating with dense and porous	Line of sight technique
Dynamic mixing method [122-124]	0.05-1.3 $\mu$ m	High adhesive strength	Line of sight technique, expensive; produces amorphous coatings
Dip coating [125,126]	0.05-0.5 mm	Inexpensive; coatings applied quickly; can coat complex substrates	Requires high sintering temperatures; thermal expansion mismatch
Sol-gel [127, 128]	<1 $\mu$ m	Can coat complex shapes; Low processing temperatures; relatively cheap as coatings are very thin	Some processes require controlled atmosphere processing; expensive raw materials
Electrophoretic deposition [129,130]	0.1-2mm	Uniform coating thickness, rapid deposition rates; can coat complex substrates	Difficult to produce crack-free coatings; requires high sintering temperatures
Biomimetic coating [131-132]	<30 $\mu$ m	Low processing temperatures; can form bonelike apatite; can coat complex shapes, can incorporate growth factors	Time consuming; Requires replenishment and a constant of pH of simulated body fluid
Hot isostatic pressing [133,134]	0.2-2.0mm	Produces dense coatings	Cannot coat complex substrates; high temperature required; thermal expansion mismatch; elastic property differences; expensive; removal/interaction of encapsulation material
ESD [135,136]	0.1-200 $\mu$ m	Inexpensive; coatings applied quickly; can control coating composition and morphology	Partial amorphous coating, replenishment and a constant of pH of solution

### 1.4. Heat treatment and coating properties

Just deposited CaP coatings are almost always amorphous or contain amorphous phases. Therefore, they need a post annealing treatment to obtain crystallinity. However, we have to notice that the temperature to induce crystallization differs for coatings deposited by different techniques. At present the main post deposition heat-treatment methods, include 1 heating in air for long time [137, 138], 2 heating in inert gas for a long time, which is rarely reported [139], 3 heating with infrared for a short time [140], 4 heating in water steam at a lower temperature [141, 142], 5, heating with excimer laser equipment [143, 144].

Although the required temperatures of the post deposition heat treatment are different for CaP coatings obtained by different techniques, the temperature is considered the key factor to affect the coating phase composition and crystallinity [145, 146]. Besides, water vapor is also an important factor in the heat treatment procedure (See Table 3) [112]. Crystallization of amorphous Ca-P coatings occurs only above a certain temperature. However, heat treatment at a high temperature (e.g. above 600°C) reduces the adhesive strength of a coating to the substrate and can even result in the buckling of the coating at the surface. Further, with increase of the heat treatment temperature, the purity of the HA phase in the coating decreases [138, 147]. Therefore, a decrease in heat treatment temperature might benefit the physicochemical and mechanical properties of HA coatings as well as their *in vivo* biological behavior [148]. As the calcium phosphate compounds are sensitive to heating and may transform into another structural form during the annealing (chemical composition and crystal structure changes), variations in CaP composition can lead to different dissolution/precipitation behavior, which may have an effect on the bone response [149]. Consequently, post deposition heat-treatment is a very complex process. In order to obtain the most preferable crystallinity, phase composition and surface morphology, different heat treatment methods should be applied on similar deposited coatings.

**Table 3** Crystallinity of sputtered CaP coating after different heat treatments

Heat treatment Temperature (°C)	Crystallinity (%)	
	Without water vapor	With water vapor
As-sputtered coatings	0	0
350	0	2.5±0.5
400	1.9±0.4	2.8±0.6
450	2.0±1.0	68.0±2.0
500	62.0±2.0	65.0±1.0
600	67.0±2.0	68.0±2.0

## 1.5. Bioactivity and biocompatibility

Bioactivity refers to the material reaction in the biological environment, including release, resorption, and exchange of ions between the materials surface and the surrounding biological fluid. Biocompatibility refers to the biochemical, biomechanical and bio-physiological aspects of the tissue response, i.e. the lack of an adverse tissue response. In view of this point, calcium phosphates show a preferable tissue response in the biological environment [150,151].

### 1.5.1. Dissolution and re-precipitation

The CaP coating surface is especially crucial for the fixation mechanism of an implant in bone, because it is in direct contact with the bone and body fluid after implantation [152, 153]. Consequently, partial dissolution of CaP coatings is essential to trigger bone growth, but exceedingly rapid dissolution leads to poor bone bonding and coating disintegration [154-156]. Therefore, it is important to optimally control the coating characteristics by varying the processing conditions. For example, the characteristics and properties of an HA coating can be changed resulting in different degrees of dissolution, which will affect the clinical performance.

Dissolution and re-precipitation happens immediately when the implant comes in contact with the biological surroundings. It is generally supposed that an amorphous coating shows higher dissolution than a crystalline coating. Therefore, crystallinity is the dominant factor for the dissolution of the HA coating [157, 158]. Other factors that affect the coating solubility include Ca/P ratio, phase composition, microstructure, porosity, surface morphology and roughness, thickness, and coating texture. Most of these variables are the result of the used processing parameters. A coating with a Ca/P ratio  $> 1.67$  shows a low solubility in liquids with a pH between 6.8-7.4 and a precipitate is formed fast on the coating surface. This in contrast to coatings with a Ca/P ratio  $< 1.67$ , which dissolve fast in a solution with a pH ranging from 6.8 to 7.4 [159]. Generally, the order of relative solubility of CaP compounds is as follows:

ACP $>>$ DCP  $>$  TTCP  $>$   $\alpha$ -TCP  $>$   $\beta$ -TCP $>>$ HA;

Where ACP is amorphous calcium phosphate, DCP is monetite ( $\text{CaHPO}_4$ ), TTCP is tetracalcium phosphate ( $\text{Ca}_4\text{P}_2\text{O}_9$ ), TCP is tricalcium phosphate ( $\text{Ca}_3(\text{PO}_4)_2$ ), and HA is hydroxyapatite ( $\text{Ca}_{10}(\text{PO}_4)_6(\text{OH})_2$ ) [160, 161]. This dissolution order is in a neutral pH solution and the order will change according the change of pH. Further, it has been reported that the dissolution increases with an increase in porosity, an increase in surface area, a decrease in particle size, and a decrease in crystallinity [162-164]. As heat-treatment is a factor that influences the crystallinity of a CaP coating, this will eventually affect the dissolution behavior of the coating [149]. Protein and amino acids in the solution also have influence on the dissolution of CaP coating, because they interfere with the mineralization



process [165, 166] For example, it has been suggested that some organic macromolecules such as amino acids and proteins have a high affinity for CaP surfaces They bind to the Ca and P in the apatite crystal, which results in inhibition of the growth and formation of CaP [167-169] Finally, the ability of the osteoblast-like cells to attach, migrate, proliferate, and differentiate and eventually form bone depends on the various characteristics of the CaP coating surface

### 1.5.2. Bone response

A successful fixation of an implant in bone should occur fast, has to be initially strong and has to provide lifelong stability In view of this, both orthopedic and dental implants have been provided with CaP coatings After implantation, the Ca and P as present in the coating surface dissolve, resulting in an increased concentration of these ions in the microenvironment close to the implant This is followed by re-precipitation of Ca and P and the formation of a bone-like mineral layer [170, 171] This bone-like mineral layer is supposed to promote the adhesion of extracellular matrix, providing a preferred substrate for cell attachment and differentiated function of resident osteoblasts or committed osteoblast precursors [172] This promotion of the differentiation and expression of osteogenic cells results in a faster bone formation on CaP surfaces than on Ti substrates [173] Due to the involvement of dissolution and precipitation phenomena, the crystallinity of a CaP coating plays a major role in the cascade of biological events [173, 174-176]

Usually *in vivo* evaluation provides the basic information and is the standard in developing and designing new implant materials [177] Different animal models have been used in evaluating the implant materials, including rat, rabbit, dog, sheep, goat and pig [178-183] Transmission electron microscopy (TEM) showed that the bone-bonding behavior of calcium phosphate ceramics at the bone-implant interface was not determined by the calcium/phosphate molar ratio [184] Amorphous substances or needle-like microcrystals were observed on the surface of all ceramics already 2 weeks after implantation However, chemical or mechanical bonding between bone and ceramics was not observed On the other hand, Porter et al [185] revealed that the process of mineralization of bone is associated with the crystallinity of plasma-sprayed HA coatings Ultrastructural examination showed the formation of biological apatite crystallites only on non-heat-treated coatings within 3 hours of implantation in dog bone Further, it has been reported that the ultimate interfacial strength values of RF sputtered HA coatings are statistically greater than the mean ultimate interfacial strength for non-coated Ti implants after 3 weeks of implantation After 12 weeks of installation, these statistical differences in the mean ultimate interfacial strengths between CaP-coated and non-coated Ti implants disappeared Nevertheless, histomorphometric evaluation indicated still a greater percent bone contact length for the CaP-coated implants, In addition, the as-deposited amorphous coating showed the highest contact percentage [186]

Evidently, the coating crystallinity affects the dissolution and precipitation of the deposited films, and eventually influences the bone formation [187-189] The dissolution of the CaP coating is supposed to evoke solution mediated events, which affect circulating biocomponents, such as proteins [190], bone cells, organic matrix components, and precipitated as well as resorbed minerals [191] In addition, it has been suggested that once early bone bonding is achieved, the biodegradation of thin CaP coatings is not detrimental to bone-coating-implant fixation, and does not compromise the long term bone response to the implant surface [192] In view of this, we have to emphasize that thin film technologies offer clearly a viable alternative to plasma spraying for the deposition of CaP coatings on implants In summary, we can conclude that the biological response to CaP coatings is determined not only by the coating characteristics but also by the biological surroundings in which the coated device is placed This is a complex process, which has not been completely well understood yet

### **1.6. Objective of the research**

Considering the tight relation between CaP material and bone response, we decided to use RF magnetron sputtering to deposit and modify CaP coatings The overall objective of our studies was to deposit CaP coatings, which varied significantly in composition and structural arrangement and to evaluate their physicochemical and biological properties Therefore, we hypothesized that CaP coatings with a Ca/P ratio of 1.0, like pyrophosphate, are the driving parameter in the formation of a bioactive carbonate apatite surface Considering the aim of the study the following experimental issues were addressed

- 1 The deposition of RF magnetron sputtered coatings with different Ca/P ratio's with targets composed of calcium pyrophosphate and hydroxyapatite and the characterization of their physicochemical and dissolution behavior,
- 2 The deposition of thin CaP coatings with preferential composition and morphological structure as induced by heat treatment at lower temperature by hot steam (under 140 °C to 80°C) or at higher temperature (500-700°C) by infrared treatment ,
- 3 The deposition of thin CaP coatings by RF magnetron sputtering on polymers and the effect of a heat treatment procedure on the final coating crystallinity,
- 4 The performance of in vitro cell culture and in vivo experimental animal studies in order to determine the coating behavior under biological conditions

## References

- 1] Stupp SI, Braun PV. Science. 1997;277:1242.
- 2] Weiner S, Wagner HD. Annu Rev Mater Sci. 1998;28:271-98.
- 3] Peters F, Schwarz K, Epple M. The structure of bone studied with synchrotron x-ray diffraction, x-ray absorption spectroscopy and thermal analysis. Thermoch Acta. 2000;361:131-38.
- 4] Pidakart RMV, Chandran A, Takano Y, Turner CH. Bone mineral lies mainly outside collagen fibrils: predictions of a composite model for osteonal bone. J Biomech. 1996;29:909-16
- 5] Ziv V, Wagner HD, Weiner S. Microstructure-microhardness relations in parallel-fibered and lamellar bone. Bone. 1996;18:417-28.
- 6] Weiner S, Wagner HD. The material bone: structure-mechanical function relations. Ann Rev of Mat Sci. 1998;28:271-98.
- 7] Furseth R. Further observations on the fine structure of orally exposed and carious human dental cementum. Arch of Oral Biol. 1971;16:71-80
- 8] McLean JD, Nelson DGA. High-resolution n-beam lattice images of hydroxyapatite. Micron 1969;13:409-13
- 9] McConnell D. Crystal chemistry of hydroxyapatite. Its relation to bone mineral. Arch of Oral Biol. 1965;10:421-31.
- 10] Selvig AK. The crystal structure of hydroxyapatite in dental enamel as seen with the electron microscope. J of Ultrastr Res. 1972;41:369-75.
- 11] Tadic D, Epple M. A thorough physicochemical characterization of 14 calcium phosphate-based bone substitution materials in comparison to natural bone. Biomaterials. 2004;25:987-94.
- 12] Berry EE. The structure and composition of some calcium-deficient apatites. J of Inorg and Nucl Chem. 1967;29:317-27
- 13] Bertoni E, Bigi A, Cojazzi G, Gandol M, Panzavolta S, Roveri N. Nanocrystals of magnesium and fluoride substituted hydroxyapatite. J of Inorg Biochem. 1998;72:29-35
- 14] Bohic S, Heymann D, Pouczat JA, Gauthier O, Daculsi G. Transmission FT-IR microspectroscopy of mineral phases in calcified tissues. Comptes Rendus de l'Acad des Scis - III - Scis de la Vie. 1998;321:865-76.
- 15] el Fekri H, Savariault JM, Ben Salah A. Structure refinements by the Rietveld method of partially substituted hydroxyapatite:  $\text{Ca}_9\text{Na}_{0.5}(\text{PO}_4)_{4.5}(\text{CO}_3)_{1.5}(\text{OH})_2$ . J of All and Comp. 1999;287:114-20
- 16] Neuman WF, Neuman MW. Emerging concepts of the structure and metabolic functions of bone. Am J of Med. 1957;22:123-31.
- 17] Jackson CD. Living without oxygen: lessons from the freshwater turtle. Comp Biochem and Phys Molec and Integr Phys. 2000;125:299-315.
- 18] Craan AG. In vitro bone metabolism in hypophosphatemic mice:  $^{32}\text{P}$  and  $^{45}\text{Ca}$  release from cultured calvaria. Int J of Nucl Med and Biol. 1984;11:27-31
- 19] Posner AS, Betts F, Blumenthal NC. Properties of nucleating systems. Metab Bone Dis and Rel Res.

- 1978;1:179-83.
- 20] Eanes ED Crystal growth of mineral phases in skeletal tissues. Progr in Crystal Growth and Char. 1980;3:3-15.
- 21] Lowenstam HA, Weiner S. On Biomineralization, Oxford University Press, Oxford, 1989.
- 22] LeGeros RZ, LeGeros JP. in: J O. Nriagu, P.B Moore (eds.), Phosphate minerals, Springer, Berlin, 1984, p. 351
- 23] de Groot K. Bioceramics consisting of calcium phosphate salts. Biomaterials. 1980;1:47.
- 24] Hulbert SF, Bokros JC, Hench LL, Wilson J, Heimke G High tech ceramics. ceramics in clinical applications, past, present and future. P.Vincenzini (eds.) Milan. 1986, p 189-213.
- 25] Villarreal DR, Sogal A, Ong JL. Protein adsorption and osteoblast responses to different CaP surfaces. J Oral Implantol 1998;24:67-73
- 26] Beganskiene A, Dudko O, Sirutkaitis R, Giraitis R. Water based sol-gel synthesis of hydroxyapatite. Mater Sci. 2003, 9:383-86.
- 27] Gan L, Pilliar R Calcium phosphate sol-gel-derived thin films on porous-surfaced implants for enhanced osteoconductivity. I: Synthesis and characterization. Biomaterials. 2004; 25:5303-12.
- 28] Haake P, Allen GW. Biological reactions at phosphorus. VII: The nature of metaphosphate ion,  $\text{PO}_3$  as a reaction intermediate (I). Bioorg Chem. 1980;9:325-41
- 29] Antonucci JM, Fowler BO, Venz S. Filler systems based on calcium metaphosphates Dent Mat. 1991;7:124-29.
- 30] Park EK, Lee YE, Choi JY, Oh SH, Shin HI, Kim KH, Kim SY, Kim S Cellular biocompatibility and stimulatory effects of calcium metaphosphate on osteoblastic differentiation of human bone marrow-derived stromal cells Biomaterials 2004;25:3403-11
- 31] Bermúdez O, Boltong MG, Driessens FCM, Ginebra MP, Fernández E, Planell JA Chloride- and alkali-containing calcium phosphates as basic materials to prepare calcium phosphate cements, Biomaterials. 1994;12 1019-23
- 32] Wang X, Ma J, Wang Y, He B. Bone repair in radius and tibiae of rabbits with phosphorylated chitosan reinforced calcium phosphate cements Biomaterials 2002;23 4167-76.
- 33] Wang X, Ma J, Feng Q, Cui F Skeletal repair in rabbits with calcium phosphate cements incorporated phosphorylated chitin. Biomaterials. 2002;23.4591-4600.
- 34] Getter L, Bhaskar SN, Cutright DE. Three biodegradable calcium phosphate slurry implants in bone. J. Oral Surg. 1972;30:263-68.
- 35] Bohner M. Calcium orthophosphates in medicine from ceramics to calcium phosphate cements. Injury. 2000;31:S37-47.
- 36] Mirtchî AA, Lemaître J, Munting E. Calcium phosphate cements: study of the  $\beta$ -tricalcium phosphate-dicalcium phosphate-calcite cements. Biomaterials. 1990;11:83-88.
- 37] Kurashina K, Kurita H, Kotani A, Takeuchi H, Hirano M In vivo study of a calcium phosphate cement consisting of  $\alpha$ -tricalcium phosphate/dicalcium phosphate dibasic tetracalcium phosphate monoxide. Biomaterials 1997;18:147-51

- 38] Otsuka M, Nakahigashi Y, Matsuda Y, Fox JL, Higuchi WI, Sugiyama Y. Effect of geometrical cement size on in vitro and in vivo indomethacin release from self-setting apatite cement. *J of Contr Rel.* 1998;52:281-89.
- 39] Yoshimine Y, Akamine A, Mukai M, Maeda K, Matsukura M, Kimura Y, Makishima T. Biocompatibility of tetracalcium phosphate cement when used as a bone substitute. *Biomaterials* 1993;14:403-06.
- 40] Ciesla K, Rudnicki R. Synthesis and transformation of tetracalcium phosphate in solid phase. I. Synthesis of roentgenographically pure tetracalcium phosphate from calcium dibasic phosphate and calcite. *Polish J Chem* 1987;61:719-27.
- 41] Doi Y, Iwanaga H, Shibutani T, Moriwaki Y, Iwayama Y. Osteoclastic responses to various calcium phosphates in cell cultures. *J of Biom Mat Res.* 1999;47:424-33.
- 42] Burguera EF, Guitián F, Chow, LC A water setting tetracalcium phosphate-dicalcium phosphate dihydrate cement. *J of Biom Mat Res* 2004;71A:275-82.
- 43] Ishikawa K, Takagi S, Chow, LC Suzuki K Reaction of calcium phosphate cements with different amounts of tetracalcium phosphate and dicalcium phosphate anhydrous. *J Biom Mat Res.* 1999;46:504-10.
- 44] Bodier-Houlle P, Steuer P, Voegel JC, Cuisinier FJC First experimental evidence for human dentine crystal formation involving conversion of octacalcium phosphate to hydroxyapatite. *Acta Cryst.* 1998,D54 1377-81.
- 45] Socol G, Torricelli P, Bracci B, Iliescu M, Miroiu F, Bigi A, Werckmann J, Mihailescu I N Biocompatible nanocrystalline octacalcium phosphate thin films obtained by pulsed laser deposition. *Biomaterials* 2004; 25:2539-45.
- 46] Monma H Preparation of octacalcium phosphate by the hydrolysis of alpha-tricalcium phosphate. *J Mater Sci.* 1980;15:2428-34.
- 47] Barrère F, Layrolle P, van Blitterswijk CA, de Groot K. Biomimetic coatings on titanium: a crystal growth study of octacalcium phosphate. *J Mat Sci: Mat in Med.* 2001;12:529-34.
- 48] Leroux L, Hatim Z, Frèche M, Lacout JL Effects of various adjuvants (lactic acid, glycerol, and chitosan) on the injectability of a calcium phosphate cement. *Bone.* 1999;25:S31-S34
- 49] Jarcho M Calcium phosphate ceramics as hard tissue prosthetics. *Ch Orthop.* 1981;157:259-278.
- 50] Heughebaert M, Le Geros RZ, Gineste M, Guilhem A, Bonel G Physicochemical characterization of deposits associated with HA ceramics implanted in nonosseous sites. *J Biomed Mater Res: Appl Biomater.* 1988;22 257-68.
- 51] Ripamonti U. Osteoinduction in porous hydroxyapatite implanted in heterotopic sites of different animal models. *Biomaterials* 1996;17:31-35
- 52] Boyde A, Corsi A, Quarto R, Cancedda R, Bianco P. Osteoconduction in large macroporous hydroxyapatite ceramic implants. evidence for a complementary integration and disintegration mechanism. *Bone.* 1999;24:579-89.
- 53] Koutsopoulos S. Synthesis and characterization of hydroxyapatite crystals A review study on the analytical methods. *J Biomed Mat Res* 2002;62:600-12

- 54] Yamasaki N, Kai Nishioka TM, Yanagisawa K, Ioku K. Porous hydroxyapatite ceramics prepared by hydrothermal hotpressing. *J Mater Sci.* 1990;9:1150–51.
- 55] LeGeros RZ, Daculsi G, Orly I, Abergas T, Torres W. Solution-mediated transformation of octacalcium phosphate (OCP) to apatite. *Scann Microsc* 1989;3:129-38.
- 56] Cheng K, Shen G, Weng W, Han G, Ferreira JMF, Yang J. Synthesis of hydroxyapatite/fluoroapatite solid solution by a sol-gel method. *Mat Letters.* 2001;51:37-41.
- 57] Pach L, Komarneni S. Precipitation of hydroxyapatite film under dynamic conditions. *Mat Res Bull.* 1999;34:1859-65.
- 58] Bouler JM, LeGeros RZ, Daculsi G. Biphasic calcium phosphates: Influence of three synthesis parameters on the HA/ $\beta$ -TCP ratio. *J of Biomed Mat Res* 2000;52:66-76
- 59] Berton E, Bigi A, Cozzani G, Gandolfi M, Panzavolta S, Roveri N. Nanocrystals of magnesium and fluoride substituted hydroxyapatite, *J Inorg Biochem.* 1998; 72:29-35.
- 60] Liu HS, Chin TS, Lai LS, Chiu SY, Chung KH, Chang CS, Lui MT. Hydroxyapatite synthesized by a simplified hydrothermal method. *Cer Int.* 1997; 23:19-25
- 61] Kitsugi T, Yamamuro T, Nakamura T, Kotani S, Kokubo T, Takeuchi H. Four calcium phosphate ceramics as bone substitutes for non-weight-bearing. *Biomaterials.* 1993;14,3:216-24.
- 62] Frame JW, Browne M, Brady CL. Hydroxyapatite as a bone substitute in the jaws. *Biomaterials.* 1981;2:19-22.
- 63] Higashi S, Yamamuro T, Nakamura T, Ikada Y, Hyon SH, Jamshidi K. Polymer-hydroxyapatite composites for biodegradable bone fillers. *Biomaterials.* 1986;7:183-87.
- 64] Ge Z, Bagenard S, Lim LY, Wee A, Khor E. Hydroxyapatite-chitin materials as potential tissue engineered bone substitutes. *Biomaterials.* 2004, 25:1049-58
- 65] Lee JJ, Rouhfard L, Ross Beirne O. Survival of hydroxyapatite-coated implants: A meta-analytic review, *J Oral and Max Surg* 2000, 58 1372-79
- 66] Destainville A, Champion E, Bernache-Assollant D, Laborde E. Synthesis, characterization and thermal behavior of apatitic tricalcium phosphate, *Mat Chem and Phys.* 2003;80:269–77.
- 67] Raynaud S, Champion E, Bernache-Assollant D, Thomas P. Calcium phosphate apatites with variable Ca/P atomic ratio I. Synthesis, characterization and thermal stability of powders. *Biomaterials.* 2002, 23:1065–72
- 68] Kwon SH, Jun YK, Hong SH, Kim HE. Synthesis and dissolution behavior of  $\beta$ -TCP and HA/ $\beta$ -TCP composite powders. *J of Eur Cer Soc.* 2003;23:1039-45
- 69] Yashima M, Sakai A. High-temperature neutron powder diffraction study of the structural phase transition between  $\alpha$  and  $\alpha'$  phases in tricalcium phosphate  $\text{Ca}_3(\text{PO}_4)_2$ , *Chem Phys Letters* 2003;372:779-83.
- 70] Hsu CK. The preparation of biphasic porous calcium phosphate by the mixture of  $\text{Ca}(\text{H}_2\text{PO}_4)_2 \cdot \text{H}_2\text{O}$  and  $\text{CaCO}_3$ . *Mat Chem and Phys* 2003;80:409-20.
- 71] Eggl PS, Muller W, Schenk RK. Porous hydroxyapatite and tricalcium phosphate cylinders with two different pore size ranges implanted in the cancellous bone of rabbits. A comparative histomorphometric and histologic study of bony ingrowth and implant substitution. *Clin.Orthop* 1988,127-38.

- 72] Kurashina K, Kurita H, Kotani A, Takeuchi H, Hirano M In vivo study of a calcium phosphate cement consisting of  $\alpha$ -tricalcium phosphate/dicalcium phosphate dibasic/tetracalcium phosphate monoxide. *Biomaterials*. 1997;18:147-51
- 73] Nery EB, LeGeros RZ, Lynch KL, Lee K. Tissue response to biphasic calcium phosphate ceramic with different ratios of HA/1-TCP in periodontal osseous defects. *J Periodontol*. 1992;63:729-35.
- 74] Piattelli A, Scarano A, Mangano C Clinical and histologic aspects of biphasic calcium phosphate ceramic (BCP) used in connection with implant placement *Biomaterials*. 1996;17: 1767-70.
- 75] Peña J, Vallet-Regi M. Hydroxyapatite, tricalcium phosphate and biphasic materials prepared by a liquid mix technique. *J of Eur Cer Soc*. 2003;23:1687-96.
- 76] Ramay HRR, Zhang M Biphasic calcium phosphate nanocomposite porous scaffolds for load-bearing bone tissue engineering. *Biomaterials* 2004;25:5171-80.
- 77] Daculsi G, Weiss P, Bouler JM, Gauthier O, Millot F, Aguado E Biphasic calcium phosphate/hydrosoluble polymer composites: a new concept for bone and dental substitution biomaterials. *Bone*. 1999;25 S59-S61
- 78] Trombe JC, Montel G Some features of the incorporation of oxygen in different oxidation states in the apatitic lattice-I On the existence of calcium and strontium oxyapatites. *J Inorg Nucl Chem* 1978;40.15-21.
- 79] Bohner M. Calcium orthophosphates in medicine: from ceramics to calcium phosphate cements *Injury* 2000;31 S37-S47
- 80] Jana C, Braun M.  $^{19}\text{F}$  NMR spectroscopy of glass ceramics containing fluorapatites *Biomaterials* 1996;17:2065-69
- 81] Lugscheider E, Knepper M, Heimberg B, Dekker A, Kirkpatrick CJ. Cytotoxicity investigations of plasma sprayed calcium phosphate coatings. *J Mater Sci: Mat Med*. 1994;5:371-5.
- 82] Gineste L, Gineste M, Ranz X, Ellefterion A, Guilhem A, Rouquet N, Frayssinet P. Degradation of hydroxylapatite, fluorapatite, and fluorhydroxyapatite coatings of dental implants in dogs *J Biomed Mater Res*. 1999;48. 224-34.
- 83] Cheng K, Shen G, Weng W, Han G, Ferreira JMF, Yang J. Synthesis of hydroxyapatite/ fluoroapatite solid solution by a sol-gel method. *Mat Letters* 2001;51:37-41.
- 84] Nikčević I, Jokanović V, Mitrić M, Nedić Z, Makovec D, Uskoković D. Mechanochemical synthesis of nanostructured fluorapatite/fluorhydroxyapatite and carbonated fluorapatite/fluorhydroxyapatite. *J Sol State Chem*. 2004;177 2565-74.
- 85] Ducheyne P Bioceramics: Material characteristics versus in vivo behavior *J Biomed Mater Res: Appl Biomater* 1987;HA 219-236.
- 86] Caswell AM, Russell RG. Evidence that ecto-nucleoside-triphosphate pyrophosphatase serves in the generation of extracellular inorganic pyrophosphate in human bone and articular cartilage. *Biochem et Biophys Acta*. 1988;966:310-17.
- 87] Fleisch H. Bisphosphonates: Pharmacology and use in the treatment of tumour-induced hypercalcaemic and metastatic bone disease. *Drugs*. 1991; 42:919-44.

- 88] Ott SM. Clinical effects of bisphosphonates in involutional osteoporosis. *J Bone Miner Res*, 1993;8 S597- S606.
- 89] Fleisch H. Diphosphonates: History and mechanisms of action. *Metab Bone Dis Relate Res*. 1981;3:279-87
- 90] Charles S, Resnik MD, Donald Resnick MD. Calcium pyrophosphate dihydrate crystal deposition disease, current problem in diagnostic Radiology. 1982;11 6-40.
- 91] Masala O, McInnes EJL, O'Brien P. Modelling the formation of granules: the influence of manganese ions on calcium pyrophosphate precipitates. *Inorg Chem Acta* 2002;339:366-72.
- 92] Anee TK, Ashok M, Palanichamy M, Narayana Kalkura S. A novel technique to synthesize hydroxyapatite at low temperature. *Mat Chem and Phys*. 2003;80:725-730.
- 93] Ryu HS, Youn HJ, Hong KS, Chang BS, Lee CK, Chung SS. An improvement in sintering property of  $\beta$ -tricalcium phosphate by addition of calcium pyrophosphate. *Biomaterials*. 2002;23: 909-14.
- 94] Kitsugi T, Yamamuro T, Nakamura T, Oka M. Transmission electron microscopy observations at the interface of bone and four types of calcium phosphate ceramics with different calcium/phosphorus molar ratios. *Biomaterials* 1995;16: 1101-07
- 95] Lin FH, Lin CC, Lu CM, Liu HC, Sun JS, Wang CY. Mechanical properties and histological evaluation of sintered  $\beta$ - $\text{Ca}_2\text{P}_2\text{O}_7$  with  $\text{Na}_4\text{P}_2\text{O}_7 \cdot 10\text{H}_2\text{O}$  addition. *Biomaterials* 1995;16:793-802
- 96] Breme J, Zhou Y, Groh L. Development of a titanium alloy suitable for an optimized coating with hydroxyapatite. *Biomaterials* 1995;16: 239-44.
- 97] Dhert WJA, Klein CPAT, Wolke JGC, van de Velde EA, de Groot K, Rozing PM. In P. Vincenzini (ed). *Ceramics in Substitutive and Reconstructive Surgery*, Elsevier, Amsterdam, 1991, pp. 385-94.
- 98] Feenster L, de Groot K. In K. de Groot (ed ). *Bioceramics of Calcium Phosphates*. CRC Press, Boca Raton. FL. USA, 1983.
- 99] Ciccotti MG, Rothman RH, Hozack WJ, Moriarty L. Clinical and roentgenographic evaluation of hydroxyapatite-augmented and nonaugmented porous total hip arthroplasty. *J Arthroplasty* 1994;9:631-39
- 100] d' Antonio JA, Capello WN, Manley MT. Remodeling of bone around hydroxyapatite-coated femoral stems. *J Bone Jt Surg Am*. 1996;78:1226-34.
- 101] Toksvig-Larsen S, Jørn LP, Ryd L, Lindstrand A. Hydroxyapatite-enhanced tibial prosthetic fixation. *Clin Orthop*. 2000;370 192-200
- 102] Regner L, Carlsson L, Karrholm J, Herberts P. Ceramic coating improves tibial component fixation in total knee arthroplasty. *J Arthroplasty*. 1998;13:882-9
- 103] Klein CPAT, Patsa P, Wolke JGC, Bliëk-Hogervorst JMAD, de Groot K. Long-term in-vivo study of plasma-sprayed coatings on titanium alloys of tetra-calcium, hydroxyapatite, and  $\alpha$ -tricalcium phosphate. *Biomaterials*. 1994;15:146-50.
- 104] Brossa F, Cigada A, Chiesa R, Paracchini L, Consonni C. Adhesion properties of plasma sprayed hydroxyapatite coatings for orthopaedic prostheses. *Bio Med Mater Eng* 1993;3 127-36.
- 105] Nakashima Y, Hayashi K, Inadome T, Sugioka Y. Hydroxyapatite coating on titanium-sprayed titanium implant. In Ducheyne P, Christiansen D, (eds). *Bioceramics 6*. Oxford, UK. Butterworth-Heinemann Ltd ,



1993. p. 449–53.
- 106] Cook SD, Thomas KA, Kay JF Experimental coating defects in hydroxyapatite-coated implants. *Clin Orthop*. 1991;265:280-90.
- 107] Collier JP, Surprenant VA, Mayor MB, Wrona M, Jensen RE, Surprenant HP Loss of hydroxyapatite coating on retrieved total hip components. *J Arthroplasty* 1993;8:389-92
- 108] Dalton JE, Cook SD. In vivo mechanical and histological characteristics of HA-coated implants vary with coating vendor. *J Biomed Mater Res*. 1995;29:239-45
- 109] Nilsson KG, Cajander S, Kärrholm J. Early failure of hydroxyapatite coating in total knee arthroplasty. *Acta Orthop Scand*. 1994;65:212-14
- 110] Ellices LG, Nelson DGA, Featherstone JDB. Crystallographic changes in calcium phosphates during plasma-spraying, *Biomaterials*. 1992;13:313-16.
- 111] Liu DM, Chou HM, Wu JD, Tung MS. Hydroxylapatite coating via amorphous calcium phosphate. *Mat Chem and Phys.*, 1994, 37:39-44
- 112] Yang Y, Kim KH, Onga JL. A review on calcium phosphate coatings produced using a sputtering process - an alternative to plasma spraying. *Biomaterials*. 2005;26:327-37.
- 113] Feddes B, Vredenberg AM, Wolke JGC, Jansen JA. Initial deposition of calcium phosphate ceramic on polystyrene and polytetrafluoroethylene by RF magnetron sputtering deposition. *J Vac Sc Techn*. 2003;21A:363-68.
- 114] Jansen JA, Wolke JGC, Swann S, van der Waerden JPCM, de Groot K Application of magnetron sputtering for producing ceramic coatings on implant materials *Clin Oral Impl Res*. 1993;4:28-34.
- 115] Dijk HG, Schaeken HG, Wolke JGC, Jansen JA. Influence of annealing temperature on RF magnetron sputtered calcium phosphate coatings. *Biomaterials* 1996;17:405-10.
- 116] Dijk HG, Schaeken HG, Wolke JGC, Marce CHM, Habraken FHPM, Verhoeven J, Jansen JA. Influence of discharge power level on the properties of hydroxyapatite films deposited on Ti6Al4V with RF magnetron sputtering. *J Biomed Mater Res*. 1995;29:269-76.
- 117] Yoshinari M, Hayakawa T, Wolke JGC, Nemoto K, Jansen JA.. Influence of rapid heating with infrared radiation on RF magnetron-sputtered calcium phosphate coatings *J Biomed Mater Res* 1997;37:60-7
- 118] Gross KA, Berndt CC. Thermal processing of hydroxyapatite for coating production *J Biomed Mater Res*. 1998, 39:580–87.
- 119] Roome CM., Adam CD Crystallite orientation and anisotropic strains in thermally sprayed hydroxyapatite coatings. *Biomaterials*. 1995;16:691–696
- 120] Zeng H, Lacefield WR. The study of surface transformation of pulsed laser deposited hydroxyapatite coatings *J Biomed Mater Res*. 2000;50:239–47.
- 121] Fernandez-Pradas JM, Cleres L, Martinez E, Sardin G, Esteve J, Morenza JL Influence of thickness on the properties of hydroxyapatite coatings deposited by KrF laser ablation. *Biomaterials*. 2001;22 2171–75
- 122] Yoshinari M, Ohshiro Y, Derand T Thin hydroxyapatite coating produced by the ion beam dynamic mixing method. *Biomaterials* 1994;15:528-35.
- 123] Hayakawa T, Yoshinari M, Kiba H, Yamamoto H, Nemoto K, Jansen JA. Trabecular bone response to

- surface roughened and calcium phosphate (Ca-P) coated titanium implants. *Biomaterials*, 2002;23:1025-31
- 124] Barthell HL, Archuleta TA, Kossowsky R. Ion beam deposition of calcium hydroxyapatite. *Mater Res Soc Symp*. 1989;110 709-15.
- 125] Weng W, Baptista JL. Alkoxide route for preparing hydroxyapatite and its coatings. *Biomaterials*. 1998;19:125-31
- 126] Campbell AA, Song L, Li XS, Nelson BJ, Bottoni C, Brooks DE, DeJong ES. Development, characterization, and antimicrobial efficacy of hydroxyapatite-chlorhexidine coatings produced by surface-induced mineralization. *J Biomed Mater Res-Appl Biomater*. 2000;53:400-7.
- 127] Liu D, Yang Q, Troczynski T. Sol-gel hydroxyapatite coatings on stainless steel substrates. *Biomaterials*. 2002;23 691-8.
- 128] Chai CS, Gross KA, Ben-Nissan B. Critical ageing of hydroxyapatite sol-gel solutions. *Biomaterials*. 1998;19:2291-96.
- 129] De Sena LA, de Andrade MC, Rossi AM, Soares GDA. Hydroxyapatite deposition by electrophoresis on titanium sheets with different surface finishing. *J Biomed Mater Res*. 2002;60 1-7.
- 130] Nie X, Leyland A, Matthews A, Jiang JC, Meletis EI. Effects of solution pH and electrical parameters on hydroxyapatite coatings deposited by a plasma-assisted electrophoresis technique. *J Biomed Mater Res*. 2001;57 612-18.
- 131] Habibovic P, Barrere F, van Blitterswijk CA, de Groot K, Layrolle P. Biomimetic hydroxyapatite coating on metal implants. *J Am Ceramic Soc*. 2002;85:517-22.
- 132] Oliveira AL, Elvira C, Reis RL, Vazquez B, San Roman J. Surface modification tailors the characteristics of biomimetic nucleated on starch-based polymers. *J Mater Sci: Mater Med*. 1999; 10 827-35
- 133] Wie H, Hero H, Solheim T. Hot isostatic pressing-processed hydroxyapatite-coated titanium implants: light microscopic and scanning electron microscopy investigation. *J Oral Maxillofac Implants*. 1998; 13: 837-44
- 134] Khor KA, Yip CS, Cheang P. Post-spray hot isostatic pressing of plasma sprayed Ti-6Al-4V/hydroxyapatite composite coatings. *J of Mat Proc Tech*. 1997;71:280-87
- 135] Leeuwenburgh SCG, Wolke JGC, Schoonman J, Jansen JA. Influence of deposition parameters on morphological properties of biomedical calcium phosphate coatings prepared using electrostatic spray deposition. *Thin Solid Films*. 2005;472:105-13.
- 136] Leeuwenburgh SCG, Wolke JGC, Schoonman J, Jansen JA. Influence of precursor solution parameters on chemical properties of calcium phosphate coatings prepared using Electrostatic Spray Deposition (ESD). *Biomaterials*. 2004;25:641-49.
- 137] Ong JL, Lucas LC. Post-deposition heat treatments for ion beam sputter deposited calcium phosphate coatings. *Biomaterials*. 1994;5 337-41
- 138] García F, Arias JL, Mayor B, Pou J, Rehman I, Knowles J, Best S, León B, Pérez-Amor M, Bonfield W. Effect of heat treatment on pulsed laser deposited amorphous calcium phosphate coatings. *J Biomed Mater Res-Appl Biomater*. 1998;43:69-76.

- 139] van Dijk K, Schaeken HG, Wolke JGC, Jansen JA. Influence of annealing temperature on RF- magnetron sputtered calcium phosphate coatings. *Biomaterials*. 1996;17:405-10.
- 140] Yoshinari M, Hayakawa T, Wolke JGC, Nemoto K, Jansen JA. Influence of rapid heating with infrared radiation on RF magnetron-sputtered calcium phosphate coatings. *J Biomed Mat Res* 1997;37:60-7.
- 141] Cao Y, Weng J, Chen J, Feng J, Yang Z, Zhang X. Water vapour-treated coatings after plasma their characteristics hydroxyapatite spraying and their characteristics. *Biomaterials* 1996; 17:419-24.
- 142] Tong W, Chen J, Cao Y, Lu L, Feng J, Zhang X Effect of water vapor pressure and temperature on the amorphous-to-crystalline HA conversion during heat treatment of HA coatings. *J Biomed Mat Res*. 1997;36: 242-45.
- 143] Mariucci L, Pecora A, Carluccio R, Fortunato G Advanced excimer laser crystallization techniques. *Thin Solid Films*. 2001;383:39-44.
- 144] Voutsas AT. A new era of crystallization: advances in polysilicon crystallization and crystal engineering *Appl Surf Sci* 2003;208:250-62.
- 145] Yang Y, Kim KH, Agrawal CM, Ong JL Effect of postdeposition heating temperature and the presence of water vapor during heat treatment on crystallinity of calcium phosphate coatings. *Biomaterials*. 2003;24 5131-37
- 146] Yang Y, Kim KH, Agrawal CM, Ong JL. Influence of postdeposition heating time and the presence of water vapor on sputter-coated calcium phosphate crystallinity. *J Dent Res*. 2003 ,82:833-37
- 147] Kweh SWK, Khor KA, Cheang P Plasma-sprayed hydroxyapatite (HA) coatings with flame-spheroidized feedstock: microstructure and mechanical properties. *Biomaterials* 2000;21:1223-34.
- 148] Hwang KE , Kim CS. Interface characteristics changed by heat treatment of Ti materials with hydroxyapatite. *Mat Sci Engin C* 2003;23:401-5.
- 149] de Bruijn JD, Bovell YP, van Blitterswijk CA. Structural arrangements at the interface between plasma sprayed calcium phosphates and bone. *Biomaterials*. 1994;15:543-50.
- 150] Sanden B, Olerud C, Johansson C, Larsson S. Improved bone screw interface with hydroxyapatite coating: An in vivo study of loaded pedicle screws in sheep. *Spine*. 2001;26:2673-78
- 151] Fini M, Giavaresi G, Greggi T, Martini L, Nicoli Aldini N, Parisini P, Giardino R Biological assessment of the bone-screw interface after insertion of uncoated and hydroxyapatite-coated pedicular screws in the osteopenic sheep *J Biomed Mat Res*. 2003;66A:176-83
- 152] Kienapfel H, Sprey C, Wilke A, Griss R Implant fixation by bone ingrowth. *J Arthrop*. 1999;14:355-68
- 153] Hayakawa T, Yoshinari M, Kiba H, Yamamoto H, Nemoto K, Jansen JA. Trabecular bone response to surface roughened and calcium phosphate (Ca-P) coated titanium implants. *Biomaterials*. 2002;23:1025-31.
- 154] Chen QZ, Wong CT, Lu WW, Cheung KMC, Leong JCY, Luk KDK. Strengthening mechanisms of bone bonding to crystalline hydroxyapatite in vivo. *Biomaterials*. 2004;25 4243-54.
- 155] Maxian SH, Zawadsky JP, Dunn MG. Effect of Ca/P coating resorption and surgical fit on the bone/implant interface. 1994;28.1311-19.
- 156] Baltag I, Watanabe K, Kusakari H, Taguchi N, Miyakawa O, Kobayashi M, Ito N. Long-term changes of

- hydroxyapatite-coated dental implants. *J Biomed Mat Res* 2000;53:76-85.
- 157] Wolke JGC, de Groot K, Jansen JA. In vivo dissolution behavior of various RF magnetron sputtered Ca-P coatings. *J Biomed Mater Res*. 1998;39:524-30.
- 158] Gu YW, Khor KA, Cheang P. In vitro studies of plasma-sprayed hydroxyapatite/ Ti-6Al-4V composite coatings in simulated body fluid (SBF). *Biomaterials*. 2003;24:1603-11
- 159] Wang H, Kook Lee J, Moursi A, Lannutti JJ. Ca/P ratio effects on the degradation of hydroxyapatite in vitro. *J Biomed Mater Res*. 2003;67A:599-608.
- 160] Driessens F, Verbeeck R. Relation between physico-chemical solubility and biodegradability of calcium phosphates. In: de Putter C, de Lange GL, de Groot K, Lee AJC (eds). *Implant materials in biofunction Advances in Biomaterials*. Amsterdam. Elsevier 1988.p48-52.
- 161] Ribeiro C, Rigo ECS, Sepúlveda P, Bressiani JC, Bressiani AHA. Formation of calcium phosphate layer on ceramics with different reactivities. *Mat Sci and EnginC*. 2004;24:631-36.
- 162] LeGeros RZ. Biodegradation and bioresorption of calcium phosphate ceramics. *Clin Mater*. 1993;14 65-88.
- 163] LeGeros RZ. Properties of osteoconductive biomaterials: calcium phosphates. *Clin Orthop Relat Res*. 2002;395:81-98.
- 164] Sun L, Berndt CC, Khor KA, Cheang HN, Gross KA. Surface characteristics and dissolution behavior of plasma-sprayed hydroxyapatite coating. *J Biomed Mater Res*. 2002;62:228-36.
- 165] Serro AP, Fernandes AC, Sasamago B. Calcium phosphate deposition on titanium in the presence of fibronectin. *J Biomed Mater Res*. 2000;49 345-52.
- 166] Blumenthal NC. Mechanisms of inhibition of calcification. *Clin Ortho Relat Res*. 1989;247:279-89.
- 167] Boskey AL, Maresca M, Ullrich W, Doty SB, Butler WT, Prince CW. Osteopontin- hydroxyapatite interactions in vitro: inhibition of hydroxyapatite formation and growth in a gelatin-gel. *Bone Mineral*. 1993;22:147-59.
- 168] Chen C, Boskey AL, Rosenberg LC. The inhibitory effect of cartilage proteoglycans on hydroxyapatite growth. *Calcif Tissue Int*. 1984;36:285-90.
- 169] Gilman H, Hukins DWL. Seeded growth of hydroxyapatite in the presence of dissolved albumin. *J Inorg Biochem*. 1994;55:21-30.
- 170] LeGeros RZ, Orly I. Substrate surface dissolution and interfacial biological mineralization. In: Davies JE (ed) *The Bone Biomaterial Interface*. Toronto: University of Toronto Press; 1991. p. 76-88.
- 171] Chen QZ, Wong CT, Lu WW, Cheung KMC, Leong JCY, Luk KDK. Strengthening mechanisms of bone bonding to crystalline hydroxyapatite in vivo. *Biomaterials* 2004; 25:4243-54
- 172] Perozzollo D, Lacefield WR, Brunette DM. Interaction between topography and coating in the formation of bone nodules in culture for hydroxyapatite- and titanium-coated micromachine surfaces. *J Biomed Mater Res* 2001;56:494-503.
- 173] Hulshoff JEG, van Dijk K, de Ruijter JE, Rietveld FJR, Ginsel LA, Jansen JA. Interfacial phenomena: an in vitro study of the effect of calcium phosphate (Ca-P) ceramic on bone formation. *J Biomed Mater Res* 1998;40:464-74

- 174] Maxian SH, Di Stefano T, Melican MC, Tiku ML, Zawadsky JP Bone cell behavior on matrigel-coated Ca/P coatings of varying crystallinities J Biomed Mater Res. 1998;40:171-79
- 175] Ong JL, Carnes DL, Sogal A Effect of transforming growth factor-B on osteoblast cells cultured on 3 different hydroxyapatite surfaces Int J Oral Maxillofac Impl. 1999 , 12:217-25.
- 176] Yang Y, Bumgardner JD, Cavin R, Carnes DL, Ong JL. Osteoblast precursor cell attachment on heat-treated calcium phosphate coatings. J Dent Res. 2003 ;82:449-53.
- 177] Thomas KA Hydroxyapatite coatings Orthopedics. 1994;17:267-78.
- 178] Ong JL, Bessho K, Cavin R, Carnes DL Bone response to radio frequency sputtered calcium phosphate implants and titanium implants in vivo J Biomed Mater Res 2002;59:184-90.
- 179] Darimont G, Cloots R, Heinen E, Seidel L, Legrand R. In vivo behavior of hydroxyapatite coatings on titanium implants: a quantitative study in the rabbit. Biomaterials. 2002;23:2569-75.
- 180] Hacking SA, Tanzer M, Harvey EJ, Krygier JJ, Bobyn JD. Relative contributions of chemistry and topography to the osseointegration of hydroxyapatite coatings Clin Orthop Relat Res 2002;405:24-38.
- 181] Sanden B, Olerud C, Johansson C, Larsson S. Improved bone screw interface with hydroxyapatite coating. Spine. 2001;26:2673-78.
- 182] Vercaigne S, Wolke JGC, Naert I, Jansen JA. A histological evaluation of TiO<sub>2</sub>-grit blasted and Ca-P magnetron sputter coated implants placed into the trabecular bone of the goat. Part 2. Clin Oral Implants Res 2000 ; 11:314-24.
- 183] Buser D, Schenk RK, Steinemann S, Fiorellini JP, Fox CH, Stich H. Influence of surface characteristics on bone integration of titanium implants A histomorphometric study in miniature pigs. J Biomed Mater Res 1991, 25:889-902.
- 184] Kitsugi T, Yamamuro T, Nakamura T, Oka M Transmission electron microscopy observations at the interface of bone and four types of calcium phosphate ceramics with different calcium/ phosphorus molar ratios Biomaterials. 1995;16:1101-7
- 185] Porter AE, Hobbs LW, Benezra Rosen V, Spector M. The ultrastructure of the plasma-sprayed hydroxyapatite-bone interface predisposing to bone bonding. Biomaterials 2002; 23:725-733.
- 186] Ong JL, Bessho K, Cavin R, Carnes DL Bone response to radio frequency sputtered calcium phosphate implants and titanium implants in vivo J Biomed Mater Res 2002;59:184-90.
- 187] Kato H, Nakamura T, Nishiguchi S, Matsusue Y, Kobayashi M, Miyazaki T, Kim HM, Kokubo T, Bonding of alkali- and heat-treated tantalum implants to bone J Biomed Mater Res-Appl Biomater 2000;53:76-85.
- 188] Lee IS, Kim HE, Kim SY. Studies on calcium phosphate coatings. Surf Coat Techn. 2000;131:181-86.
- 189] Liang F, Zhou L, Wang K. Apatite formation on porous titanium by alkali and heat-treatment. Surf and Coat Techn. 2003;165:133-39
- 190] Mangano C, Bartolucci EG, Mazzocco C A new porous hydroxyapatite for promotion of bone regeneration in maxillary sinus augmentation: clinical and histologic study in humans Int J Oral Maxillofac Implants. 2003;18:23-30.
- 191] Fujui T, Ogino M Difference of bone bonding behavior among surface active glasses and sintered apatite

J Biomed Mater Res 1984;18:845-59.

- 192] Wolke JGC, de Bleeck-Hogervorst JMA, Dhert WJA, Klein CPAT, de Groot K Studies on the thermal spraying of apatite bioceramics. J Thermal Spray Technol. 1992,1:75-82

## **Chapter 2**

### **Preparation and characterization of RF magnetron sputtered Calcium pyrophosphate coatings**

In press: J Biomed Mat Res. Part A, 2005

Yan Yonggang, J. G.C. Wolke, Li Yubao, J.A. Jansen

## Introduction

Calcium phosphate (Ca-P) materials have been used as bone substitute or bone graft in dentistry, orthopedic- and reconstructive surgery because of their good biocompatibility and osteointegrative properties [1]. However, due to their brittle nature, the use of bulk Ca-P ceramics is limited to unloaded situations. To solve this problem, it has been proposed to apply Ca-P bioceramics as thin coatings on metallic substrates, resulting in implants that have the excellent biocompatible properties of calcium phosphate as well as the advantageous mechanical properties of metal. At the moment, various techniques are available for the deposition of calcium phosphate on metal implants, e.g. hot pressing, plasma or flame spraying, ion-beam sputter deposition, frit enameling, electrophoretic deposition, and sol-gel deposition [2-9].

Previous work by our group investigated the use of radiofrequency (RF) magnetron sputter deposition as a method of applying thin adherent calcium phosphate coatings to titanium implants. The results showed that the deposited films had an excellent adhesiveness and a good biological response, both *in vitro* and *in vivo* [10-13].

Recently, a lot of attention has been paid to pyrophosphate ceramics. These pyrophosphates are used as artificial bone filler and can be useful in a clinical setting characterized by abnormal bone resorption. The results of an *in vitro* osteoblast cell culture and *in vivo* animal study demonstrated already that pyrophosphate is biocompatible with bone cells [14-19]. Further, synthetic pyrophosphate can inhibit osteoclastic bone resorption and therefore is used for the treatment of bone diseases, such as tumor hypercalcemia and osteoporosis [20-21]. Besides as bone substitute, pyrophosphate ceramic can also be useful as coating on medical- and oral implants.

Consequently, the objective of the present study was to characterize the physicochemical and dissolution behavior of calcium-pyrophosphate coatings obtained by RF magnetron sputtering.

## Materials and Methods

### *Ca-P coating deposition*

For the experiments commercially pure titanium (cpTi) disc were provided with various Ca-P sputter coatings. The discs measured 1mm in thickness and had a diameter of 12 mm. All discs were Al<sub>2</sub>O<sub>3</sub>-blasted on one side. The following coatings were prepared:

1-Calcium pyrophosphate- coating with a thickness of 2  $\mu\text{m}$  (Pyro).

2-Hydroxyapatite coating- coating with a thickness of 2  $\mu\text{m}$  (HA).

RF magnetron sputter coatings were made by using a commercially available RF sputter deposition system (Edwards ESM 100). The target materials were calcium pyrophosphate ( $\beta\text{-Ca}_2\text{P}_2\text{O}_7$ ) and hydroxylapatite ( $\text{Ca}_5(\text{PO}_4)_3\text{OH}$ ) granules (diameter 0.5-1.0mm). The test specimens were mounted on a rotating and water-cooled substrate holder. The distance



between target and substrate was 80 mm. Before sputtering the metal substrates were cleaned by etching for 10 min with argon ions. During deposition, the argon pressure was kept at  $5 \times 10^{-3}$  mbar and the sputter power was 400W.

After deposition, half of the coated specimens were subjected to an additional infrared heat treatment (HT) for 30 sec at 300°C (Quad Ellipse Chamber, Model E4-10-P, Research Inc.). Thereafter, the crystallographic structure of the coatings was evaluated. Depending on the results, the heat-treatment procedure was repeated on new specimens till a crystalline coating structure was obtained. In each new heat-treatment cycle the temperature was increased with 50°C.

Before and after annealing, coatings were characterized as follows:

- The crystallographic structure of each film was determined by thin film X-ray diffraction (XRD) using a Philips  $\theta$ -2 $\theta$  diffractometer using a  $\text{CuK}\alpha$  -radiation.
- The infrared spectra of the films on the substrates were obtained by reflection Fourier transform infrared spectroscopy (FTIR) (Perkin-Elmer).
- The surface topology of the films was examined using scanning electron microscopy (SEM) using a Jeol JSM-35.
- The elemental composition of the films was determined with an energy dispersive spectroscopy (EDS). Repetitive measurements at different locations on the coating surface were performed.

### ***In vitro bioactivity assay***

All coated specimens were incubated in 4 ml Simulated Body Fluid buffer (SBF) with a pH of 7.2 at 37°C for 4 weeks (Table 1). The experiment was performed in triplicate. At time points, 1, 2, 3 and 4 weeks, the SBF buffer solution was refreshed. For each sample, the Ca and P concentration in the solutions was determined in triplicate, respectively by OCPC (ortho-cresolphthalein complexone) method and spectrophotometer (Vitatron).

At the end of the experiment, coated samples were retrieved out of the SBF solution. After rinsing in aqua and drying at room temperature, the specimens were characterized by using XRD, FTIR, SEM and EDS.

**Table 1** Simulated Body Fluid (SBF)

Ions	Na	K <sup>+</sup>	Ca <sup>2+</sup>	Mg <sup>2+</sup>	Cl	HCO <sub>3</sub>	HPO <sub>4</sub>	SO <sub>4</sub> <sup>2-</sup>
SBF	142.0	5.0	2.5	1.5	147.8	4.2	1.0	0.5
Blood Plasma	142.0	5.0	2.5	1.5	103.0	27.0	1.0	0.5

Buffered with tris(hydroxymethyl) aminomethane (50 mM), set at pH 7.2 with 1.0N hydrochloric acid (Li 1993).

## Results

### Coating characterization before and after heat treatment

#### X-ray diffraction

The XRD patterns of the as-sputtered coatings showed an amorphous structure with no clear peaks (Figure 1). Further, a clear difference was observed in temperature as required to obtain crystallization between HA and pyrophosphate coatings (Figure 1). Infrared heat-treatment at 550°C changed the amorphous sputtered HA coatings into a crystalline apatite structure with reflections 002, 211, 112, 202, resp. 25.9°, 31.9°, 32.4° and 34.0° in 2-Theta, comparative with the XRD pattern of HA powder (JCPDS #09-0432). In contrast, the sputtered amorphous pyrophosphate coating required an annealing temperature of 650°C to alter into crystalline beta-calcium pyrophosphate structure with reflections lines 201, 202, 008 and 212, which correspond to peaks at 26.6°, 27.7°, 29.5° and 30.7° in 2-Theta (JCPDS#09-0346). Also, for the crystalline pyrophosphate coatings an additional reflection peak was seen at 27.6° in 2-Theta corresponding to titanium oxide (TiO<sub>2</sub>). This indicated oxidation of these substrates during the heat treatment procedure.

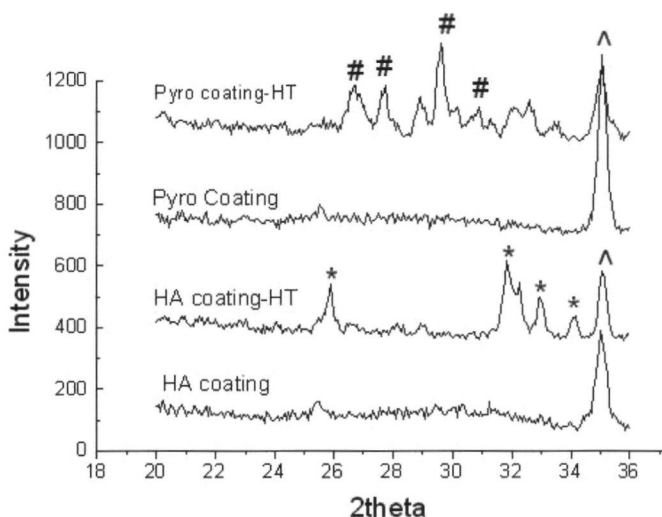


**Figure 1:** XRD patterns of sputtered calcium phosphate coatings. The major peaks have been marked: # = Pyro, \* = HA, and ^ = substrate

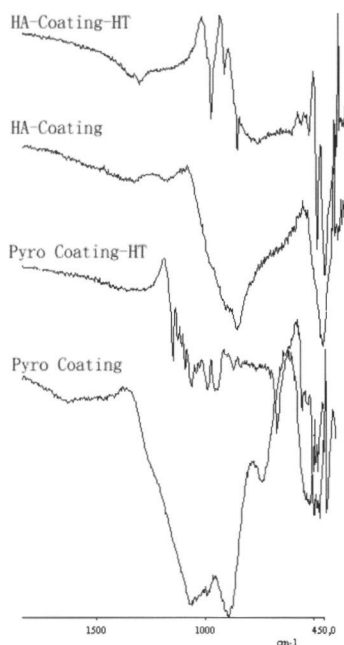


**Figure 2:** IR spectra of magnetron sputtered calcium phosphate coatings.

### **Fourier transform infrared spectroscopy**

FTIR measurements showed for all the amorphous coatings two clusters of bands from 900-1150 and from 550-600  $\text{cm}^{-1}$  attributed to the major absorption modes associated with the presence of phosphate (Figure 2). Heat treatment of the amorphous HA coatings resulted in the appearance of the hydroxyl band at 630  $\text{cm}^{-1}$ , characteristic for hydroxylapatite and the appearance of various P-O bands at a wavelength of 587, 630, 965, 1009, 1083  $\text{cm}^{-1}$  (Figure 2). Heat treatment of the sputtered amorphous pyrophosphate coatings resulted in the appearance of various P-O bonds at the wavelength around 1202, 1163, 1125, 1095, 1081, 993, 957, 644, 608, and 522  $\text{cm}^{-1}$ , which are characteristic for the beta-calcium pyrophosphate structure (Figure 2).

### **Scanning electron microscopy**

SEM examination of the sputtered coatings showed an excellent coverage of the substrate surface. Heat treatment was found to have no evident effect on the HA as well as pyrophosphate coating morphology (Figure 7A, 7D, 7G, and 7J).

### **Energy dispersive spectroscopy**

EDS analysis revealed that Ca/P ratio of amorphous as well as crystalline HA- and Pyro coatings varied between respectively 1.9-2.0 and 0.76-0.8.

### ***Coating characterization after soaking in SBF***

#### **In vitro bioactivity assay**

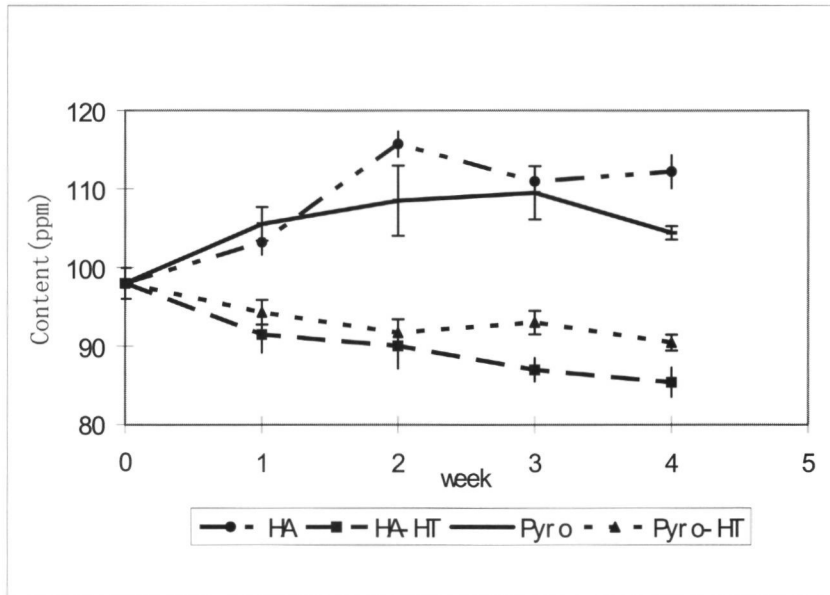
Figure 3 and 4 show the calcium and phosphate concentrations in the SBF buffer for the various coatings during the 4-week incubation period.

Partial dissolution of the amorphous coatings was observed characterized by a sharp increase in Ca concentration in the SBF solution from 1 to 2 weeks of incubation. Thereafter, the Ca concentration remained about constant. A similar dissolution pattern was observed for the P concentration. After 4 weeks of incubation, amorphous HA coatings showed only a significant higher release of P as compared to the Pyro coatings (ANOVA and Tukey multiple comparison test,  $P < 0.001$ ).

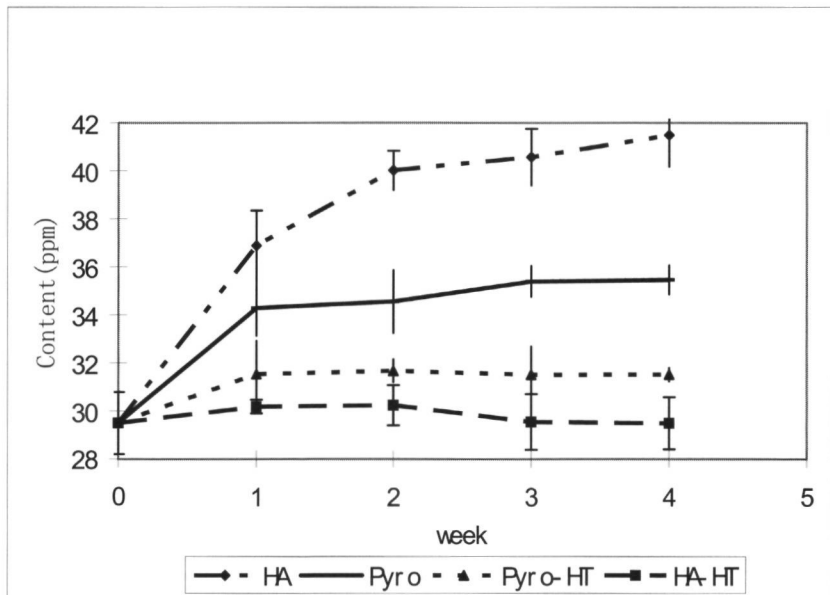
In contrast with the amorphous specimens, all heat-treated coatings appeared to induce a very limited decrease in Ca and an increase in P in the SBF solution during the 4 weeks incubation. Further, we observed that the HA heat-treated coatings did not cause a significant higher release of Ca and P in the SBF solution than the Pyro heat-treated coatings (ANOVA and Tukey multiple comparison test,  $P > 0.05$ ).

#### **X-ray diffraction**

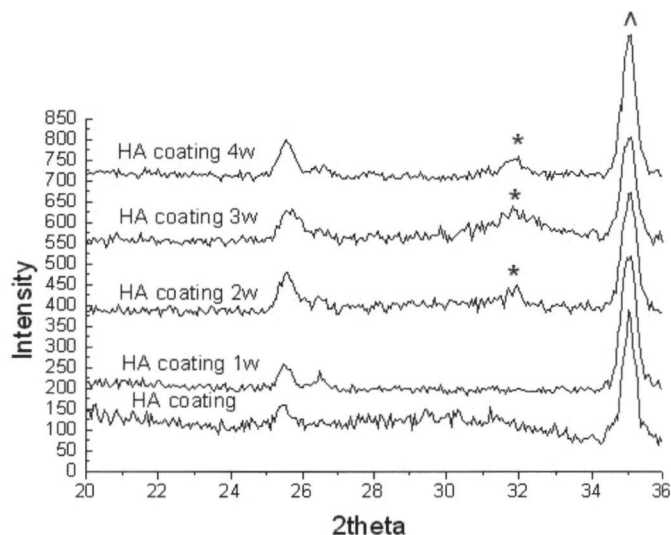
The XRD evaluation confirmed that all types of Ha and Pyro coatings were still present after 4 weeks of incubation in SBF. Further, for both types of amorphous sputter coatings the XRD pattern remained almost the same during the incubation (Figure 5A and 5C). Only for the HA coatings, dissolution of amorphous material resulted in the appearance of some minor crystalline peaks at  $26^\circ$  and  $31\text{--}33^\circ$  2-Theta (Figure 5A). Also, the XRD pattern of the heat-treated HA coatings did not change during incubation (Figure 5B). On the other hand, for the Pyro heat-treated coatings a  $\beta$ -TCP peak appeared at  $31^\circ$  2-Theta already 1 week after incubation in SBF (Figure 5D).



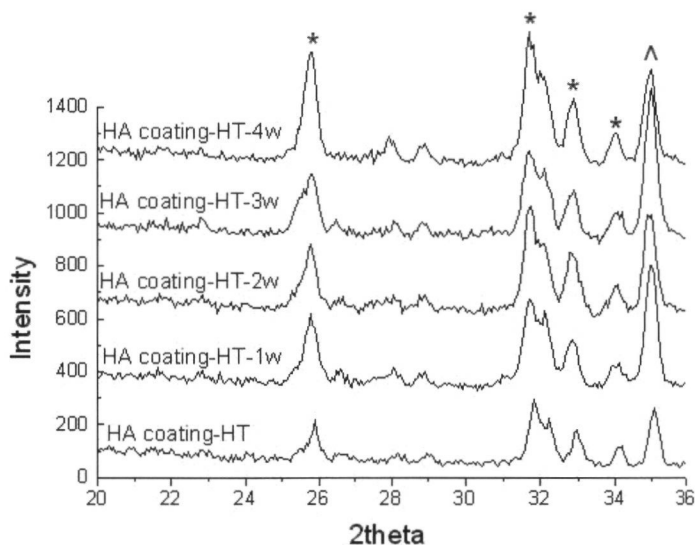
**Figure 3:** Calcium release of various magnetron sputtered Ca-P coatings in SBF at 37° C.



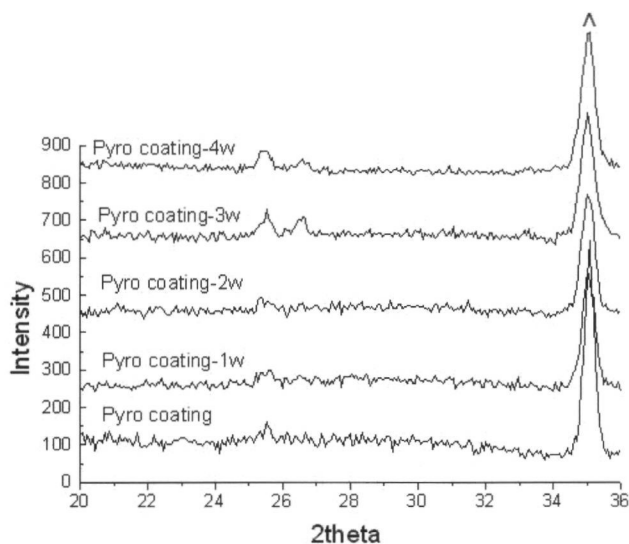
**Figure 4:** Phosphate release of various magnetron sputtered Ca-P coatings in SBF at 37° C.



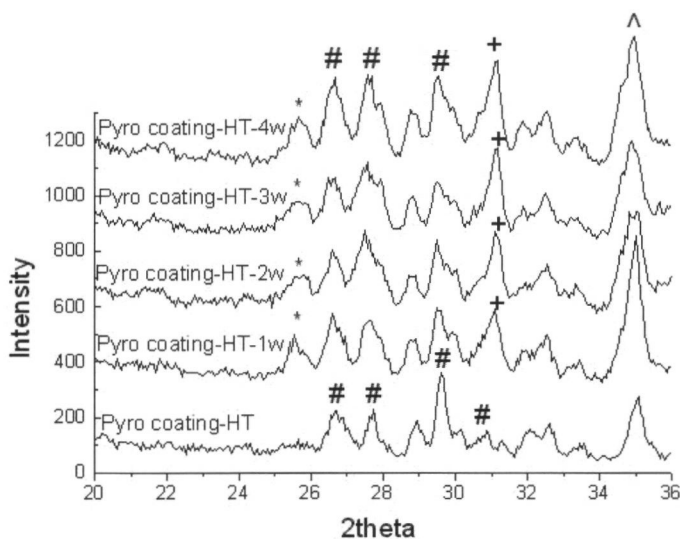
**Figure 5a:** The X-ray diffraction pattern of amorphous HA coating after 4 weeks incubation in SBF at 37° C. (\* = HA peaks)



**Figure 5b:** The X-ray diffraction pattern of heat-treated HA coating after 4 weeks incubation in SBF at 37° C. (\* = HA peaks)



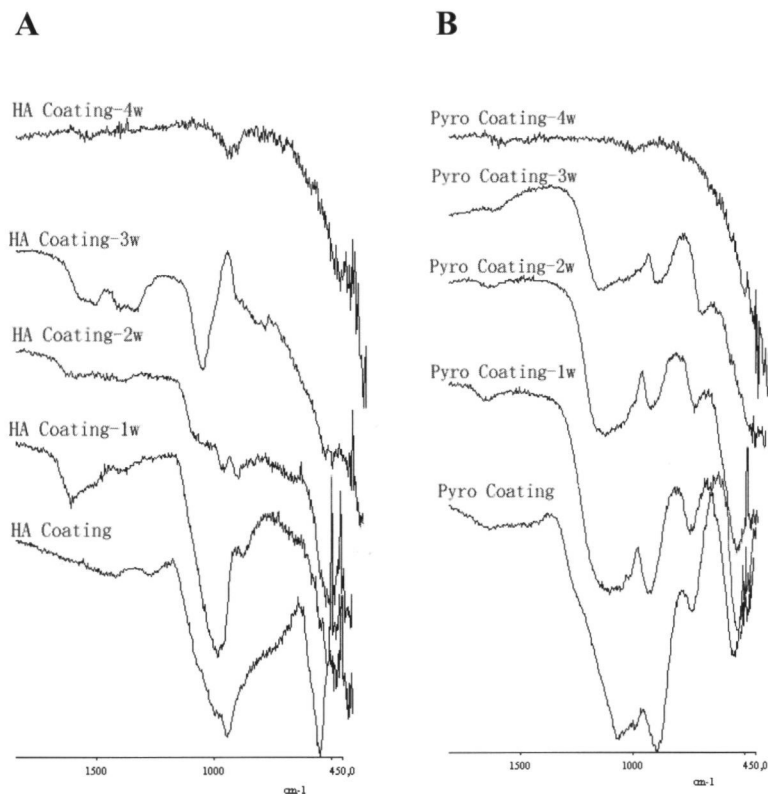
**Figure 5c:** The X-ray diffraction pattern of amorphous pyrophosphate coating after 4 weeks incubation in SBF at  $37^\circ\text{C}$ . (^ = substrate peaks)



**Figure 5d:** The X-ray diffraction pattern of amorphous HA coating after 4 weeks incubation in SBF at  $37^\circ\text{C}$ . (# = Pyro, \* = HA, + = TCP, and ^ = substrate peaks)

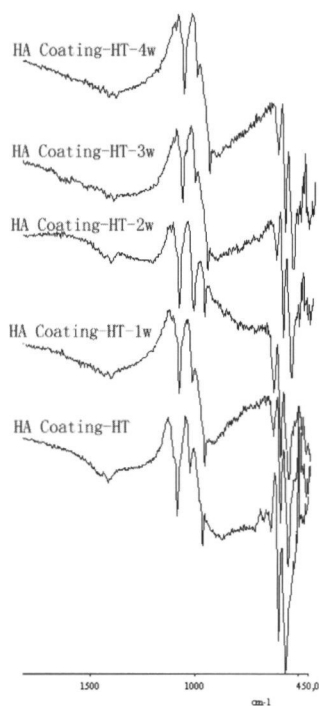
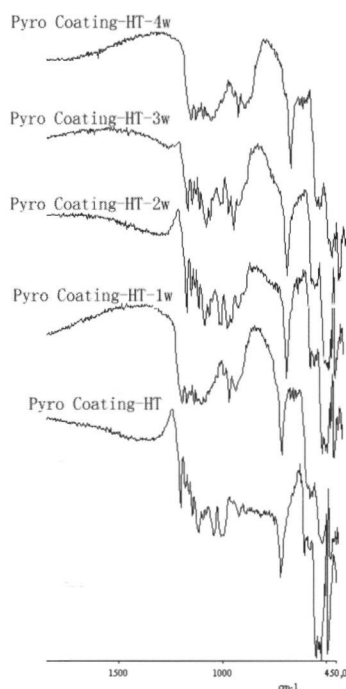
### **Fourier transform infrared spectroscopy**

FTIR spectra confirmed the partial dissolution of both amorphous HA and Pyro coatings, which was characterized by the disappearance of PO-bonds around  $700\text{ cm}^{-1}$  for amorphous HA coatings at 4 weeks of incubation and around  $1000\text{--}1100\text{ cm}^{-1}$  for amorphous Pyro coatings at 3 weeks of incubation (Figure 6A and 6B). For the heat-treated HA and heat treated pyrophosphate coatings no significant changes were seen in the FTIR bands (Figure 6C and 6D).



**Figure 6a-b:**IR spectra of amorphous HA and pyrophosphate coatings after 4 weeks incubation in SBF at  $37^{\circ}\text{C}$ .



**C****D**

**Figure 6c-d:** IR spectra of heat-treated HA and pyrophosphate coatings after 4 weeks incubation in SBF at 37° C

### **Scanning electron microscopy**

SEM evaluation revealed no clear changes in coating surface morphology during the incubation in SBF (Figure 7). Only, occasionally drying artefacts were observed as characterized by the appearance of cracks in the coated layer (Figure 7H).

### **Energy dispersive spectroscopy**

EDS examination showed that the Ca/P ratio of the amorphous Pyro coatings increased during the 4 weeks of incubation, while the Ca/P ratio of the amorphous HA coatings decreased. The Ca/P ratio of the heat-treated pyrophosphate coatings showed a slight increase during incubation and the Ca/P ratio of the HA heat-treated coatings stayed the same (Table 2).

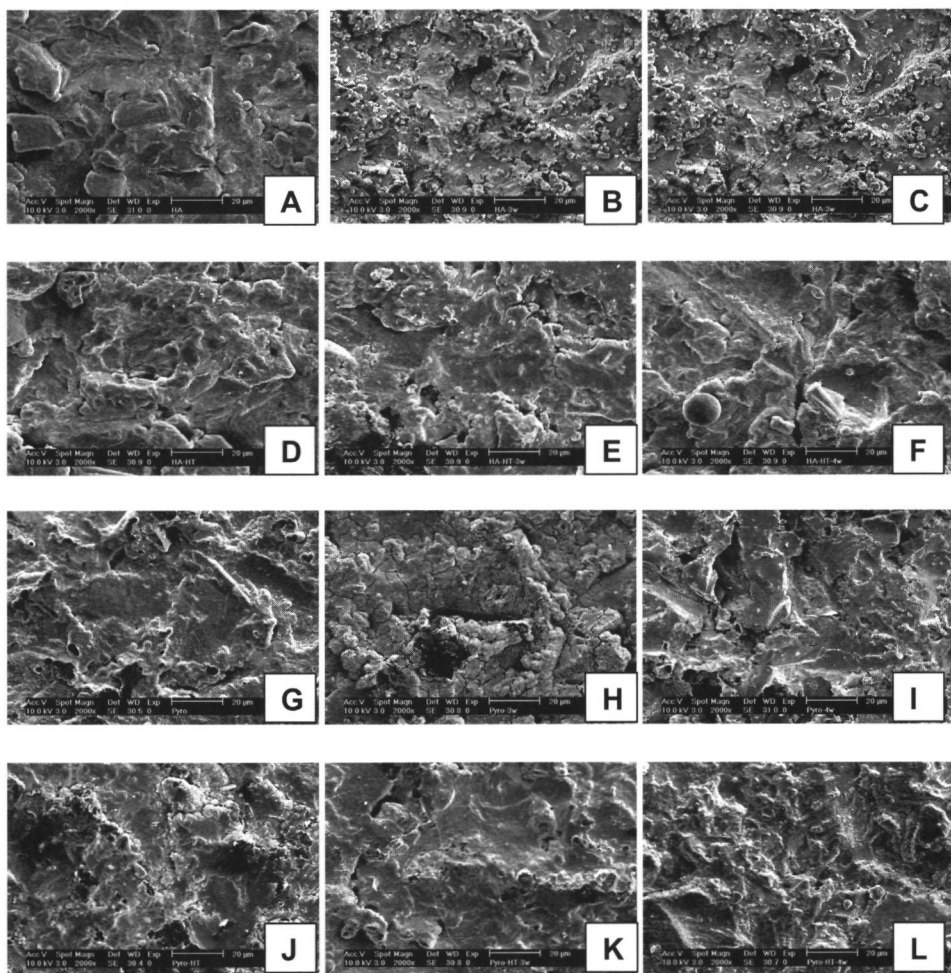


**Figure 7:** SEM graphs of as-sputtered and heat-treated coatings and after incubation in SBF; A = HA coating, B = HA coating 3 wk in SBF, C = HA coating 4 wk in SBF, D = HA HT, E = HA HT 3 wk in SBF, F = HA HT 4 wk in SBF, G = Pyro coating, H = Pyro coating 3 wk in SBF, I = Pyro coating 4 wk in SBF, J = Pyro HT, K = Pyro HT 3 wk in SBF, L = Pyro HT 4 wk in SBF.

**Table 2:** EDS measurement Ca/P ratio of as sputtered CaP coatings in SBF

Week	HA	HA-HT	Pyro	Pyro-HT
0	1.98	2.01	0.76	0.78
1	1.90	1.93	1.06	0.80
2	1.56	1.93	1.02	0.86
3	1.67	2.06	1.23	0.86
4	1.15	1.99	1.24	0.92

## Discussion

The aim of this study was to investigate the applicability of RF magnetron sputter sputtering for the production of calcium pyrophosphate coatings on titanium substrates. The results demonstrated that it is possible to deposit a dense, adherent calcium pyrophosphate coating by choosing the appropriate deposition parameters.

XRD analysis demonstrated that the as deposited CaP coatings had an amorphous structure. The post heat treatment induced the crystal growth within the coatings, resulting in a crystalline structure. Further for the pyrophosphate coatings, the post heat treatment resulted in an increase of thickness of the TiO<sub>2</sub> layer. This increase is not considered to be a disadvantage for the long-term bone response. It has already reported that the growth of the titanium oxide layer can even enhance the bonding to bone [22].

XRD revealed that different crystal phases could be obtained after heat treatment of the amorphous CaP coatings with IR-irradiation, depending on the temperature during heating. Heat treatment below 650° C did not result in crystallization of amorphous pyrophosphate coatings. Under these conditions only the amorphous HA coating transformed into a crystalline apatite structure. However, after heat treatment at temperature of 650° C, the amorphous pyrophosphate coating changed into a crystalline  $\beta$ -Ca<sub>2</sub>P<sub>2</sub>O<sub>7</sub> structure. The reason for this difference in crystallization behavior is not completely clear yet; we assume that the activation energy for the crystallization of apatite coatings is lower then for the pyrophosphate coatings. Unfortunately, at the moment no scientific data are available to confirm this theory. Nevertheless, our results confirmed again that IR-irradiation is an excellent method to crystallize thin amorphous calcium phosphate coating in a fast and reproducible way.

SEM examination showed that all as-sputtered and heat-treated coatings had a homogeneous and dense structure. Additional EDS measurements proved that the Ca/P ratio of the magnetron sputtered coatings as used in this study was higher than the theoretical value for HA, i.e. 2.0 instead of 1.67. For the pyrophosphate coatings, the Ca/P ratio was found to be lower than theoretical value, i.e. 0.76 instead of 1.0. Concerning the high Ca/P ratio of the HA, several studies have been published where preferential sputtering of calcium was

observed, probably due to the possibility of the phosphorus ions being pumped away before they are deposited on the substrate [23]. Besides, surface effects during the sputtering process and sputtering power are also important parameters that can affect the final Ca/P ratio of sputtered coatings [24]. An explanation for the decrease in Ca/P ratio of the pyrophosphate is the structure of the pyrophosphate anion. It has been described that pyrophosphates have a great tendency to occur in polymorphic phases and to consist of two  $\text{PO}_4$  tetrahedral bridged by a mutual oxygen atom [25]. Consequently, we can assume that the possibility of pyrophosphate ions being pumped away during sputtering is very low, due to the complex structure as compared to the orthophosphate anion. Further, it has to be noticed that  $\text{PO}_4$  reaches the substrate surface easier and is much more volatile than Ca ions [25].

In addition to structural changes, the solubility of the various types coatings was investigated during incubation in simulated body fluid. A partial dissolution of the amorphous HA and Pyro coatings was observed characterized by the disappearance of the PO-bonds around  $700\text{ cm}^{-1}$  in the IR spectra. In contrast, all heat-treated sputter coatings were observed to be stable under the test conditions. No dissolution or precipitate deposition was seen. These results corroborate with earlier studies [26], in which it was also shown that as-deposited calcium phosphate coatings were amorphous and dissolved in SBF solution with the same ionic concentrations as human blood plasma, but without any organic additives. However, heat-treated CaP coatings remained intact when immersed in SBF and showed no formation of a CaP precipitate. Only immersion of heat-treated specimens in SBF with increased ionic concentrations, so-called  $\text{SBF}_x$  with  $x > 1.4$ , resulted in the formation of a precipitate.

The EDS measurements demonstrated that incubation of the amorphous coatings in SBF had an effect on the Ca/P ratio, i.e. pyrophosphate coatings surface showed an increase in Ca/P ratio from 0.76 to 1.24, while the Ca/P ratio of the HA coatings decreased from 1.98 to 1.15 during incubation. This indicates again that a sputter coated amorphous Ca/P film easily dissolves and exchanges in SBF, resulting in a change in Ca/P ratio. This in contrast to heat-treated coatings, which are stable and hardly change in Ca/P ratio. Evidently, the dissolution is determined by the crystallinity of the deposited coatings, which is also in agreement with earlier findings using the same medium [29]

## **Conclusion**

Based on the results of this study, it can be concluded that magnetron sputtering can be successfully used to deposit pyrophosphate coatings on metal substrates. Homogeneous and dense coating morphologies were obtained. All the as-sputtered coatings were amorphous and after IR-irradiation the coatings altered into a crystalline phase. The activation energy for the crystallization of amorphous pyrophosphate coating is higher as compared to amorphous hydroxylapatite coating. The amorphous coatings were instable in the simulated body fluid and dissolved partially within 4 weeks of incubation. All heat-treated coatings appeared to be stable in simulated body fluid. These results suggest that magnetron sputtering of calcium

pyrophosphate coating is a promising method for deposition of a bioceramic coating. Of course, the final bone biocompatibility of these coatings has to be proven in follow-up cell culture and experimental animal studies.

## References

- 1] de Groot K, Klein CPAT, Wolke JGC, de Blicck-Hogervorst JMA. In. Handbook of bioactive ceramics. Vol. 2, Yamamuro T, Lhench L, and Wilson J (eds). CRC Press, Boca Raton, FL 1990:p3.
- 2] de Groot K, Geesink R, Klein CPAT, Serclian P. Plasma sprayed coatings of hydroxyapatite. *J Biomed Mater Res* 1987;21:1375-81.
- 3] Barthell HL, Archuleta TA, Kossowsky R. Ion beam deposition of calcium hydroxyapatite. *Mater Res Soc Symp Proc.* 1989;110:709-15
- 4] Oguchi H, Ishikawa K, Ojima S, Hirayama Y, Seto K, Eguchi G. Evaluation of a high velocity flame spraying technique for hydroxy apatite. *Biomaterials* 1992;13:471-77
- 5] Ducheyne P, Radin S, Heughebaert M, Heughebaert JC. Calcium phosphate ceramic coatings on porous titanium effect of structure and composition on electrophoretic deposition, vacuum sintering and in vitro dissolution *Biomaterials.* 1990;11:244-54.
- 6] Rajiv K, Singh F, Qian F, Nagabushnam V, Dammodaran R, Moudgil BM. Excimer laser deposition of hydroxyapatite thin films. *Biomaterials.* 1994;15:522-28
- 7] Cotell CM, Chnsey DB, Grabowski K S, Sprague JA Pulsed laser deposition of hydroxyapatite thin films on Ti-6Al-4V. *J Appl Biomater* 1992;2:87-93.
- 8] Yoshinari M, Ohtsuka Y, Derand T, Thin hydroxyapatite coating produced by ion beam dynamic mixing method. *Biomaterials* 1994;15: 29-535
- 9] Wolke JGC, de Blicck-Hogervorst JMA, Dhert WJA, Klein CPAT, de Groot K. Studies on thermal spraying of apatite bioceramics. *J Therm Spray Tech.* 1992;1 79-90.
- 10] Jansen JA, Wolke JGC, Swann S, van der Waerden JPCM, de Groot K. Application of magnetron sputtering for producing ceramic coatings on implant materials *Clin Oral Impl Res.* 1993;4:28-34
- 11] Dyk K, Schaeken HG, Wolke JGC, Jansen JA. Influence of annealing temperature on RF magnetron sputtered calcium phosphate coatings *Biomaterials* 1996;17:405-10
- 12] Dijk K, Schaeken HG, Wolke JGC, Maree CHM, Habraken FHPM, Verhoeven J, Jansen JA. Influence of discharge power level on the properties of hydroxyapatite films deposited on Ti6Al4V with RF magnetron sputtering. *J Biomed Mat Res.* 1995;29:269-76
- 13] Yoshinari M, Hayakawa T, Wolke JGC, Nemoto K, Jansen JA Influence of rapid heating with infrared radiation on RF magnetron-sputtered calcium phosphate coatings. *J Biomed Mater Res* 1997;37:60-7.
- 14] Kasuga T, Nogami M, Niinomi M Preparation of bioactive calcium pyrophosphate glass-ceramics. *J Mater Sci Lett* 2001;20:1249-51.
- 15] Brown WE, Eidelman N, Tomazic B. Octacalcium phosphate a precursor in biomineral formation. *Adv Dent Res.* 1987;1:306-13.
- 16] Nordström EG, Niemi L, Miettinen J. Reaction of bone to HA, carbonate-HA, hydroxyapatite + calcium orthophosphate and to hydroxyapatite + calcium ortho- and pyrophosphate. *Biom Mat and Engin.* 1992;2:115-22.
- 17] Cheung HS, Story MT, McCarty DJ Mitogenic effects of hydroxyapatite and calcium pyrophosphate dihydrate crystals on cultured mammalian cells *Arthritis Rheum.* 1984;27:668-74
- 18] Kamakura S, Sasano Y, Shimizu T, Hatori K, Suzuki O, Kagayama M, Motegi K Implanted octacalcium phosphate is more resorbable than  $\beta$ -tricalcium phosphate and hydroxyapatite. *J Biomed Mater Res.* 2002;59:29-34.
- 19] Kamakura S, Sasano Y, Homma H, Suzuki O, Ohki H, Kagayama M, Motegi K. Implantation of octacalcium phosphate (OCP) in rat skull defects enhances bone repair. *J Dent Res.* 1999;78 1682-87.
- 20] Fleisch H. Bisphosphonates: Pharmacology and use in the treatment of tumour-induced hypercalcaemic and metastatic bone disease. *Drugs.* 1991;42:919-44.
- 21] Ott, SM. Clinical effects of bisphosphonates in involutional osteoporosis *J Bone Miner Res.* 1993;8:597-606.

- 22]Kitsugi T, Nakamura T, Oka M, Yan W, Goto T, Shibuya T, Kokubo T, Miyaji S Bone bonding behavior of titanium and its alloy when coated with titanium oxide ( $\text{TiO}_2$ ) and titanium silicate ( $\text{Ti}_4\text{Si}_3$ ). *J Biomed Mater Res* 1996;32:149-56.
- 23]Yamashita K, Arashi T, Kitagaki K, Yamasa S, Umegaki T Preparation of apatite thin films through rf-sputtering from calcium phosphate glasses. *J Am Ceram Soc.* 1994,77:2401-7.
- 24]Yang Y, Kim KH, Ong JL. A review on calciumphosphate coatings produced using a sputtering process - an alternative to plasma spraying. *Biomaterials.* 2005;26:327-37.
- 25]Toy ADF. Phosphorus, chapter 20. In comprehensive inorganic chemistry. Bailer JC, Emeleus HJ, Nyholm R, Trotman-Dickenson AF (eds). Pergamon Press Oxford, 1973;2:509-14.
- 26]van der Wal E, Wolke JGC, Jansen JA, Vredenberg AM. Initial reactivity of RF magnetron sputtered calcium phosphate thin films in simulated body fluids *App Surf Sc* Accepted Sept 2004.
- 27]Wolke JGC, de Groot K, Jansen JA. In vivo dissolution behavior of various RF magnetron sputtered Ca-P coatings *J Biomed Mater Res.* 1998;39:524-30.





## **Chapter 3**

### **The influence of discharge power and heat treatment on calcium phosphate coatings prepared by RF magnetron sputtering deposition.**

Submitted: Biomaterials, 2005

Yan Yonggang, J. G.C. Wolke, Li Yubao, J.A. Jansen

## Introduction

In the biomedical field, coatings are frequently applied onto the surface of metallic dental and orthopedic implants in order to improve their biological performance. Because of its similarity to the inorganic component of bone and teeth, calcium phosphate (CaP) ceramics are considered as a suitable class of materials for use as such a surface coating [1]. Therefore, CaP coatings on metallic substrates have been developed, which are currently used in loaded situations, like total joint replacements and dental root implants. In this way the mechanical strength of titanium and the biocompatibility of CaP are combined [2].

As demonstrated in various publications, CaP coatings show a favorable bone response compared with non-coated titanium implants. At the moment, various techniques are available for the deposition of calcium phosphate on metal implants [3-11]. Over the past few years, we have made use of an RF magnetron sputter coating technique to produce thin adherent CaP coatings on implants. The results showed that the deposited films had a good biological response, both in vitro and in vivo. The osteogenic capacity of CaP was shown to be dependent on the physicochemical properties, such as the coating composition, coating crystal as well as molecular structure and coating crystallinity. [12-19]. However, the final bone response can also be influenced by the structural arrangement of calcium phosphate ceramics, and besides HA other calcium phosphate ceramics like dicalcium phosphate and pyrophosphate play a role in the mechanism for the formation of a carbonated-apatite deposit. The capacity of biomaterials to initiate the formation of a carbonated-apatite layer is indicative for their bioactivity [20-23].

In view of the above mentioned, previous studies in our laboratory demonstrated that the dissolution behavior in simulated body fluid (SBF) of RF magnetron sputtered dicalcium pyrophosphate (DCPP) coatings was similar as compared to HA coatings. Further, rat bone marrow stromal cells proliferated and differentiated only on crystalline magnetron sputtered DCPP as well as HA coatings, while crystalline HA coatings induced an earlier osteogenic effect than the crystalline DCPP coatings [24]. Despite these favorable results, it has to be noticed that the physicochemical evaluation of pyrophosphate coatings is not as well studied as those of calcium phosphate coatings. Especially, investigations of mixtures of both materials are scarce.

Therefore, the objective of the present study was to characterize the physicochemical properties of dicalcium pyrophosphate and hydroxylapatite coatings obtained by RF magnetron sputtering.

## **Materials and Methods**

### ***Ca-P coating deposition***

For the experiments commercially pure titanium (cpTi) disc were provided with various Ca-P sputter coatings. The discs measured 1mm in thickness and had a diameter of 12 mm. All discs were Al<sub>2</sub>O<sub>3</sub>-blasted on one side.

RF magnetron sputter coatings were made by using a commercially available RF sputter deposition system provided with two separate targets (Edwards ESM 100). The target materials were dicalcium pyrophosphate ( $\beta$ -Ca<sub>2</sub>P<sub>2</sub>O<sub>7</sub>) and hydroxylapatite (Ca<sub>5</sub>(PO<sub>4</sub>)<sub>3</sub>OH) granules (diameter 0.5-1.0mm). The test specimens were mounted on a rotating and water-cooled substrate holder. The distance between target and substrate was 80 mm. Before sputtering the metal substrates were cleaned by etching for 10 min with argon ions. During deposition, the argon pressure was kept at  $5 \times 10^{-3}$  mbar. The composition of the target materials were characterized after sputtering by energy dispersive spectroscopy (Table 1).

In total five coating groups were prepared:

- 1 HA; at a discharge power of 400W for both targets;
2. mixture HA/Pyro; at a discharge power of 600W for the HA target and 200W for DCP target;
3. mixture HA/Pyro; at a discharge power of resp. 400W and 400W;
4. mixture HA/Pyro; at a discharge power of resp. 200W and 600W;
5. Pyro; at a discharge power of 400W for both targets.

Coating thicknesses of 2 $\mu$ m were produced and the deposition rate for Pyro and HA was analyzed with a step measurement. The results are listed in Table 2.

After deposition, half of the coated specimens were subjected to an additional infrared heat treatment (HT) for 30 sec at 550, 650 and 750°C (Quad Ellipse Chamber, Model E4-10-P, Research Inc.).

Before and after annealing, coatings were characterized as follows:

- The crystallographic structure of each film was determined by thin film X-ray diffraction (XRD) using a Philips  $\theta$ -2 $\theta$  diffractometer using a CuK $\alpha$  -radiation;
- The infrared spectra of the films on the substrates were obtained by reflection Fourier transform infrared spectroscopy (FTIR)(Perkin-Elmer);
- The surface topology of the films was examined using scanning electron microscopy (SEM) using a Jeol JSM-35.

The elemental composition of the films was determined with an energy dispersive spectroscopy (EDS). Repetitive measurements at different locations on the coating surface were performed.

**Table 1** Ca/P ratio of the target material after sputtering of the Ca-P coatings

	Ca/P ratio Surface	Ca/P ratio Starting material
HA	1.1	1.67
Pyro	1.56	1.0

**Table 2** Deposition rate of the films deposited at different discharge power level on a rotated substrate holder

	200 W	400W	600W
HA (nm/h)	70	141	210
Pyro (nm/h)	68	140	208

## Results

### *X-ray diffraction*

The XRD patterns of the as-sputtered coatings showed an amorphous structure with no clear peaks, only the underlying substrate peaks were visible (Figure 1a-d)

At 550°C, the amorphous coating HA was transformed into a crystalline apatite structure with main reflection lines at (002), (211) and (112), which correspond to peaks at 25.9°, 31.9° and 32.4° (2-Theta). The amorphous HA/Pyro (600W/200W) changed into two crystalline phases, an apatite structure with peaks at 25.9°, 31.9° and 32.4° (2-Theta) and a beta-calcium pyrophosphate structure with peaks at 26.6°, 27.7° and 29.5° (2-Theta). HA/Pyro (400W/400W) coatings alter into three crystalline phases, an apatite structure with peaks at 25.9°, 31.9° and 32.4° (2-Theta), a beta-calcium pyrophosphate structure with peaks at 26.6°, 27.7° and 29.5° (2-Theta) and a beta-tricalcium phosphate structure with peaks at 25.9°, 27.7° and 31° (2-Theta). For the amorphous HA/Pyro (200W/600W) the formation of beta-calcium pyrophosphate could be detected, with peaks at 26.6°, 27.7° and 29.5° (2-Theta).

On the other hand, the Pyro coating remained unchanged and required a higher infrared heat-treatment to obtain crystallization (Figure 1a-d).

After heat treatment at 650°C, the heated HA, HA/Pyro (600W/200W), HA/Pyro (400W/400W) and HA/Pyro (200W/600W) coatings showed the same results as the coatings heated at 550°C, while the amorphous Pyro coatings changed into a crystalline beta-calcium pyrophosphate structure with reflection lines 201, 202, 008 and 212, which correspond to peaks at 26.6°, 27.7°, 29.5° and 30.7° (2-Theta). For all the coatings heated at 750°C the formation of TiO<sub>2</sub> with peaks at 27.6° and 36.0° (2-Theta) appeared, and also peaks developed around 27.7° and 31° during the heat treatment, which attributed to beta-TCP formation.

The X-ray diffraction data of all the heat-treated coatings are listed in Table 3.

**Table 3** The phase composition of the sputtered coatings at different discharge power ratio at different annealing temperature from XRD analysis

Discharge power	550°C	650°C	750°C
(HA:Pyro: w/w)			
2x 400: 0	HA	HA	HA+TCP+TiO <sub>2</sub>
600:200	HA+Pyro	HA+Pyro	HA+Pyro+TCP+TiO <sub>2</sub>
400:400	HA+Pyro+TCP	HA+Pyro+TCP	HA+TCP+ TiO <sub>2</sub>
200:600	Pyro	Pyro	Pyro+TCP+TiO <sub>2</sub>
0: 2x 400	-----	Pyro	Pyro+TCP+TiO <sub>2</sub>

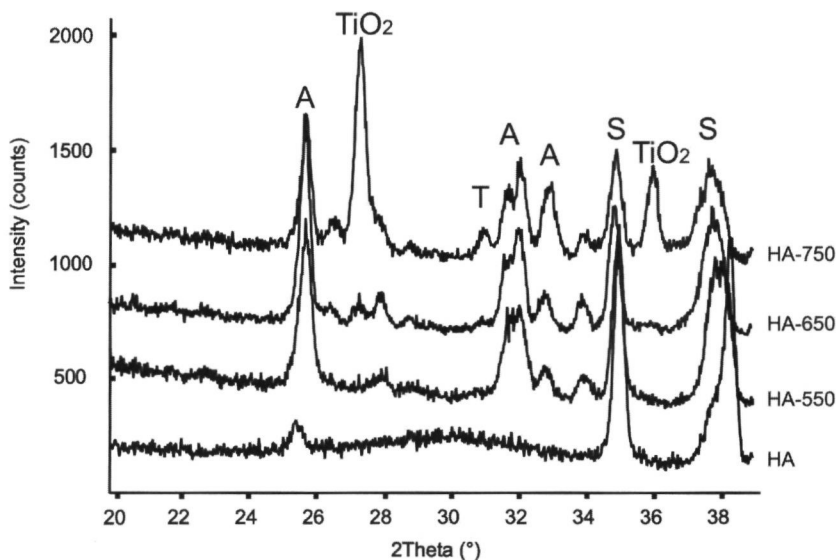


**Figure 1a:** XRD patterns of as-sputtered and heat-treated HA coatings, two target at a discharged power of 400W. (A: apatite, P: dicalcium pyrophosphate, T: beta-tricalcium phosphate, TiO<sub>2</sub>: titaniumoxide and S: titanium substrate).

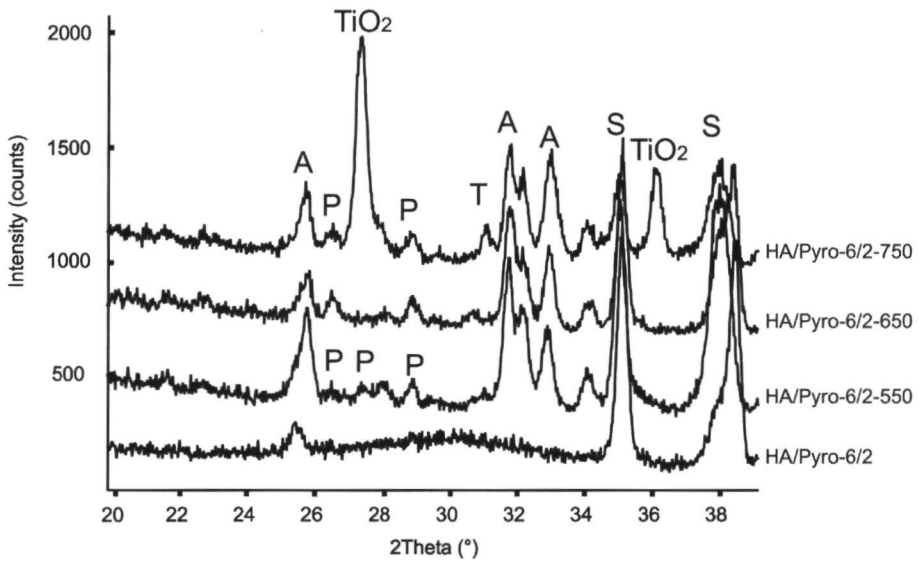


**Figure 1b:** XRD patterns of as-sputtered and heat-treated HA-Pyro coatings, at a discharged power of HA/Pyro= 600W/200W. (A: apatite, P: dicalcium pyrophosphate, T: beta-tricalcium phosphate, TiO<sub>2</sub>: titaniumoxide and S: titanium substrate).

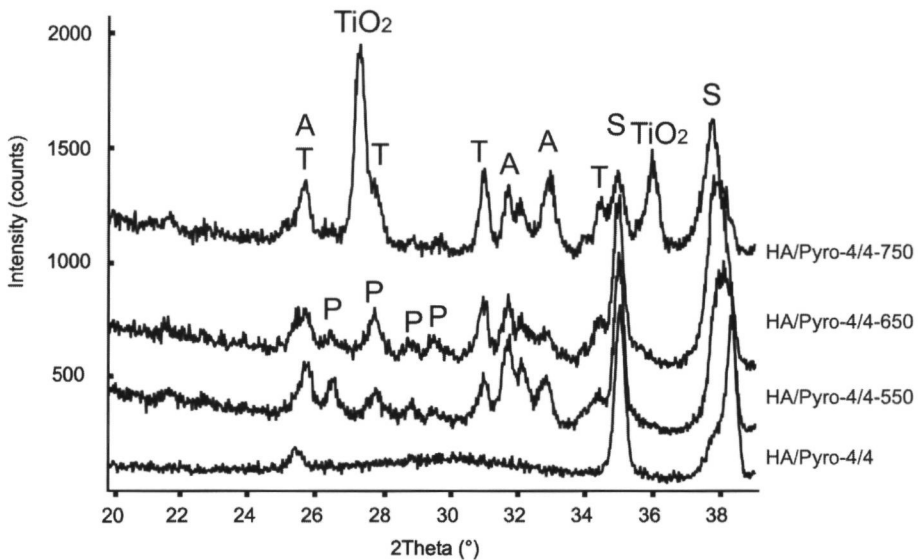


**Figure 1c:** XRD patterns of as-sputtered and heat-treated HA-Pyro coatings, at a discharged power of HA/Pyro= 400W/400W. (A: apatite, P: dicalcium pyrophosphate, T: beta-tricalcium phosphate, TiO<sub>2</sub>: titaniumoxide and S: titanium substrate).

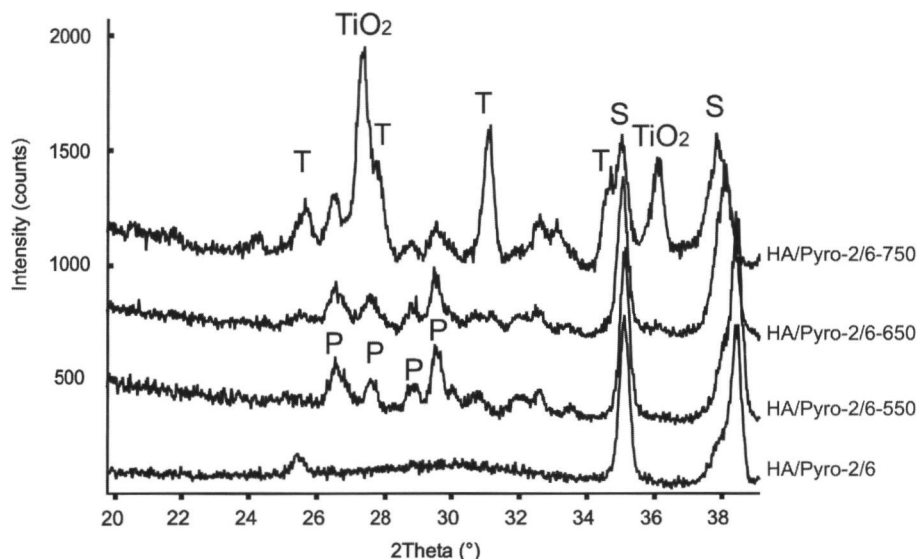


**Figure 1d:** XRD patterns of as-sputtered and heat-treated HA/Pyro coatings, at a discharged power of HA/Pyro= 200W/600W. (P: dicalcium pyrophosphate, T: beta-tricalcium phosphate, TiO<sub>2</sub>: titaniumoxide and S: titanium substrate).

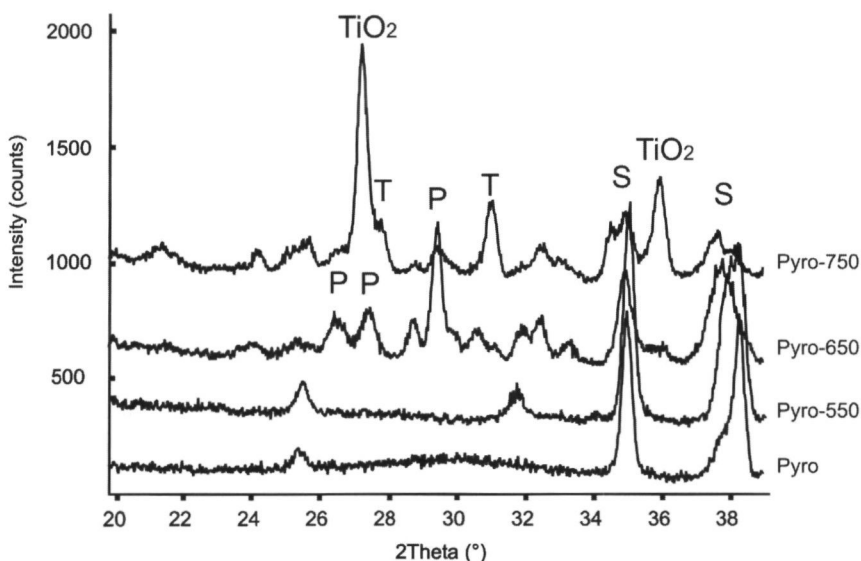


**Figure 1e:** XRD patterns of as-sputtered and heat-treated Pyro coatings, two target at a discharged power of 400W. (P: dicalcium pyrophosphate, T: beta-tricalcium phosphate, TiO<sub>2</sub>: titaniumoxide and S: titanium substrate).

## **FTIR spectroscopy**

### ***As-sputtered coatings***

FTIR measurements showed for all the amorphous coatings two clusters of bands from 900-1200 and from 500-600  $\text{cm}^{-1}$  attributed to the major absorption modes associated with the presence of phosphate (Figure 2a-d).

### ***Infrared heat-treatment at 550°C.***

FTIR of the HA and HA/Pyro (600W/200W) coatings resulted in the appearance of the hydroxyl band at 630  $\text{cm}^{-1}$ , characteristic for hydroxylapatite and the appearance of various P-O bonds at a wavelength of 567, 587, 965, 1009, 1083  $\text{cm}^{-1}$ . The spectrum of the heat treated HA/Pyro (400W/400W) and HA/Pyro (200W/600W) coatings revealed characteristics of a mixture of apatite and beta-calcium pyrophosphate phases with various P-O bonds at 567, 587, 965, 1009, 1083, 1095, 1125, 1163 and 1202  $\text{cm}^{-1}$ . The Pyro coatings resulted in the appearance of various P-O bonds at the wavelength around 567, 644, 965, 1009, 1083, 1095, 1125, 1163 and 1202  $\text{cm}^{-1}$ , which are characteristic for the beta-calcium pyrophosphate structure. [21]

### ***Infrared heat-treatment at 650°C.***

FTIR showed identical FTIR spectra as obtained after the heat treatment at 550°C.

### ***Infrared heat-treatment at 750°C.***

At this temperature only a change of the Pyro coating could be observed. The spectrum showed various P-O bonds at the wavelength around 551, 571, 596, 947 and 975  $\text{cm}^{-1}$ , which are characteristic for the beta-tricalcium phosphate.

## ***Scanning electron microscopy***

SEM examination showed that, besides the HA/Pyro (200W/600W) coating, all the other amorphous coatings resulted in a uniform coverage of the titanium substrate. In contrast, the HA/Pyro (200W/600W) had a different morphology, i.e. the surface crystals grew vertically on top of the coating. (Figure 3g).

SEM revealed that at 550°C no changes of the morphology of heated coatings were observed. On the other hand, at 650°C the HA/Pyro (200W/600W) and the Pyro coatings changed in morphology (Figure 3a-f). During the heat treatment the plate-like crystals of the HA/Pyro (200W/600W) coatings melted, resulting in a smooth appearance of the coating (Figure 3h). The surface morphology of the heated Pyro coating was characterized by a flat appearance with micropores and needle-like crystals due to the melting and recrystallization of the coating (Figure 3j). At 750°C, no further change in the morphology could be found.

EDS analysis of the different coatings are listed in Table 4.



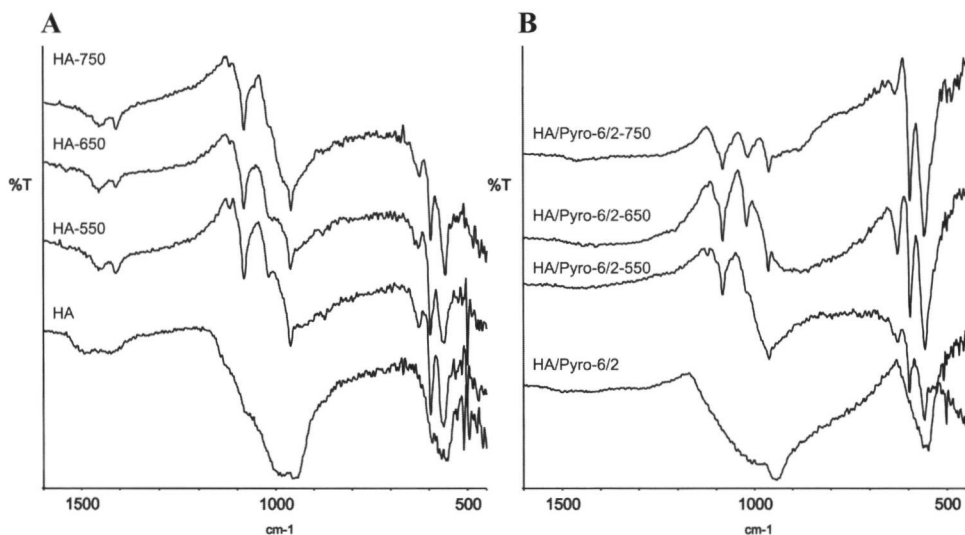


**Figure 2a-b:** IR spectra of as-sputtered and heat-treated Ha and Ha/Pyro coatings, (A) two target at a discharged power of 400W and (B) at a discharged power of HA/Pyro= 600W/200W.

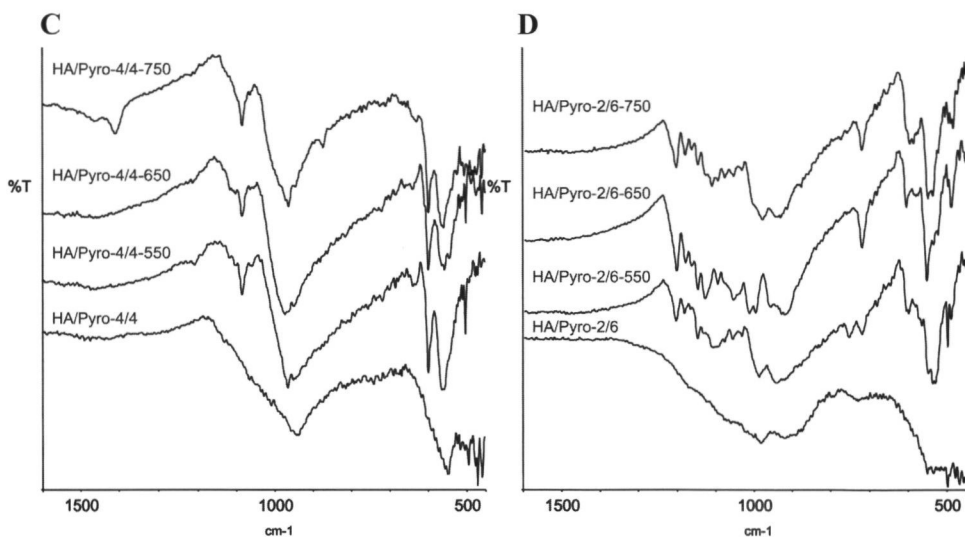


**Figure 2c-d:** IR spectra of as-sputtered and heat-treated Ha/Pyro coatings, (C) at a discharged power of HA/Pyro= 400W/400W and (D) at a discharged power of HA/Pyro= 200W/600W.

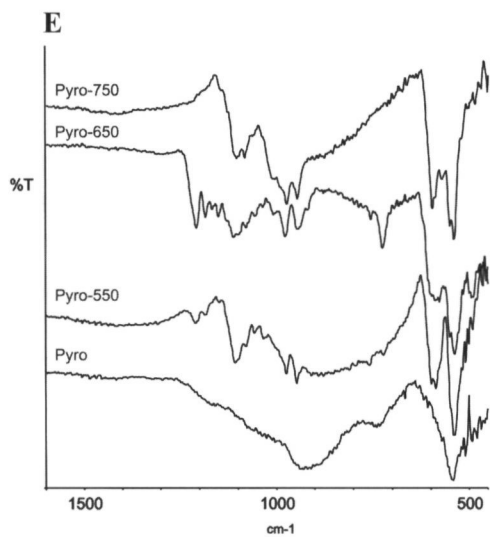
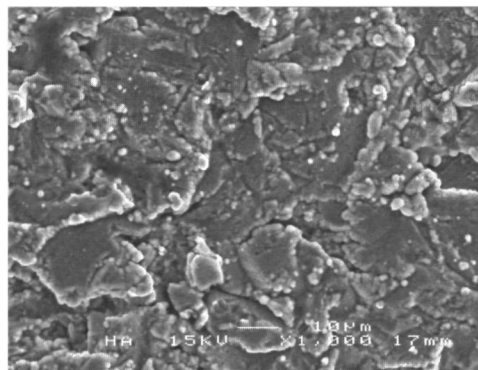
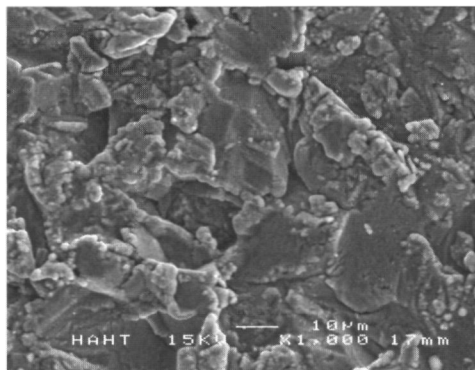


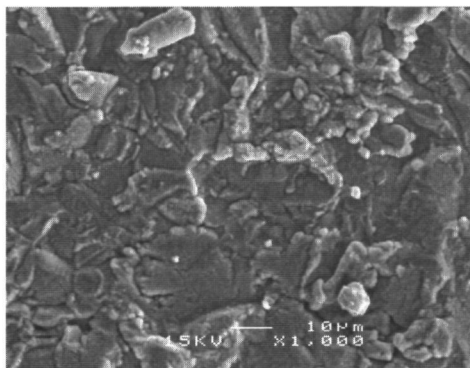
**Figure 2e:** IR spectra of as-sputtered and heat-treated Pyro coatings, two target at a discharged power of 400W.



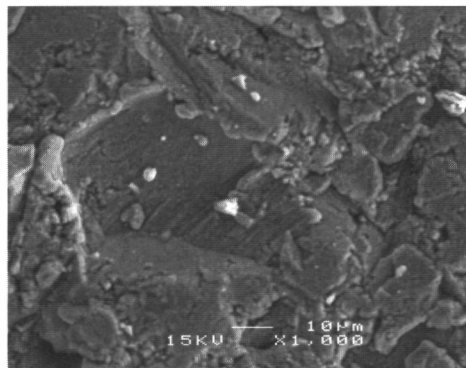
a: HA coating



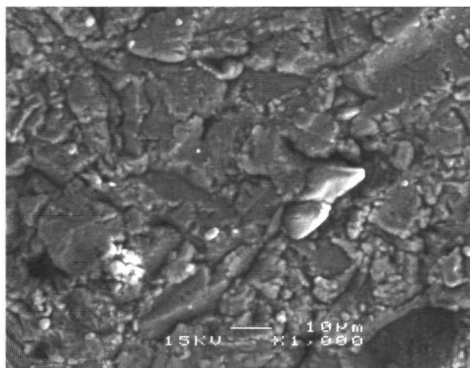
b: HA coating-HT



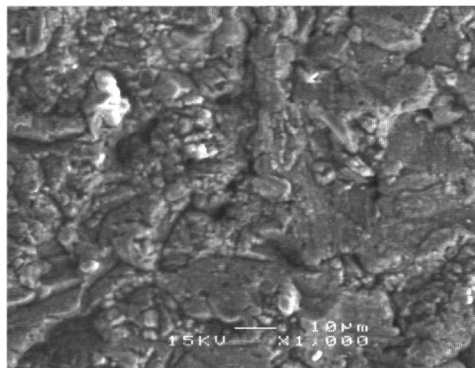
c: HA/Pyro=600W/200W coating



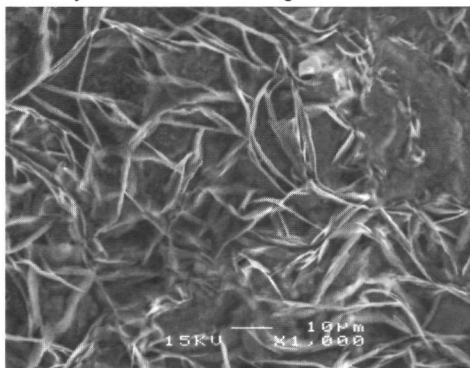
d: HA/Pyro=600W/200W coating-HT



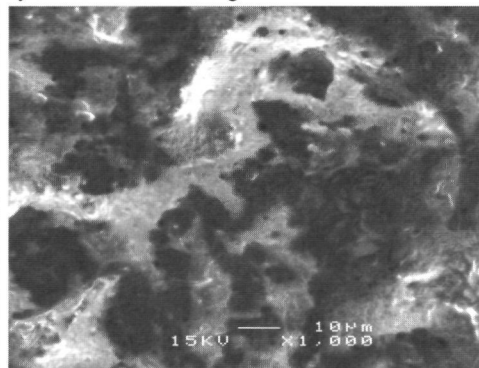
e: HA/Pyro=400W/400W coating



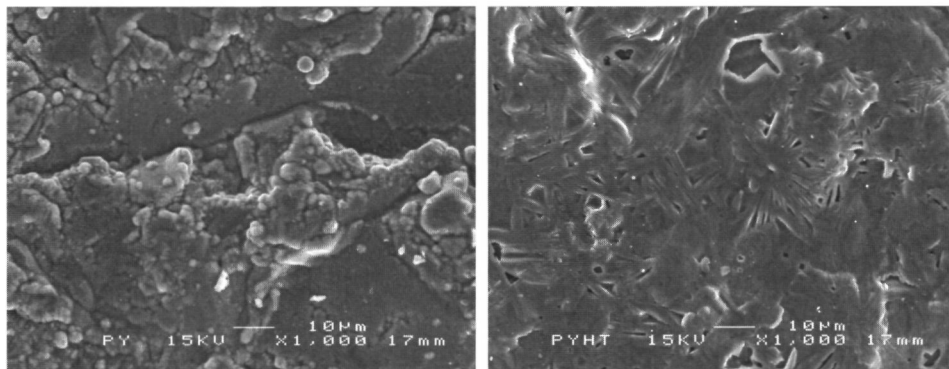
f: HA/Pyro=400W/400W coating-HT



g: HA/Pyro=200W/600W coating



h: HA/Pyro=200W/600W coating-HT



i: Pyro coating

j: Pyro coating -HT

**Figure 3a-j:** SEM micrographs of magnetron sputtered Ca-P coatings, as sputtered and heat-treated at 650°C. (1000x)

**Table 4** Ca/P ratio of all the sputtered and heat treated coatings

<b>Discharge power</b> (HA:Pyro: w/w)	<b>Ca/P</b> amorphous coating	<b>Ca/P heat treated</b> 550°C	<b>Ca/P heat treated</b> 650°C	<b>Ca/P heat treated</b> 750°C	<b>Calculated</b> Ca/P
2x 400: 0	2.00	2.00	2.01	2.10	1.67
600:200	1.82	1.84	1.82	1.85	1.50
400:400	1.51	1.53	1.49	1.55	1.34
200:600	0.55	0.57	0.56	0.88	1.17
0:2x 400	0.76	0.78	0.78	1.19	1.00

## Discussion

The aim of this study was to investigate the applicability of RF magnetron sputter sputtering for the production of mixtures of hydroxylapatite and calcium pyrophosphate coatings on titanium substrates. The results demonstrated that it is possible to deposit dense and adherent mixtures of hydroxylapatite and calcium pyrophosphate coatings by choosing the appropriate deposition parameters.

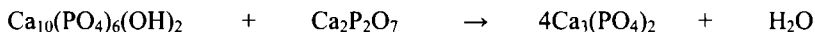
RF magnetron sputter deposition is a rather complex process to describe in physical parameters, especially when used to sputter multi-compounds like hydroxylapatite and pyrophosphate. There are, besides target composition, two main process parameters, which can be varied to influence the physical and chemical properties of the coating: working gas pressure and discharge power. In our study, we changed the discharge power and the Argon pressure was kept constant. In literature, there is discrepancy about the exact process of

building a layer. It is generally accepted that during the sputtering process the deposited layers are built up atom for atom or ion for ion. Although other researchers found that particles are ejected as a neutral and as a negatively charged particle, they suggested that Phosphorus and Calcium were ejected as neutral, while Oxygen was escaped from the target as a negative ion [25]. We observed that besides all the mentioned particles, also clusters of phosphate materials are sputtered. XRD revealed that a mixture of crystalline pyro and hydroxylapatite coatings (400W/400W) consisted of an apatite, beta-pyrophosphate and beta-tricalciumphosphate structure. The Ca/P ratio of this coating is 1.5, when a coating is built up from atoms or ions, the heat treatment of this coating will only result in the formation of a tricalcium phosphate. In this study, we found a mixture of several phases and therefore we assume that molecules and clusters of ortho- and pyrophosphate materials play an important role in building a calcium phosphate layer.

The EDS analysis showed that the Ca/P ratio of the sputtered coatings was higher than the theoretical values for HA and HA/Pyro (600W/200W and 400W/400W) coatings and lower for the HA/Pyro (200W/600W) and Pyro coatings. Concerning the high Ca/P ratio of the coatings, several studies have been published where preferential sputtering of calcium was observed, probably due to the possibility of the phosphorus ions being pumped away before they are deposited on the substrate [26]. An explanation for the decrease in Ca/P ratio of the other coatings is the structure of the pyrophosphate anion. It has been published that pyrophosphates have a great tendency to occur in polymorphic phases and to consist of two  $\text{PO}_4$  tetrahedral bridged by a mutual oxygen atom [27]. Consequently, we hypothesize that the possibility of pyrophosphate ions being pumped away during sputtering is very low, due to the complex structure as compared to the orthophosphate anion. Further, it has to be noticed that  $\text{PO}_4$  reaches the substrate surface easier and is much more volatile than Ca ions [28,29]. Also the impact of a particle with the target material may lead to structural rearrangements such as the introduction of interstitials or vacancies. It may also introduce lattice defects such as stoichiometry modifications. In our sputtering system, we observed a preferential sputtering of the outer layer of the target material, the Ca/P ratio of the pyrophosphate target increased in time from 1.0 to 1.56, while for the hydroxylapatite target material a decrease was found (1.67 to 1.1). It is clear that a cascade of events occurs during sputtering of calcium phosphate materials. As a result, the exact mechanism of how the sputtered layer is built up, is not completely understood. Therefore, research efforts in this area should have more attention.

Furthermore, the crystallization of the amorphous as sputtered coatings is depending on the temperature during infrared heating. At 650°C or higher the XRD all the amorphous coatings showed a crystalline structure. Further, the post heat treatment at 750°C resulted in an increase of thickness of the  $\text{TiO}_2$  layer. This increase is not considered to be a disadvantage for the long-term bone response. It has already been reported that the growth of the titanium oxide layer can even enhance the bonding to bone [30].

Finally, XRD analysis demonstrated that the mixing of HA and Pyro resulted in the formation of beta-tricalcium phosphate phase. From literature, it is known that apatite and pyrophosphate forms tricalcium phosphate around 650°C according to the following reaction [31].



It has been described that tricalcium phosphate is generally considered as a more resorbable biomaterial than dense hydroxylapatite and is used to overcome the low biodegradation of hydroxylapatite.

### Conclusion

Based on the results of this study, it can be concluded that magnetron sputtering can be successfully used to deposit dicalcium pyrophosphate and hydroxylapatite coatings on metal substrates. All the as-sputtered coatings were amorphous and after IR-irradiation the coatings altered into a crystalline phase. The crystallization temperature of amorphous pyrophosphate coating is higher as compared to amorphous hydroxylapatite coating. The obtained coatings had a Ca/P ratio varying from 0.55 to 2.0 and different phase compositions or mixtures of apatite, beta-pyrophosphate and beta-tricalciumphosphate structures were formed. The phase compositions of the sputtered coatings are determined not only by the discharged power ratio of the hydroxylapatite and dicalcium pyrophosphate target, but also by the annealing temperature. These results suggest that magnetron sputtering of mixtures of apatite and calcium pyrophosphate coating is a promising method for forming a ceramic coating.

## References

- 1] de Groot K., Klein CPAT, Wolke JGC, de Bleeck-Hogervorst JMA. In Handbook of bioactive Ceramics, 2. Yamamuro T, Lhench L, Wilson J (eds). CRC Press, Boca Raton, FL. 1990. p3.
- 2] Ramselaar MMA, Driessens FCM, Kalk W, de Wijn JD, van Mullen PJ. *J Mater Med.* 1991;2:63
- 3] de Groot K, Geesink R, Klein CPAT, Serclian P. Plasma sprayed coatings of hydroxylapatite. *J Biomed Mater. Res.* 1987;21:1375-81.
- 4] Barthell HL, Archuleta TA, Kossowsky R. *J Mater Res Soc Symp.* 1989;110:709-14.
- 5] Oguchi H, Ishikawa K, Ojima S, Hirayama Y, Seto K, Eguchi G. Evaluation of a high-velocity flame-spraying technique for hydroxyapatite. *Biomaterials.* 1992;13:471-77.
- 6] Ducheyne P, Radin S, Heughebaert M, Heughebaert JC. *Biomaterials.* 1990;11:244-54
- 7] Rajiv K, Singh K, Qian F, Nagabushnam V, Dammodaran R, Moudgil BM. Excimer laser deposition of hydroxyapatite thin films. *Biomaterials.* 1994;15:522-8
- 8] Cotell CM, Chrisey DB, Grabowski KS, Sprague JA. *Appl Biomater.* 1992;8:87-93.
- 9] Yoshinari M, Ohtsuka Y, Derand T. Thin hydroxyapatite coating produced by the ion beam dynamic mixing method. *Biomaterials.* 1994;7:529-35
- 10] Wolke JGC, de Bleeck-Hogervorst JMA, Dhert WJA, Klein CPAT, de Groot K. *J Therm Spray Techn.* 1992;1:75-82.
- 11] Jansen JA, Wolke JGC, Swann S, van der Waerden JPCM, de Groot K. Application of magnetron sputtering for producing ceramic coatings on implant materials. *Clin Oral Impl Res.* 1993;4:28-34
- 12] Kivrak N, Cuncy A. *J Am Ceram Soc.* 1998;81:2245-53.
- 13] Hardoun P, Chopin D, Devyver B, Flautre B, Blary MC, Guigui P, Anselme K. *J Mater Sci Med.* 1991;3:212-8
- 14] Kitsugi T, Yamamuro T, Nakamura T, Oka M. Transmission electron microscopy observations at the interface of bone and four types of calcium phosphate ceramics with different calcium/phosphorus molar ratios. *Biomaterials.* 1995;16:1101-7
- 15] Ryu HS, Youn HJ, Hong KS, Chang BS, Lee CK, Chung SS. An improvement in sintering property of  $\beta$ -tricalcium phosphate by addition of calcium pyrophosphate. *Biomaterials.* 2002;23:909-14.
- 16] Sun JS, Huang YC, Tsuang YH, Chen LT, Lin FH. Sintered dicalcium pyrophosphate increases bone mass in ovariectomized rats. *J Biomed Mat Res.* 2002;62:246-53
- 17] Ducheyne P, Radin S, King L. The effect of calcium phosphate ceramic composition and structure on in vitro behavior. I. Dissolution. *J Biomed Mater Res.* 1993;27:25-34.
- 18] Radin S, Ducheyne P. The effect of calcium phosphate ceramic composition and structure on in vitro behavior. II. Precipitation. *J Biomed Mater Res.* 1993;27:35-45.
- 19] Nordström EG, Niemi L, Miettinen J. Reaction of bone to HA, carbonate-HA, hydroxyapatite + calcium orthophosphate and to hydroxyapatite + calcium ortho- and pyrophosphate. *Biomed Mat Eng.* 1992;115-21.
- 20] Cheung HS, Story MT, McCarty DJ. Mitogenic effects of hydroxyapatite and calcium pyrophosphate dihydrate crystals on cultured mammalian cells. *Arthritis Rheum.* 1984;27:668-74.
- 21] Kamakura S, Sasano Y, Homma H, Suzuki O, Ohki H, Kagayama M, Motegi K. Implantation of octacalcium phosphate (OCP) in rat skull defects enhances bone repair. *J Dent Res.* 1999;78:1682-87.
- 22] van Dijk K, Schaeken HG, Wolke JGC, Maree CHM, Habraken FHPM, Verhoeven J, Jansen JA. Influence of discharge power level on the properties of hydroxyapatite films deposited on Ti6Al4V with RF magnetron sputtering. *J Biomed Mat Res.* 1995;29:269-76.
- 23] Yamashita K, Arashi T, Kitagaki K, Yamasa S, Umegaki T. *J Am Ceram Soc.* 1994;77:2401-2406
- 24] Yan Y, Wolke JGC, Yubao L, Jansen JA. *J Biomed Mater Res.* Accepted 2005.
- 25] Feddes B, Vredenberg AM, Wolke JGC, Jansen JA. *J Appl Phys.* 2003;93:662-670.
- 26] Zalm PC. Quantitative sputtering. In Handbook of ion beam processing technology. JJ Cuomo, SM

- Rossmagel, HR Kaufman (eds). Park Ridge, NJ; Noyes Publications;1989.78-111.
- 27] Toy ADF Phosphorus, chapter 20: In Comprehensive inorganic chemistry. Bailor JC, Emelcus HJ, Nyholm R, Trotman-Dickenson AF (eds). Pergamon Press, Oxford, 1973;2 509-14.
- 28] Fowler BO, Moreno EC, Brown WE Infra-red spectra of hydroxyapatite, octacalcium phosphate and pyrolysed octacalcium phosphate Arch Oral Bio 1966;11:477-92.
- 29] Schmitz JP, Hollinger JO, Milam SB. Reconstruction of bone using calcium phosphate bone cements: a critical review. J Oral Maxillofac Surg. 1999;57:1122-6.
- 30] Kitsugi T, Nakamura T, Oka M, Yan W, Goto T, Shibuya T, Kokubo T, Miyaji S. Bone bonding behavior of titanium and its alloy when coated with titanium oxide ( $\text{TiO}_2$ ) and titanium silicate ( $\text{Ti}_5\text{Si}_3$ ). J Biomed Mater Res. 1996;32 149-56
- 31] Kamakura S, Sasano Y, Shimizu T, Hatori K, Suzuki O, Kagayama M, Motegi K Implanted octacalcium phosphate is more resorbable than beta-tricalcium phosphate and hydroxyapatite. J Biomed Mater Res. 2002;59 29-34.



## **Chapter 4**

### **In vitro evaluation of different heat-treated RF magnetron sputtered calcium phosphate coatings**

Submitted: Biomaterials, 2005

Yan Yonggang, J. G.C. Wolke, Li Yubao, J.A. Jansen

## **Introduction**

With the advances in ceramics technology, many kinds of synthetic calcium phosphate (Ca-P) materials have been used as bone substitutes. These materials have been prepared and studied extensively *in vitro* and *in vivo* [1-3]. Beside hydroxylapatite (HA), a naturally occurring mineral and the predominant mineral component of vertebrate bone and tooth enamel, tricalcium phosphate (TCP) has also been widely used in the clinical applications [4, 5]. Although some materials used have been called "hydroxylapatite" by some investigators, they actually vary widely in composition with calcium/phosphorus ratios ranging from 2.0 to as low as 1.3. Therefore, it can be difficult to compare and rationalize the results of studies by different investigators with "hydroxylapatite" materials [6, 7]. The previous studies showed that except the calcium phosphate primary ( $\text{Ca}(\text{H}_2\text{PO}_4)_2$ ), which is too acidic, most other CaP ceramics are biocompatible [8-10]. Meanwhile bone responses to the implant surface are affected not only by the surface chemical compositions but also by the surface structure and morphological properties [11-14]. Usually HA is considered as the end product of the biological mineralization process, while dicalcium pyrophosphate (DCPP) with a formula of  $\text{Ca}_2\text{P}_2\text{O}_7$  is one of the intermediate products in this process [15]. Although many studies suggested that crystalline dicalcium pyrophosphate is biocompatible, little is known about DCPP coating properties *in vitro* and *in vivo*. On the other hand, due to their brittle nature the bulk Ca-P ceramics have been proposed to be applied as thin coatings on metallic substrates, resulting in implants that have the excellent biocompatible properties of calcium phosphate as well as the advantageous mechanical properties of metal [16, 17]. Previously our group investigated the use of radio frequency (RF) magnetron sputter deposition as a method of applying thin adherent calcium phosphate coatings to titanium implants [18-20]. The results have shown that both calcium pyrophosphate and hydroxylapatite films deposited are amorphous and change into a crystalline structure after heat treatments of either infrared or water steam [21]. The morphological properties and the compositions are different after these heat treatments, which can result in a different biological response. Consequently, the objective of the present study was to compare the response of different heat-treated Radio Frequent (RF) magnetron sputtered CaP surfaces in simulated body fluid (SBF) as well as the behavior of bone-like cells on these surfaces.

## Materials and Methods

### *Ca-P coating deposition*

Ca-P sputter coatings were applied onto commercially pure titanium (cpTi) discs. The discs were cut from cpTi rods with a diameter of 12 mm and a thickness of 1 mm. The discs were then subjected to an aluminium oxide grit blasting procedure and subsequently cleaned with ethyl alcohol rinses. The final roughness (Ra)-value of the surfaces was 1-1.3  $\mu\text{m}$ . The following coatings were provided on the discs with a commercially available RF sputter deposition system (Edwards ESM 100).

Calcium pyrophosphate with a thickness of 2  $\mu\text{m}$  (A-DCPP),

Hydroxyapatite with a thickness of 2  $\mu\text{m}$  (A-HA)

The target materials were calcium pyrophosphate ( $\beta\text{-Ca}_2\text{P}_2\text{O}_7$ ) and hydroxylapatite ( $\text{Ca}_5(\text{PO}_4)_3\text{OH}$ ) granules (diameter 0.5-1.0 mm). The test specimens were mounted on a rotating and water-cooled substrate holder. The target to substrate distance was 80 mm. Before sputtering the metal substrates were cleaned by etching for 10 min with argon ions. During deposition, the argon pressure was kept at  $5 \times 10^{-3}$  mbar and the sputter power was 400 W.

After deposition, one third of the coated specimens were subjected to an additional infrared heat treatment for 30 sec, the HA coatings were heated at 550°C (I-HA) and the DCPD coatings at 650°C (I-DCPD) (Quad Ellipse Chamber, Model E4-10-P, Research Inc.). The other one third of the coated specimens were heated at 140°C and 0.4 MPa in water steam, the HA coatings for 8 hours (S-HA) and the DCPD coatings for 16 hours (S-DCPD).

Before and after the different heat treatments the deposited films were characterized using the following techniques.

The crystallographic structure of each film was determined by thin film X-ray diffraction (XRD) using a Philips  $\theta$ - $2\theta$  diffractometer using a  $\text{CuK}\alpha$  -radiation. The infrared spectra of the films on the substrates were obtained by reflection Fourier transform infrared spectroscopy (FTIR) (Perkin-Elmer). The surface topology of the films was examined using scanning electron microscopy (SEM) using a Jeol JSM-35. The elemental composition of the films was determined with energy dispersive spectroscopy (EDS).

### *In vitro bioactivity assay*

Coated specimens were incubated in 4 ml Simulated Body Fluid buffer (SBF) with a pH of 7.2 at 37°C for 4 weeks (Table 1). For each treatment procedure, the experiment was performed in triplicate and SBF was refreshed once a week. At the end of the experiment, coated samples were retrieved out of the SBF solution. After rinsing in aqua and drying at room temperature, the specimens were characterized by using XRD, FTIR, SEM and EDS. For each sample, the Ca and P concentration in the solutions was determined in triplicate by ICP (Inductively Coupled Plasma).

**Table 1:** Composition of Simulated Body Fluid (SBF)

Ions	Na <sup>+</sup>	K <sup>+</sup>	Ca <sup>2+</sup>	Mg <sup>2+</sup>	Cl <sup>-</sup>	HCO <sub>3</sub> <sup>-</sup>	HPO <sub>4</sub> <sup>-</sup>	SO <sub>4</sub> <sup>2-</sup>
SBF	142.0	5.0	2.5	1.5	147.8	4.2	1.0	0.5
Blood Plasma	142.0	5.0	2.5	1.5	103.0	27.0	1.0	0.5

Buffered with tris(hydroxymethyl) aminomethane (50mM), set at pH 7.2 with 1.0N hydrochloric acid (Li 1993).

### ***Rat bone marrow cell assay***

Rat bone marrow (RBM) cells were isolated and cultured using the method described by Maniopoulos [22]. RBM cells were obtained from femora of male Wistar rats. Femora were washed 4 times in culture medium  $\alpha$ -MEM (Minimal Essential Medium; MEM Gibco BRL, Life Technologies B.V. Breda, The Netherlands) with 0.5-mg/ml gentamycin and 3  $\mu$ g/ml fungizone. Epiphyses were cut off and diaphyses flushed out with 15 ml culture medium  $\alpha$ -MEM, supplemented with 10 % FCS (foetal calf serum, Gibco), 50  $\mu$ g/ml ascorbic acid (Sigma, Chemical Co., St.Louis, MO, USA), 50  $\mu$ g/ml gentamycin, 10 mM Na  $\beta$ -glycerophosphate (Sigma) and  $10^{-8}$  M dexamethasone (Sigma). Cells were incubated in a humidified atmosphere of 95 % air, 5 % CO<sub>2</sub> at 37°C. The medium was changed every two or three days.

After 6 days of primary culture, cells were detached using trypsin/ EDTA (0.25% w/v trypsin/0.02% EDTA). The cells were concentrated by centrifugation at 1500 rpm for 5 min. and resuspended in a known amount of media (5 ml). Cells were counted by a Coulter® counter and resuspended in medium ( $2.0 \times 10^5$  cells/1000 $\mu$ l). The cell suspension was used for the seeding and culturing experiments.

Cells were presented to the various substrates in a cell suspension. The substrates were seeded with  $2.0 \times 10^4$  cells/1000 $\mu$ l). Substrates with cells were cultured in 24-wells plate for 8 and 16 days. The medium was changed every two or three days.

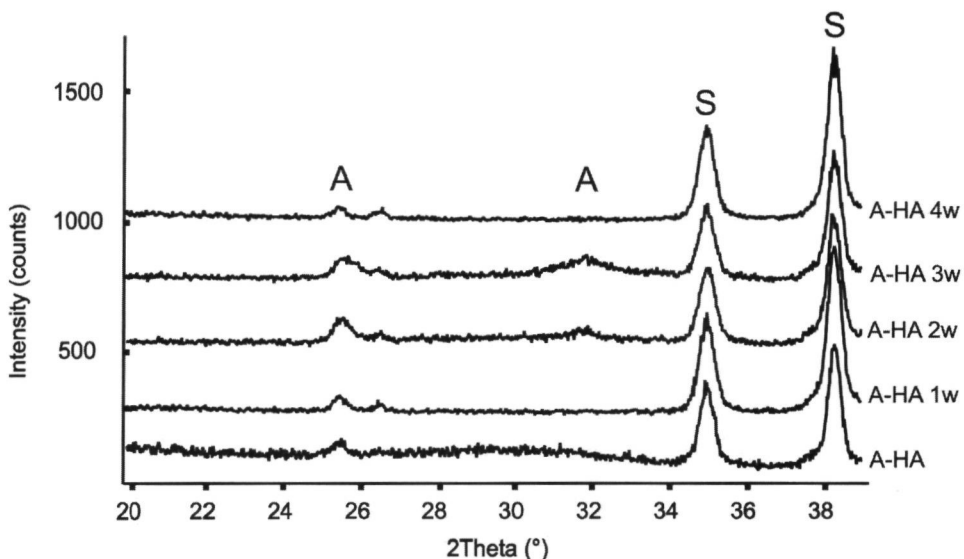
At the end of the incubation times, samples were taken out of the well-plates and washed twice with PBS. Subsequently, cells were fixed for 30 minutes in 2% glutaraldehyde, and then substrates were washed twice with 0.1 M sodium-cacodylate buffer (pH 7.4), dehydrated in a graded series of ethanol and dried by tetramethylsilane. The specimens were sputter-coated with gold and examined and photographed using a Jeol 6310 SEM at an acceleration voltage of 10kV.

## **Results**

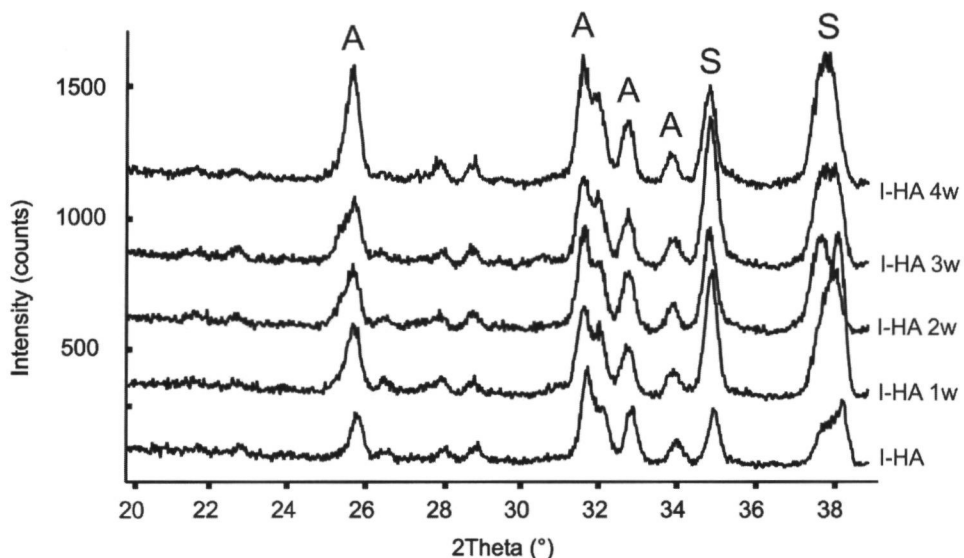
### ***Surface phase changes of the Ca-P sputtered coatings after incubation in SBF***

Figure 1 shows the XRD patterns of the sputtered coatings before and after incubation in SBF. As-sputtered HA coating heated at 550°C with infrared radiation showed a crystalline apatite structure with reflections at 002, 211, 112, 202, resp. 25.9°, 31.9°, 32.4° and 34.0° 2-

Theta, which is comparative with the XRD pattern of HA powder (JCPDS #09-0432). The sputtered amorphous pyrophosphate coating required an annealing temperature of 650°C to alter into crystalline beta-calcium pyrophosphate structure with reflection lines 201, 202, 008 and 212, which correspond to peaks at 26.6°, 27.7°, 29.5° and 30.7° in 2-Theta (JCPDS#09-0346). The four week incubation of A-HA coatings in SBF resulted in the formation of small peaks around 25.9°, 26.6°, 31-33°, indicating apatite formation (Figure 1a). In contrast, no peaks appeared for A-DCPP coatings during SBF incubation (Figure 1d). The I-HA and S-HA coatings showed a stable XRD pattern during the incubation (figure 1b, 1c). For the I-DCPP coatings, peaks appeared around 25.9°, 29° and 31°, which indicate the transformation of calcium pyrophosphate into a tricalciumphosphate (TCP) phase (Figure 1e). For the S-DCPP coatings, peaks developed around 27.7 and 31° during SBF incubation, which could be attributed to TCP formation (Figure 1f).



**Figure 1a:** XRD patterns of amorphous HA coating after 4 weeks incubation in SBF at 37° C. (A: apatite and S: titanium substrate).



**Figure 1b:** XRD patterns of infrared heat-treated HA coating after 4 weeks incubation in SBF at 37° C. (A: apatite and S: titanium substrate).

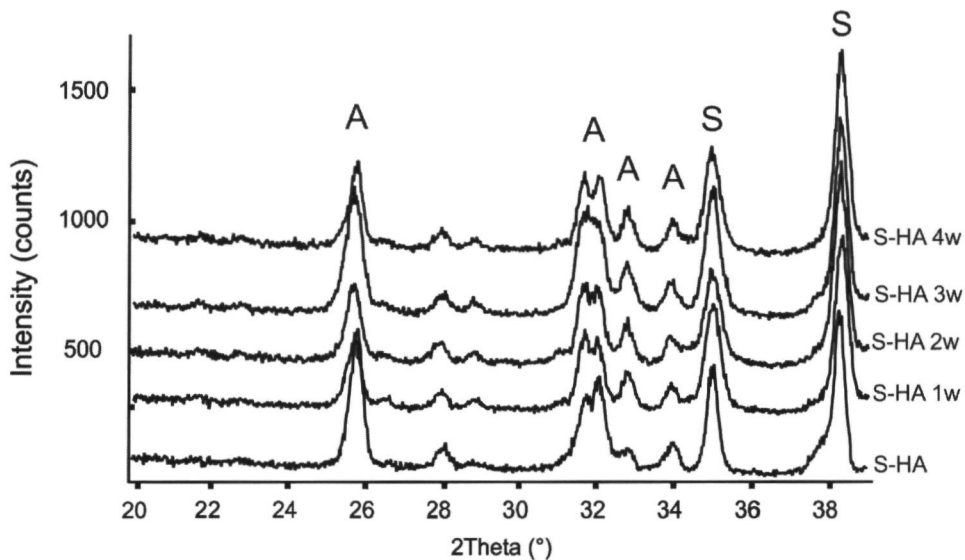


**Figure 1c:** XRD patterns of steam heat-treated HA coating after 4 weeks incubation in SBF at 37° C. (A: apatite and S: titanium substrate).

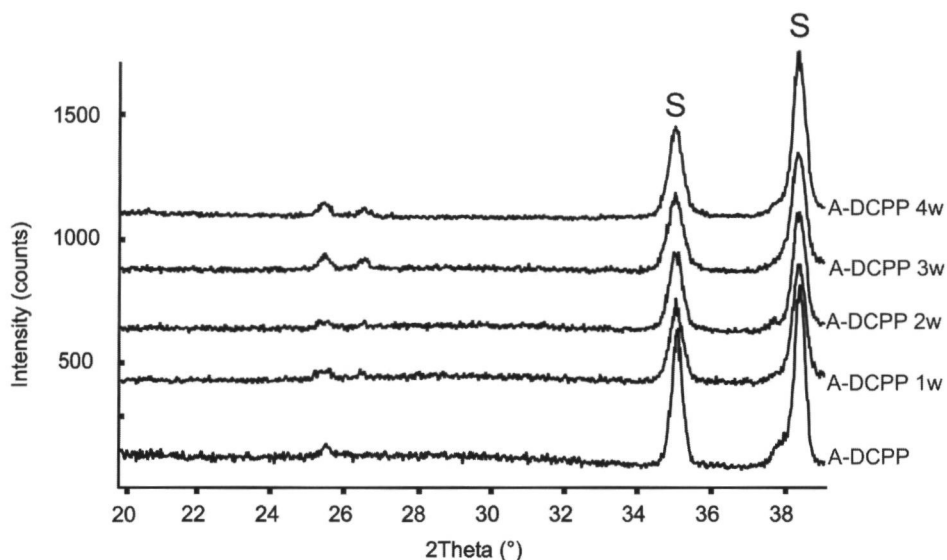


**Figure 1d:** XRD patterns of amorphous DCP coating after 4 weeks incubation in SBF at 37° C. (S: titanium substrate).

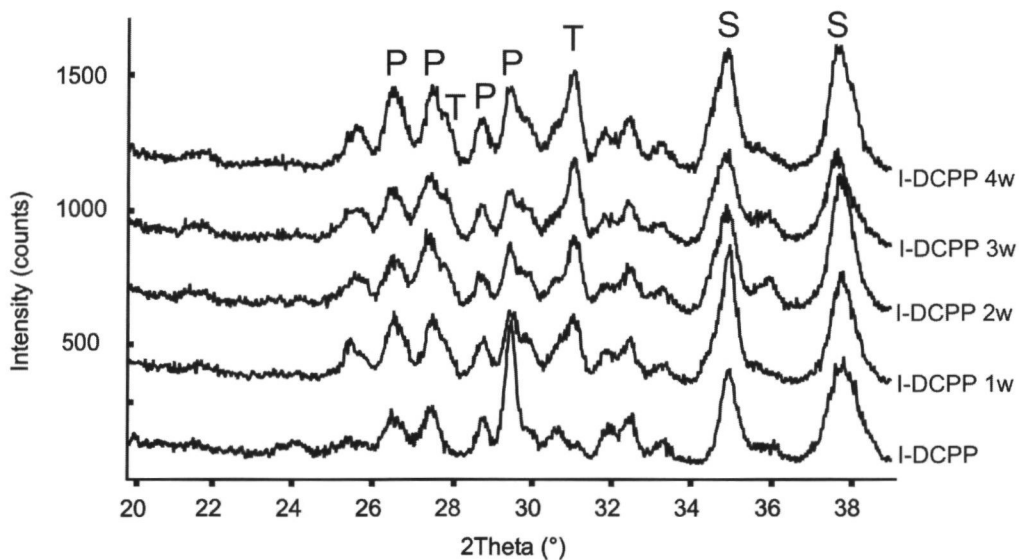


**Figure 1d:** XRD patterns of amorphous DCP coating after 4 weeks incubation in SBF at 37° C. (P: dicalcium pyrophosphate, T: beta-tricalcium phosphate and S: titanium substrate).

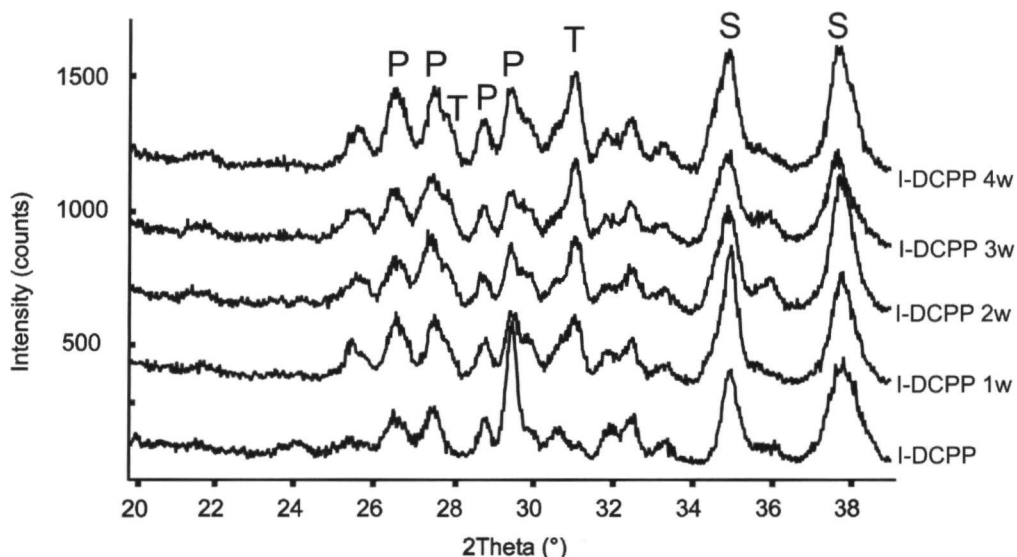


**Figure 1e:** XRD patterns of infrared heat-treated DCP coating after 4 weeks incubation in SBF at 37° C. (P: dicalcium pyrophosphate, T: beta-tricalcium phosphate and S: titanium substrate).

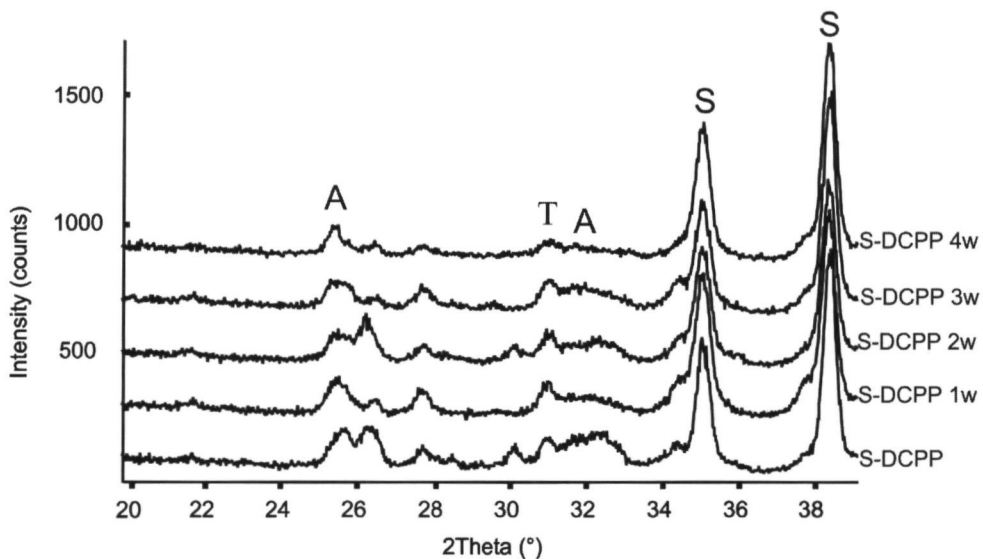


**Figure 1e:** XRD patterns of steam heat-treated DCP coating after 4 weeks incubation in SBF at 37° C. (P: dicalcium pyrophosphate, T: beta-tricalcium phosphate and S: titanium substrate).



### ***CaP coating surface structure changes before and after incubation in SBF***

Figure 2 depicts the FTIR spectra of the as-sputtered, heated and SBF incubated coatings. All as-sputtered DCPD and HA coatings show two clusters of peaks from 900-1150 and from 550-600  $\text{cm}^{-1}$ , which can be attributed to the major absorption modes of phosphate bonds (Figure 2). During incubation in SBF, these peaks decreased in size, indicating dissolution of these amorphous coatings (Figure 2a, 2d). Infrared heat treatment of the DCPD coatings resulted in the appearance of various P-O bonds that did split up into many peaks at a wavelength around 1300 to 950  $\text{cm}^{-1}$ , which is characteristic for the beta-calcium pyrophosphate structure. I-HA coatings showed the appearance of the various P-O bonds at a wavelength of 948, 965, 1009, 1083, and 1124  $\text{cm}^{-1}$ , which is characteristic for an apatite structure. During soaking in SBF, a weak peak developed around 1470  $\text{cm}^{-1}$  for both I-HA and S-HA coatings indicating the formation of carbonated apatite (Figure 2b, 2c). I-DCPD and S-DCPD coatings showed stable FTIR spectra, almost no changes could be observed during immersion in the SBF (Figure 2e, 2f).

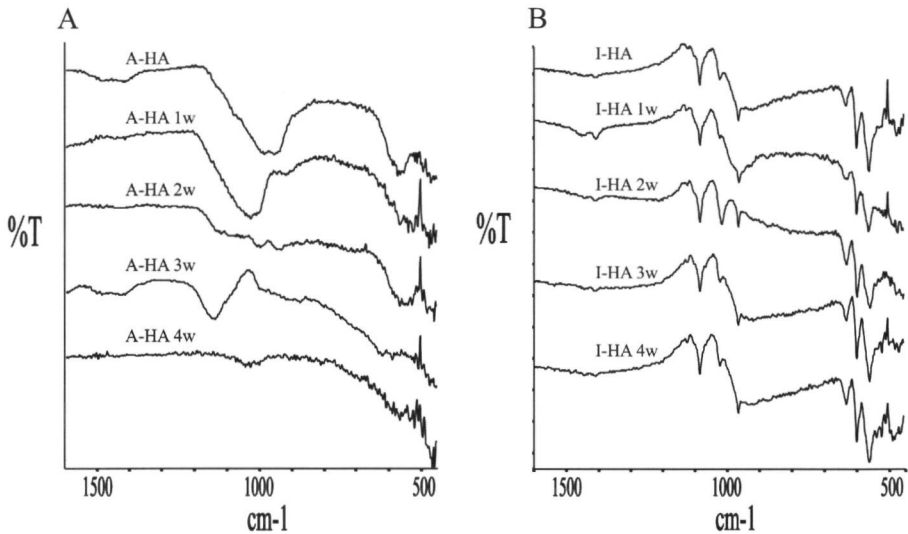


**Figure 2a-b:** IR spectra of Ha coatings after 4 weeks incubation in SBF at 37° C. (A) as-sputtered coatings and (B) infrared heat-treated coatings

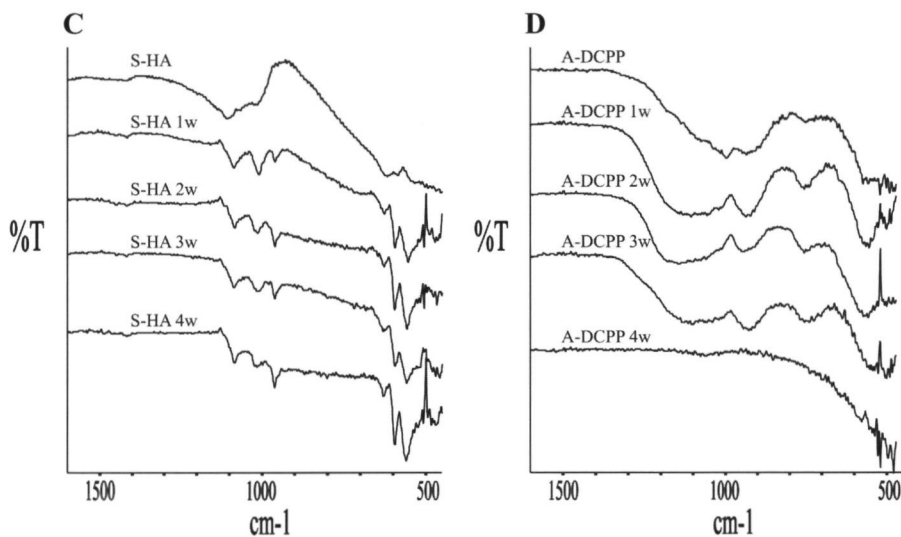


**Figure 2c-d:** IR spectra of Ha and DCPD coatings after 4 weeks incubation in SBF at 37° C. (C) steam heat-treated coatings and (D) as-sputtered coatings.

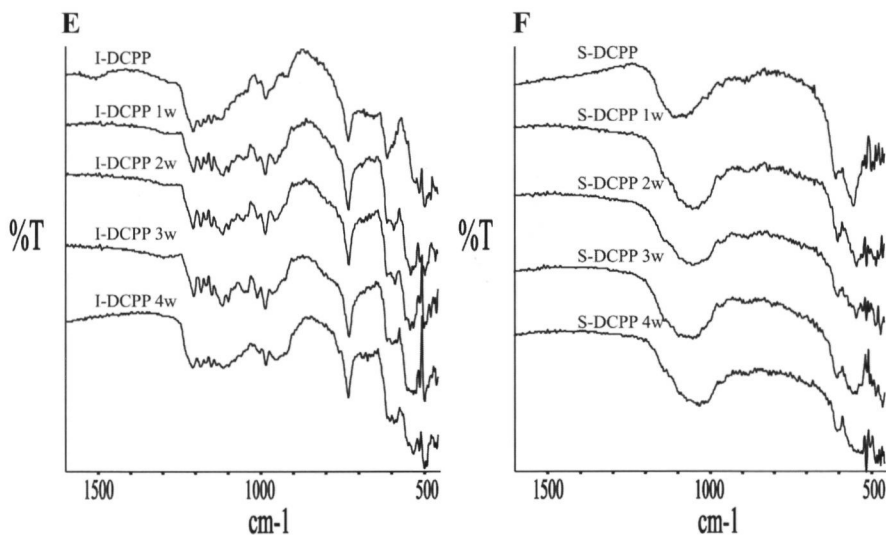


**Figure 2e-f:** IR spectra of Ha and DCPD coatings after 4 weeks incubation in SBF at 37° C. (E) infrared heat-treated coatings and (F) steam heat-treated coatings.

### ***Compositional changes of the sputtered CaP coating surfaces during incubation in SBF***

Table 2 lists the Ca/P ratio changes of the coating surfaces before and after incubation in SBF as determined by Energy Dispersive Spectroscopy. The Ca/P ratio of both amorphous HA and DCPD coatings was found to change significantly. The Ca/P ratio of the A-HA coatings changed from 2.0 to 1.12, and the Ca/P ratio of the A-DCPD coatings from 0.76 to 1.23. In contrast, the Ca/P ratio of the I-HA coating changed less, i.e. from 2.01 to 1.76, and the Ca/P ratio of the S-HA coatings changed from 1.91 to 1.68 after incubation in the SBF. For both I-HA and S-HA coatings, the changes in Ca/P ratio mainly occurred during the first week of incubation. Further, the Ca/P ratio of the I-DCPD coatings increased gradually during incubation, i.e. from 0.76 to 1.26 while the Ca/P ratio of S-DCPD coatings remained more or less stable around 1.5 during incubation in SBF.

**Table 2** EDS measurement of the Ca/P ratio of the coatings after incubation in SBF

Week	A-HA	I-HA	S-HA	A-DCPD	I-DCPD	S-DCPD
0	1.98	2.01	1.91	0.76	0.76	1.62
1w	1.74	1.73	1.78	1.16	1.15	1.48
2w	1.70	1.83	1.67	0.90	1.19	1.51
3w	1.54	1.70	1.67	0.97	1.21	1.49
4w	1.12	1.76	1.68	1.23	1.26	1.55

### ***ICP measurements of Ca and P concentration changes in the SBF***

Figure 3 and 4 show the calcium and phosphate concentration for the different calcium phosphate coatings in SBF buffer during the 4 week incubation period.

For the amorphous coatings, an increase of Ca concentration was observed up to 3 weeks of incubation. Thereafter, the Ca concentration remained stable. The P concentration in the SBF increased up to 4 weeks of incubation.

In contrast with the amorphous specimens, all heat-treated coatings adsorbed Ca and P within the 4 week incubation period, which is characterized by a slight decrease in Ca as well as P concentration during the immersion in SBF.

### ***Surface morphology changes of the CaP coatings after soaking in SBF***

SEM pictures of the as-sputtered, heated and SBF incubated coatings are shown in Figure 5. SEM examination of the as-sputtered coatings showed an excellent coverage of the substrate surface (Figure 5a, 5d). Infrared heat treatment induced no changes in the coating morphology (Figure 5b, 5e), while steam heating resulted in the deposition of a precipitate on the coated surface (Figure 5c, 5f). After incubation in SBF, the amorphous coatings dissolved almost completely (Figure 6a, 6d), while both I-HA and I-DCPD coatings did not show any change during the incubation in SBF (Figure 6b, 6e). On the other hand, on the S-HA and S-DCPD surfaces precipitation was seen with a different morphological structure compared

with before incubation in SBF (Figure 6c, 6f).

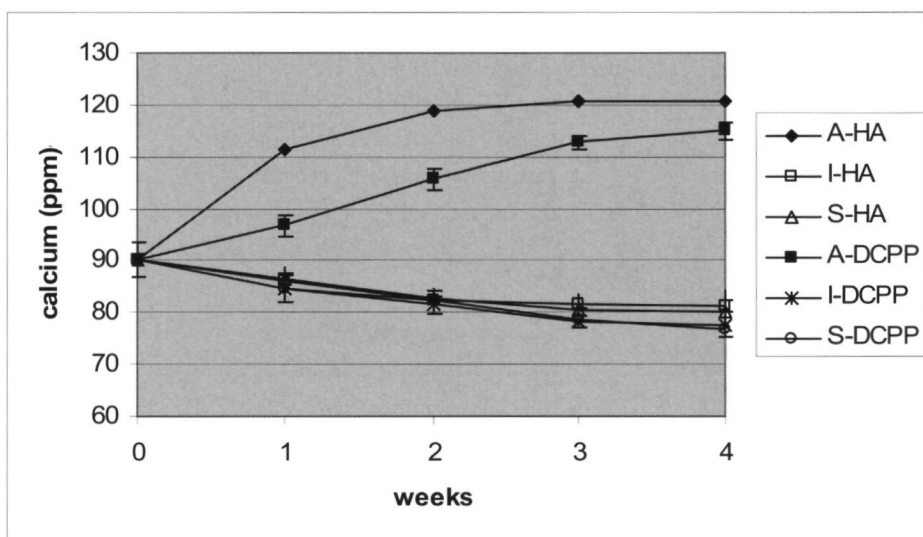


**Figure 3** Calcium concentration measurements in SBF

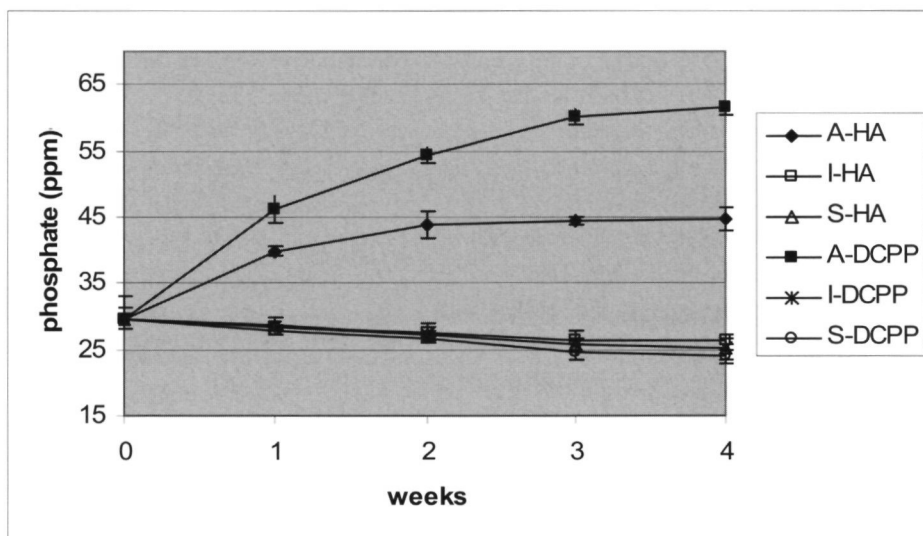


**Figure 4** Phosphate concentration measurements in SBF

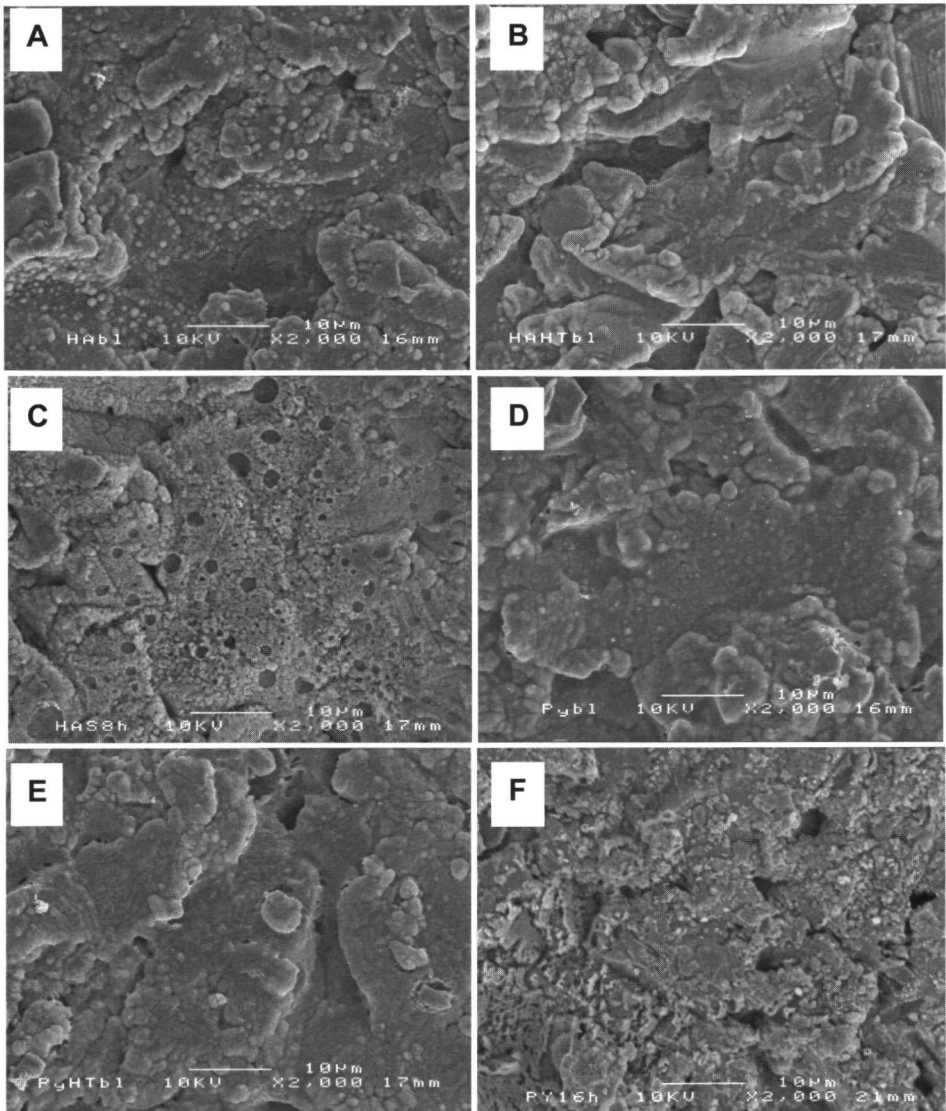


**Figure 5** SEM micrographs of different sputtered CaP surface;  
 A: A-HA surface, B: I-HA surface, C: S-HA surface, D: A-DCPP surface,  
 E: I-DCPP surface and F: S-DCPP surface

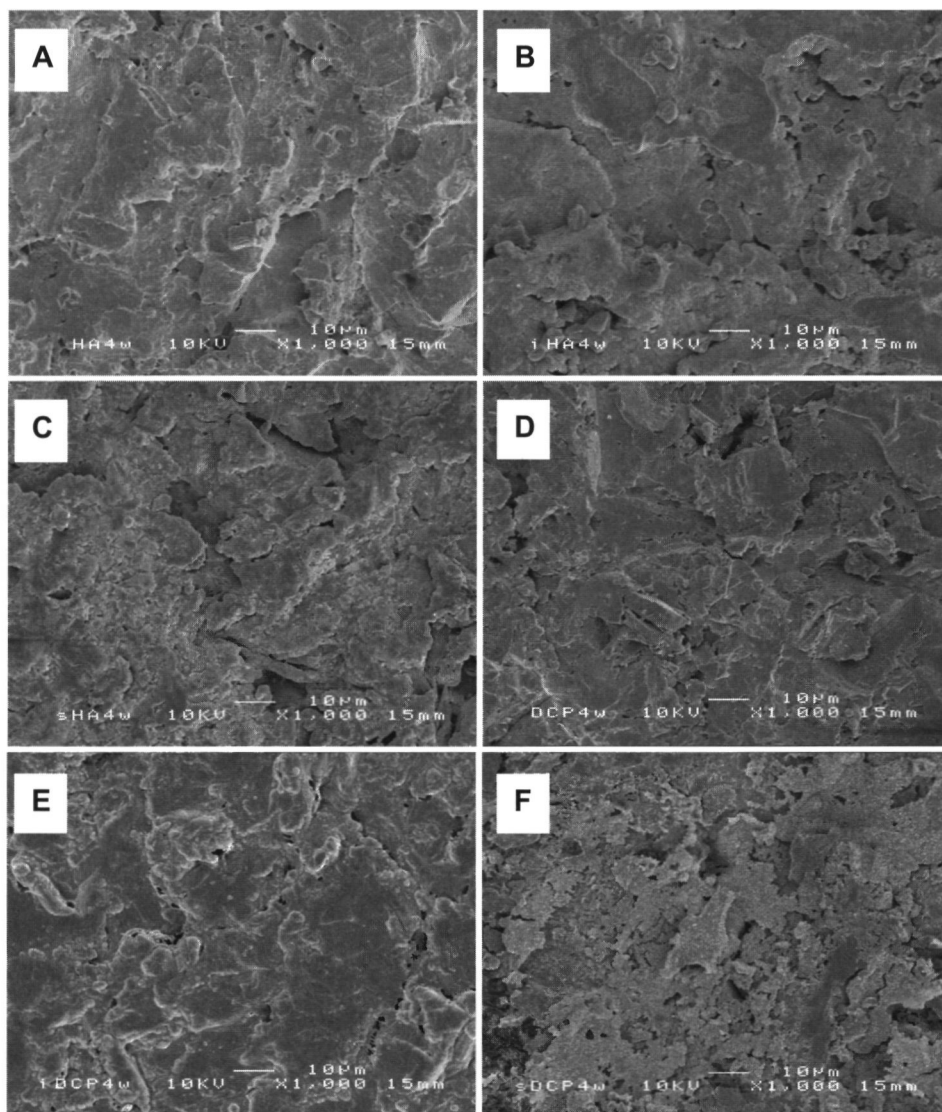


**Figure 6** SEM micrographs of different CaP surfaces after incubation in SBF for 4 weeks;  
A: A-HA surface, B: I-HA surface, C: S-HA surface, D: A-DCPP surface,  
E: I-DCPP surface and F: S-DCPP surface

### ***Behavior of RBM cells on the various CaP coatings***

SEM confirmed the presence of cells on all four types of heat-treated CaP coating at both incubation times. Nevertheless, clear differences were seen. On the I-HA coatings, the cells proliferated well and formed a multilayer of cells with extensive collagen fibre formation and surface mineralization in the form of globular accretions (Figure 7a). On the S-HA surfaces, the cell proliferation was combined with the deposition of very fine mineralization particles (Figure 7b). The same was observed for the S-DCPP coatings, although the number of cells appeared to be somewhat less. On the I-DCPP surface a multilayer of cells was observed, but the deposition of calcified globuli was very limited.

Additional EDS measurements showed that the Ca/P ratio of the I-HA coating decreased to  $1.96 \pm 0.05$  at day 8 and  $1.91 \pm 0.05$  at day 16, while the Ca/P ratio of the S-HA coatings remained stable at  $1.77 \pm 0.02$  during incubation. The Ca/P ratio of the I-DCPP coatings at 8 days was found to be  $1.15 \pm 0.01$  and at 16 days  $1.23 \pm 0.02$ , while the Ca/P ratio of S-DCPP coatings increased to  $1.52 \pm 0.01$  at day 8 and  $1.51 \pm 0.01$  at day 16 of incubation.

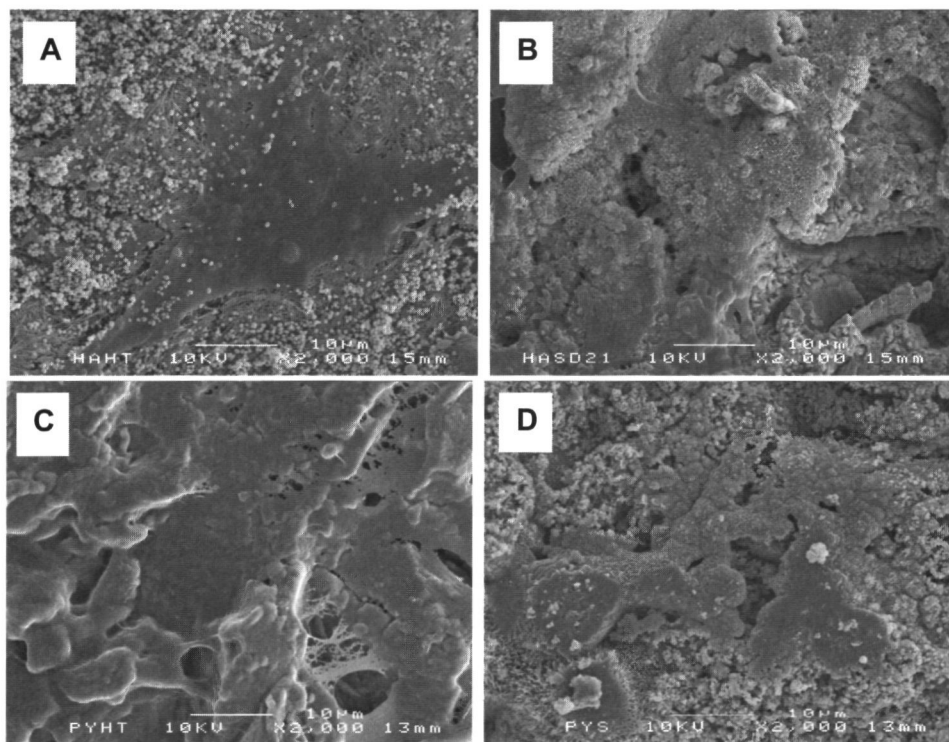
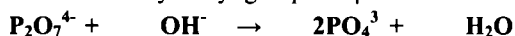


**Figure 7** SEM micrographs of RBM cells after 16 days of incubation on different CaP surfaces. A: I-HA surface, B: S-HA surface, C: I-DCPP surface and D: S-DCPP surface.

## Discussion

Based on the results, we have clearly seen that *in vitro* behavior of RF sputtering CaP coatings is strongly affected by the surface characteristics induced by different heat treatments. As-deposited RF sputtered CaP coatings are amorphous and need heat treatment to obtain crystallinity [23]. As a consequence, incubation of as-sputtered CaP coatings in simulated body fluid (SBF) results in partial dissolution of the surface. This process is initiated by the release of  $\text{Ca}^{2+}$ ,  $\text{HPO}_4^{2-}$  and  $\text{PO}_4^{3-}$ . This exchange of ions from the coating surface continues until the concentration of  $\text{Ca}^{2+}$ ,  $\text{HPO}_4^{2-}$  and  $\text{PO}_4^{3-}$  reaches supersaturation, then the dissolution and precipitation equals. When the SBF is refreshed, the equilibrium is broken and the dissolution restarts. In this way the RF sputtered amorphous CaP coatings dissolve gradually in the SBF. Although HA is considered the most stable phase among all the calcium phosphate phases in a SBF environment, the amorphous HA coatings show dissolution in the SBF, similar to the amorphous pyrophosphate coatings.

Therefore, post-heat treatment is an essential process to control the crystallinity and morphology of the CaP coatings. However, different heat treatment procedures can have a great influence on the morphology and interfacial properties of the coating surface, which can influence the surface reaction in SBF. Heat treatment at a high temperature (e.g., above  $600^\circ\text{C}$ ) in air reduces the adhesive strength of a sputtered CaP coating to the underlying substrate surface and can even result in the buckling of the coating at the surface. Also it is known, that with increasing temperature of the heat treatment, the purity of the HA phase in the coating decreases [19, 24]. To avoid alteration of the basic properties of sputtered CaP coatings, we decided to heat the coatings either with infrared at high temperature ( $500\text{--}700^\circ\text{C}$ ) for a very short time (30 seconds) or water steam at a lower temperature for a long time ( $140^\circ\text{C}$ ). The results showed that both infrared and water steam heat treatment changed the amorphous coating into the crystalline phase. After the different heat treatment procedures, the sputtered CaP coatings were stable in SBF and CaP crystals nucleated on the surface [25]. In our present study, the I-HA coatings had an initial Ca/P ratio 1.97, which indicates the presence of a surplus of positive ions ( $\text{Ca}^{2+}$ ). Consequently, the negative ions as present in the SBF, like  $\text{CO}_3^{2-}$  and  $\text{HPO}_4^{2-}$ , will be attracted to the coating surface. This is followed by an accumulation of positive ions in SBF and their subsequent precipitating on the surface. During this process, ions exchange and gradually a hydroxy-carbonate apatite (HCA) layer is formed. On the other hand, the formation of TCP phase within the heat treated DCPD coatings is the result of the surface reaction of calcium pyrophosphate into a  $\beta$ -TCP phase. This result is in line with observations of Yubao et al [26], who found that pyrophosphate reacts with a hydroxyl group and  $\beta$ -TCP is formed.



Further, the DCPD coating showed a deficit of  $\text{Ca}^{2+}$  (Ca/P ratio of 0.76). Therefore, this surface has a high initial affinity for positive ions, like  $\text{Ca}^{2+}$  and  $\text{Mg}^{2+}$ , after incubation in SBF, which is followed by the deposition of a TCP and HA phases. Occasionally, it is



claimed that this kind of reactions on CaP surfaces has bone-like characteristics. Nevertheless, we have to emphasize that a lot of major bone components (like cells, collagen, blood vessels) are lacking [27, 28]. In view of this, the deposit can only be considered as a more natural matrix for osteoblast adhesion and differentiation.

Further, the changes in Ca/P ratio of both A-HA and A-DCPP coatings indicated that these surfaces are chemically unstable in SBF, resulting in a decrease in Ca/P ratio for A-HA and an increase for A-DCPP coatings. Meanwhile, the Ca/P ratio of I-HA and S-HA surfaces showed a tendency to change into the direction of stoichiometric HA, i.e. 1.67. A similar trend was observed for the heat treated DCPD surfaces. This agrees with the existing theories, since the crystal HA phase is the most stable phase in SBF [29]. All changes could be associated with changes in the Ca and P concentration of the SBF. Evidently, a relation exists between change in coating Ca/P ratio and the deposition of a precipitate out of the SBF. The SEM photographs of infrared steam heated CaP surfaces indicated that much more precipitate was formed on S-HA surface as well as S-DCPD surfaces compared with the infrared treated coatings.

Our previous study showed that amorphous DCPD and HA coatings did not support the proliferation and differentiation of rat bone marrow cells [30]. In the current study, some significant differences were observed on the various heated CaP coating surfaces. On both I-DCPD and I-HA coatings, a thick multilayer of bone-like cells was seen. Also, on the S-HA and S-DCPD coatings, the cells did proliferate and differentiate. Nevertheless, the morphology of the cells and mineral deposit differed compared with the infrared heated coatings. We suppose that this is still due to small differences in the dissolution properties of these coatings. All these results corroborate with our earlier studies dealing with the behavior of bone marrow cells on magnetron sputtered CaP coatings [31]. The EDS measurement of the Ca/P ratio of the coatings after cell culturing revealed for S-HA, I-DCPD and S-DCPD coatings similar changes occurred as for the SBF incubated specimens. Only for I-HA coatings the Ca/P ratio after 16 days of culturing was higher compared with the SBF incubated ones. Again, this can be due to small differences in dissolution behavior associated with coverage by the cell layer and at the same time deposition of mineralized matrix by the bone-like cells. This explanation is supported by an earlier study with very thin highly crystalline magnetron deposited coatings [29]. This study proved that incubation in SBF as well as incubation in cell cultures and the subsequent deposition of a calcified layer are two different phenomena.

## Conclusion

Overall, we conclude that different heat treatment procedures for the sputtered HA and DCPD coatings influence the surface characteristics of these coatings, whereby a combination of crystallinity and specific phase composition (Ca/P ratio) strongly affect the *in vitro* bioactivity of sputtered CaP coatings. This conclusion is supported by our observation that

Both sputtered amorphous A-HA coating and A-DCPP coatings are chemically active in SBF and release Ca and P into the SBF. In contrast, heat treated surfaces release less Ca and P as well as a precipitate is formed on these surfaces.

The Ca/P ratio of heat treated HA and DCPD coatings shows a tendency to change into the direction of stoichiometric HA during incubation in SBF.

Rat bone marrow cells can proliferate and differentiate on heat treated HA and DCPD coatings.

Finally, it has to be noticed that SBF incubation studies are not completely comparable with cell culture studies.

## References

- 1] Ducheyne P. Bioceramics: Material characteristics versus *in vivo* behavior. J Biomed Mater Res Appl Biomater 1987;21A 219-36.
- 2] Lin FH, Hon KH. A study on synthesized hydroxyapatite bioceramics. Ceram Int 1989;5 530-6.
- 3] Kitsugi T, Yamamuro T, Nakamura T, Kotani S, Kokubo T. Four calcium phosphate ceramics as bone substitutes for non-weight-bearing. Biomaterials. 1993;4:216-24.
- 4] Rangavittal N, Landa-Canovas AR, Gonzalez-Calbet JM, Vallet-Reg M. Structural study and stability of hydroxyapatite and  $\beta$ -tricalcium phosphate. Two important bioceramics. J Biomed Mater Res. 2000;51:660-8.
- 5] McAndrew MP, Gorman PW, Lange TA. Tricalcium phosphate as a bone graft substitute in trauma. preliminary report. J Orthop Trauma. 1988;2:333-9.
- 6] Black J. Ceramics and composites. In: Orthopaedic biomaterials in research and practice. New York: Churchill Livingstone, 1988;191-211.
- 7] Jarcho M. Calcium phosphate ceramics as hard tissue prosthetics. Clin Orthop. 1981;157:259-78.
- 8] Dorozhkin SV, Epple M. Biological and medical significance of calcium phosphates. Angew Chem Int Ed Eng. 2002;41 3130-46.
- 9] Klein CPAT, Driessen AA, de Groot K, van den Hooff A. Biodegradation behavior of various calcium phosphate materials in bone tissue. J Biomed Mater Res 1983;17:769-84.
- 10] Kitsugi T, Yamamuro T, Nakamura T, Oka M. Transmission electron microscopy observations at the interface of bone and four types of calcium phosphate ceramics with different calcium/phosphorus molar ratios. Biomaterials. 1995;16:1101-7.
- 11] ter Brugge PJ, Wolke JGC, Jansen JA. Effect of calcium phosphate coating composition and crystallinity on the response of osteogenic cells in vitro. Clin Oral Impl Res 2003;14:472-80.
- 12] Ducheyne P, Qui Q. Bioactive ceramics. the effect of surface reactivity on bone formation and bone cell function. Biomaterials 1999; 20:2287-2303.
- 13] Ferraz MP, Fernandes MH, Santos JD, Monteiro, FJ. HA and double-layer HAP2O5/CaO glass coatings influence of chemical composition on human bone marrow cells osteoblastic behavior. J Mater Sci: Mater in Med. 2001;12 629-38.
- 14] Hulshoff JEG, van Dijk K, de Ruijter JE, Rietveld FJR., Ginsel LA, Jansen JA. Interfacial phenomena: an in vitro study to the effect of calcium phosphate (Ca-P) ceramic on bone formation. J Biomed Mater Res. 1998;40:464-74.
- 15] Cheung HS, Story MT, McCarty DJ. Mitogenic effects of hydroxyapatite and calcium pyrophosphate dihydrate crystals on cultured mammalian cells. Arthr Rheum. 1984;27:668-74.
- 16] de Groot K, Geesink R, Klein CPAT, Serekian P. Plasma sprayed coatings of hydroxyapatite. J Biomed Mater Res 1987;21:1375-81.
- 17] Wolke JGC, de Bleeck-Hogervorst JMA, Dhert WJA, Klein CPAT, de Groot K. Studies on thermal spraying of apatite bioceramics. J Therm Spray Techn. 1992; 1:79-90.
- 18] Jansen JA, Wolke JGC, Swann S, van der Waerden JPCM, de Groot K. Application of magnetron sputtering for producing ceramic coatings on implant materials. Clin Oral Impl Res. 1993;4:28-34.
- 19] van Dijk K, Schaeken HG, Wolke JGC, Jansen JA. Influence of annealing temperature on RF-magnetron sputtered calcium phosphate coatings. Biomaterials. 1996;17:405-10.
- 20] van Dijk K, Schaeken HG, Wolke JGC, Marrec CHM, Habraken FHPM, Verhoeven J, Jansen JA. Influence of discharge power level on the properties of hydroxyapatite films deposited on Ti6Al4V with RF-magnetron sputtering. J Biomed Mater Res 1995;29 269-76.
- 21] Yonggang Y, Wolke JGC, Yubao L, Jansen JA. Surface characteristics of RF-magnetron sputtered calcium

- phosphate coatings at different heat treatments *Key engineering materials* 2005;284-286 235-39.
- 22]Maniatopoulos C, Sodek J, Melcher AH. Bone formation in vitro by stromal cells obtained from bone marrow of young adult rats. *Cell and Tiss Res.* 1998;254:17–330.
- 23]Yoshinari M, Hayakawa T, Wolke JGC, Nemoto K, Jansen JA. Influence of rapid heating with infrared radiation on RF-magnetron-sputtered calcium phosphate coatings. *Biomed Mater Res.* 1997;37:60-7.
- 24]Jansen JA, ter Brugge PJ, van der Wal E, Vredenberg AM, Wolke JGC. Osteocapacities of calcium phosphate ceramics In: *Bio-implant interface: Improving biomaterials and tissue reactions.* Ellingsen JE, Lyngstadaas SP (eds). CRC Press, 2003,305-22.
- 25]Gross KA, Berndt CC, Goldschlag DD, Iacono VJ. In vitro changes of hydroxyapatite coatings *Int J Oral Maxillofac Impl* 1997;12:589-97.
- 26]Yubao L, Klein CPAT, de Wijn J, van de Meer S, de Groot K. Shape change and phase transition of needle-like non-stoichiometric apatite crystals. *J Mater Sc: Mater in Med.* 1994;5:263-8.
- 27]Leng Y, Chen J, Qu S TEM study of calcium phosphate precipitation on HA/TCP ceramics. *Biomaterials.* 2003;24 2125-31.
- 28]Shi D, Jiang G, Bauer J. The effect of structural characteristics on the in vitro bioactivity of hydroxyapatite *J Biomed Mater Res.* 2002; 63:71-8
- 29]Yan Y, Wolke JGC, de Ruijter JE, Yubao L, Jansen JA. Growth behaviour of Rat Bone Marrow (RBM) cells on RF-magnetron sputtered hydroxyapatite and dicalcium pyrophosphate coatings *J Biomed Mater Res.* 2005, in press
- 30]ter Brugge, PJ, Wolke, JGC, Jansen, JA. Effect of calcium phosphate coating crystallinity and implant surface roughness on differentiation of rat bone marrow cells *J Biomed Mater Res.* 2002,60.70-7

## **Chapter 5**

### **Growth behavior of Rat Bone Marrow (RBM) cells on RF magnetron sputtered hydroxyapatite and dicalcium pyrophosphate coatings**

Accepted: J Biomed Mat Res. Part A, 2005

Yonggang Yan, J. G.C. Wolke, A. De Ruijter, Li Yubao, J.A. Jansen

## **Introduction**

Worldwide an estimated number of 1 million patients annually need implants (orthopedic and, or dental) for the replacement of joints of natural teeth. Treatment does not always result in a solution. For example, loosening occurs in 5-40% of the inserted orthopedic and dental implants [1, 2]. This situation is attributed to inadequate local bone conditions and impaired bone healing.

Bone formation is a complex process that involves proliferation of osteoprogenitor cells, their differentiation into osteoblasts, finally resulting in the secretion of abundant bone matrix proteins, which coordinate the mineralization process [3-7]. In view of the bone formation process, it is known that most so-called bioactive implant materials show a direct bone bonding through a calcified layer at the implant interface. One of the preferred bioactive materials for the manufacturing of bone replacing devices is the calcium phosphate ceramic hydroxylapatite (HA). The favorable bone response of this material is supposed to be due to its similarity in terms of chemical composition and crystal structure with the calcium phosphate phase of bone mineral [8-11]. However, on basis of the structural arrangement of bone and the sequence of the biological mineralization process, it can be reasoned that besides HA other calcium phosphate ceramics, like dicalcium phosphate and pyrophosphate, play an important role in the bone formation towards implant surfaces [12]. For example, HA has to be considered as the end product of the biological mineralization process, while dicalcium pyrophosphate ( $\text{Ca}_2\text{P}_2\text{O}_7$ , DCP) is one of the intermediate products in this process [13].

To support and explore this hypothesis, in previous studies dicalcium pyrophosphate coatings were obtained by RF magnetron sputter deposition and the physicochemical as well as dissolution behavior of these coatings was determined in simulated body fluid (SBF) [14, 15]. The results showed that DCP coatings displayed similar properties as HA in the SBF, also heat-treated coatings appeared to be more stable in the SBF than amorphous coatings. The aim of the present study was to evaluate the in vitro cell behavior of RF magnetron deposited DCP coatings in comparison with HA coatings. We hypothesized that the proliferation and differentiation of bone-like cells on DCP surfaces would be at least very similar to HA surfaces.

## Materials and Methods

### *Substrates*

For the experiments commercially pure titanium discs with a diameter of 12 mm and thickness of 1.5 mm were used. All discs were  $\text{Al}_2\text{O}_3$ -blasted on one side ( $R_a = 1.0\text{-}1.3\mu\text{m}$ ). After ultrasonic cleaning in isopropanol, the discs were provided with the following coatings:

- Dicalcium pyrophosphate coating, with a thickness of 2  $\mu\text{m}$ ;
- Hydroxylapatite coating, with a thickness of 2  $\mu\text{m}$ .

The coating procedure was performed using a commercially available RF magnetron sputter unit (Edwards ESM 100, Crawford, England). The target material used in the deposition process was a copper disc provided with either pyrophosphate or hydroxylapatite granulate. The process pressure was  $5 \times 10^{-3}$  mbar and the sputter power was 400 W. The deposition rate of the films was 100-150 nm/hour sputtering. After deposition, half of the coated specimens were subjected to an additional infrared heat treatment for i.e. 30 sec at 550°C for the HA coatings and at 650°C for the DCPD coatings. Before and after heat-treatment, the coatings were characterized by thin film X-ray diffraction (Philips, PW3710, Almelo, The Netherlands), Fourier transform infrared (FTIR, Perkin Elmer, Fremont, CA, USA) and a scanning electron microscope (SEM, Jeol 6310, Tokyo, Japan) equipped with an energy dispersive spectroscopy in order to determine the coating Ca/P ratio.

### *Cell isolation*

Rat bone marrow (RBM) cells were isolated and cultured using the method described by Maniopoulos [16]. RBM cells were obtained from femora of male Wistar rats. Femora were washed 4 times in culture medium  $\alpha$ -MEM (Minimal Essential Medium; MEM Gibco BRL, Life Technologies B.V. Breda, The Netherlands) with 0.5-mg/ml gentamycin and 3  $\mu\text{g}/\text{ml}$  fungizone. Epiphyses were cut off and diaphyses flushed out with 15 ml culture medium  $\alpha$ -MEM, supplemented with 10 % FCS (foetal calf serum, Gibco), 50  $\mu\text{g}/\text{ml}$  ascorbic acid (Sigma, Chemical Co., St.Louis, MO, USA), 50  $\mu\text{g}/\text{ml}$  gentamycin, 10 mM Na  $\beta$ -glycerophosphate (Sigma) and  $10^{-8}$  M dexamethasone (Sigma). Cells were incubated in a humidified atmosphere of 95 % air, 5 %  $\text{CO}_2$  at 37°C. The medium was changed every two or three days.

After 6 days of primary culture, cells were detached using trypsin/ EDTA (0.25% w/v trypsin/0.02% EDTA). The cells were concentrated by centrifugation at 1500 rpm for 5 min. and resuspended in a known amount of media (5 ml). Cells were counted by a Coulter® counter and resuspended in medium ( $2.0 \times 10^5$  cells/1000 $\mu\text{l}$ ). The cell suspension was used for the seeding and culturing experiments.

### ***Cell seeding and culturing***

Cells were presented to the substrates in a cell suspension. The substrates were seeded with  $2.0 \times 10^4$  cells/1000 $\mu$ l. Substrates with cells were cultured in 24-wells plate for 0 (16 hrs) to 24 days. The medium was changed every two or three days.

Two complete separate studies were performed. In each study, each assay was done in fourfold.

### ***DNA analysis***

DNA content was determined at day 1, 3, 5, 8 and 12. For the DNA assay, medium was removed and the cell layers were washed twice with PBS. The substrates were put in a 10ml tube containing 1 ml milliQ water. For isolation of the DNA, the 10ml tubes were incubated at 37°C for one hour. After that the tubes were placed at -70°C for 2 hrs. After thawing, samples were sonicated for 10 min. After that samples were ready for use. For analysis, a PicoGreen dsDNA Quantitation Kit (Molecular Probes, Leiden, The Netherlands) was used, according to the instructions of the kit. Briefly, 100  $\mu$ l sample was added to 100  $\mu$ l PicoGreen working solution. After 2-5 minutes of incubation in the dark, the DNA was measured on a fluorescence curve reader with excitation filter 365nm and emission filter 450nm.

### ***Alkaline phosphatase***

Alkaline phosphatase was measured at day 1, 3, 5, 8 and 12. Medium was removed and cell layer was washed twice with PBS. 0.5 ml of MilliQ was added to each well. Cells were harvested in 10-ml tubes and cell suspension was sonicated for 10 min, and then centrifuged at 2000 rpm, room temperature. Aliquots of the supernatant were removed for determination of protein concentration. The supernatant was stored at -20 °C until the assay was performed. For the assay, 96 well plates were used. 80  $\mu$ l of sample and 20  $\mu$ l of buffer solution (5 mM MgCl<sub>2</sub>, 0.5M 2-amino-2methyl-1-propanol) was added. 100 $\mu$ l of substrate solution (5mM paranitrophenylphosphate) was added to the well and the plate was incubated for 1 hrs at 37°C. The reaction was then stopped by adding 100 $\mu$ l of stop solution (0.3 M NaOH). For the standard curve, serial dilutions of 4-nitrophenol were added to final concentrations of 0 to 25nM. 80 $\mu$ l of standard and 20 $\mu$ l of buffer solution was added to the wells. The plate was read in an ELISA reader at 405nm. Samples and standards were assayed in triplicate.

### ***Osteocalcin***

Cell layers were collected on days 8, 12, 16 and 24. Cell layers were washed twice in PBS, scraped in 1 ml PBS and homogenized by sonication for 10 minutes. Appropriate dilutions of this suspension were used for quantification of osteocalcin. The suspension was stored at -20°C until the assay was performed. Osteocalcin was measured using an enzyme immunoassay kit (Biomedical Technologies Inc., Stoughton, MA, USA). Briefly, 100  $\mu$ l of



sample was added to the wells and the plate was incubated at 4°C, for 24 hrs. After this period, wells were washed 3 times with 0.3 ml wash buffer. 100 µl of osteocalcin anti-serum was added to the well and the plate was incubated for 1 hr at 37°C. The plate was then washed three times and 100 µl of donkey anti-goat IgG peroxidase was added and incubated for 1 hr at RT. 1 Volume of TMB solution was mixed with 1 volume of hydrogen peroxidase solution. The plate was washed 3 times with wash buffer. 100 µl of substrate solution was added to the wells and the plate was incubated for 30 minutes at RT (in the dark). 100 µl of stop solution was added to the wells and absorbency read at 450 nm. Osteocalcin stock was diluted to generate standards from 0.25 to 20 ng/ml. Samples and standards were assayed in 6-fold.

### ***Scanning electron microscopy (SEM)***

After day 8 and 16 of incubation, samples were washed twice with PBS. Fixation was done for 30 minutes in 2% glutaraldehyde, then substrates were washed twice with 0.1 M sodium-cacodylate buffer (pH 7.4), dehydrated in a graded series of ethanol and dried by tetramethylsilane. The specimens were sputter-coated with gold and examined and photographed using a Jeol 6310 SEM at an acceleration voltage of 15 kV and equipped with energy dispersive spectroscopy (EDS).

### ***Statistical analysis***

All data were statistically evaluated with GraphPad<sup>®</sup> Instat 3.05 software (GraphPad Software Inc, San Diego, CA, USA) using an one-way Analysis of Variance (ANOVA) followed by a Tukey-Kramer Multiple Comparison test for further evaluation of the data. Differences were considered significant at *p*-values less than 0.05.

## **Results**

### ***Coating surface analysis***

XRD characterization and Ca/P ratio of the various coatings is shown in Figure 1. Both HA and DCPD coating changed from an amorphous into an almost 100% crystalline structure after heat treatment with infrared at 550°C and 650°C for 30 seconds. Heat-treated HA coatings had a crystalline apatite structure, as characterized by the reflections 002, 211, 112, 202 resp. 25.9°, 31.9°, 32.4° and 34.0° 2-Theta (JCPDS #09-0432). The heat-treated DCPD coatings showed a crystalline beta-calcium pyrophosphate structure with reflection lines 201, 202, 008 and 212, which correspond to peaks at 26.6°, 27.7°, 29.5° and 30.7° in 2-Theta (JCPDS#09-0346).

FTIR showed for all the amorphous HA and DCPD coatings two clusters of peaks from 900-1150 and from 550-600 cm<sup>-1</sup>, which can be attributed to the major absorption modes associated with the presence of phosphate (Figure 2). Infrared heat treatment resulted for the

HA sputter coatings in the appearance of the various P-O bonds at a wavelength of 948, 965, 1009, 1083, and 1124  $\text{cm}^{-1}$ , which are characteristic for an apatite structure. Heat treatment of the DCPD coatings resulted in the appearance of various P-O bonds at a wavelength around 1300 to 950  $\text{cm}^{-1}$ , which split up into many peaks that are characteristic for the beta-calcium pyrophosphate structure.

The Ca/P ratios of the two types of coating were significantly different and were about 2 for HA and about 0.8 for DCPD (Table 1).

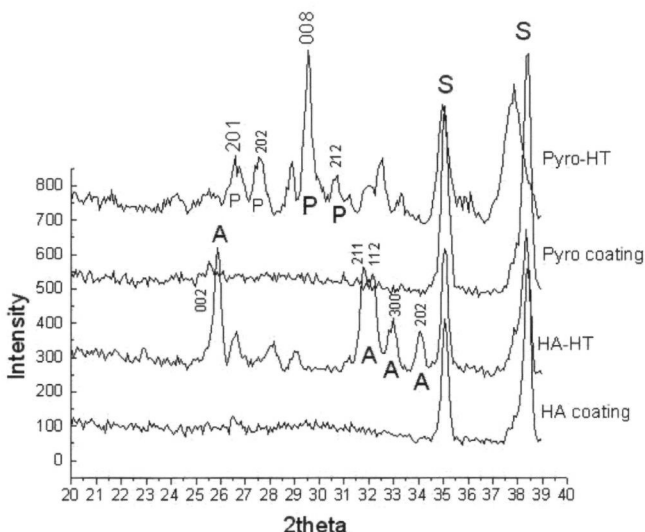


**Figure 1:** XRD patterns of the sputtered CaP coatings. The numbers indicate the major reflection lines for HA and dicalcium pyrophosphate. (A: apatite, P: pyrophosphate and S: titanium substrate)

**Table 1:** the Ca/P ratios of the sputtered coatings surface (n = 5)

Coatings	Ca/P ratio
Sputtered HA coatings	$2.01 \pm 0.05$
Sputtered HA coatings-HT	$1.97 \pm 0.06$
Sputtered Pyro coatings	$0.76 \pm 0.03$
Sputtered Pyro coatings-HT	$0.76 \pm 0.04$

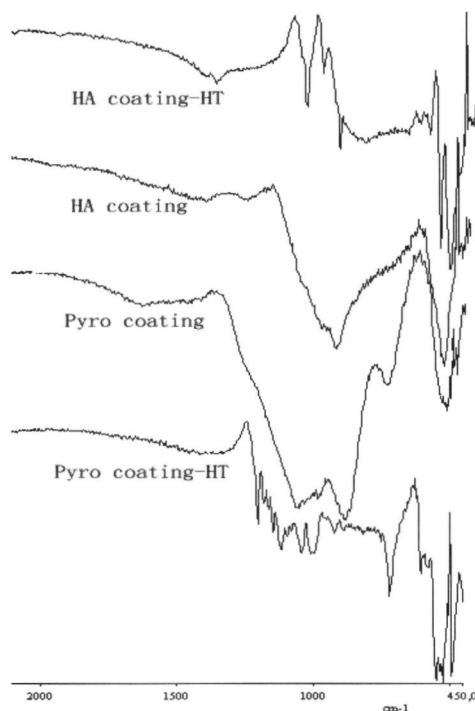


**Figure 2:** FTIR spectra of the various CaP coatings before and after infrared heat treatment (Y axis is in transmittance).

### ***DNA analysis***

Some differences existed in total amount of DNA, but overall the two separately performed studies showed the same results. The data from the DNA assay of the first study are shown in Figure 3 ( $P < 0.05$ ). DNA content remained low till day 3 with no significant difference between the four CaP coatings (as-sputtered HA coating, as-sputtered DCP coating, heated HA coating and heated DCP coating). From day 3 on, DNA content did still not change for both amorphous coatings. This in contrast to both heat-treated coatings. For heat-treated HA, an increase in DNA can be seen starting at day 5 of incubation. This increase continued till day 8. Statistical analysis confirmed the following significant difference: DNA content for HA heat-treated at 5 days  $<$  DNA content for HA treated at 8 days = DNA content for HA treated at 12 days. For heat-treated DCP coatings an increase of DNA content was seen at day 8 and continued till day 12 of incubation. Statistical testing revealed the following significant differences ( $P < 0.05$ ): DNA content heat-treated DCP at 5 days = DNA content heat-treated DCP at 8 days  $<$  DNA content heat-treated DCP at 12 days. Finally, statistical testing also showed that increase of DNA content started earlier on the heat treated HA

coatings; DNA content heat treated HA at 8 days > DNA content heat treated DCPD at 8 days, while at 12 days DNA content heat treated HA < than DNA content heat treated DCPD.

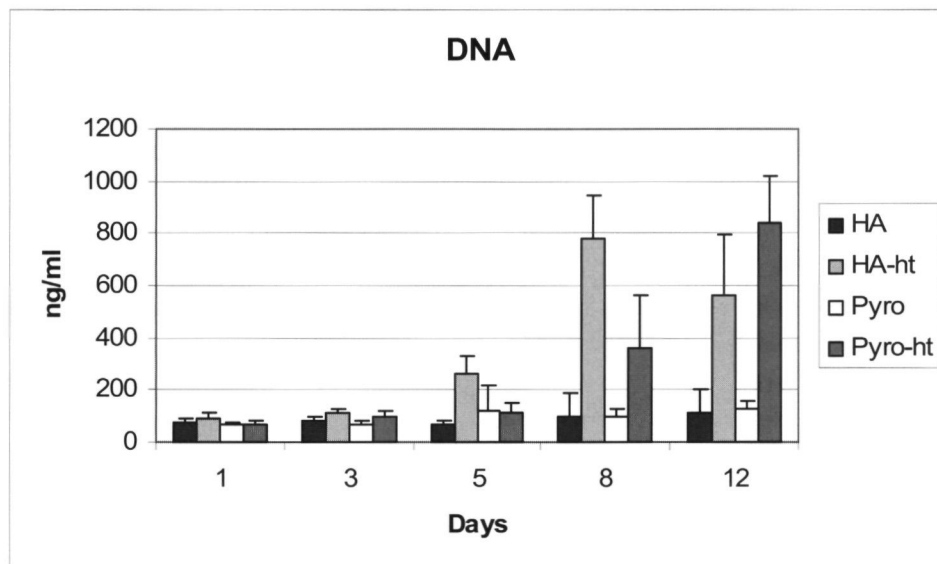


**Figure 3:** DNA content of the RBM cells on all different coating surfaces at the end of the various incubation times. Values are mean  $\pm$  SD.

### *Alkaline phosphatase*

Again no large differences in alkaline phosphatase activity existed for the two separate experimental runs. The data of the first study are shown in Figure 4. For both amorphous coatings no significant increase in AP expression was seen. This in contrast to the heat-treated coatings, which showed a continuous increase during incubation. For the heat-treated HA coatings this increase becomes significant compared with the preceding incubation times at day 8 and for heat-treated DCPD at day 12. In addition, no significant difference in alkaline phosphatase expression exists between heat treated HA and heat-treated DCPD at 12 days of incubation.

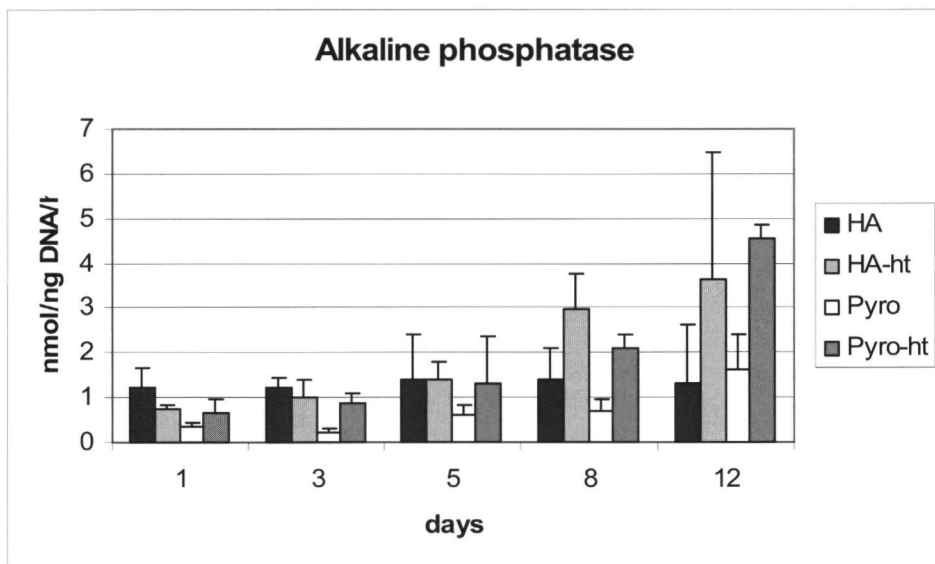


**Figure 4** Alkaline phosphatase expression of the RBM cells on all different coating surfaces at the end of the various incubation times. Expression was normalized for protein content. Values are mean  $\pm$  SD.

### ***Osteocalcin***

Overall, no differences existed in osteocalcin expression between the two separate experimental runs. The results of the first experimental run are shown in Figure 5. For the amorphous coatings, osteocalcin expression was very low for all incubation times and neither an increase or decrease occurred during time. For the heat treated DCPD coatings, osteocalcin expression appeared to increase starting at day 16 of incubation, but statistical testing showed that these differences were not significant compared with 8 and 12 days of incubation. On the other hand, osteocalcin expression on the heat treated HA coatings was significantly increased compared with 8 and 12 days of incubation. In addition at 16 days of incubation, the osteocalcin expression on the heat treated HA coatings was significantly higher compared with the heat-treated DCPD coatings. No difference in osteocalcin expression on heat treated HA coatings existed between 16 and 24 days of incubation.

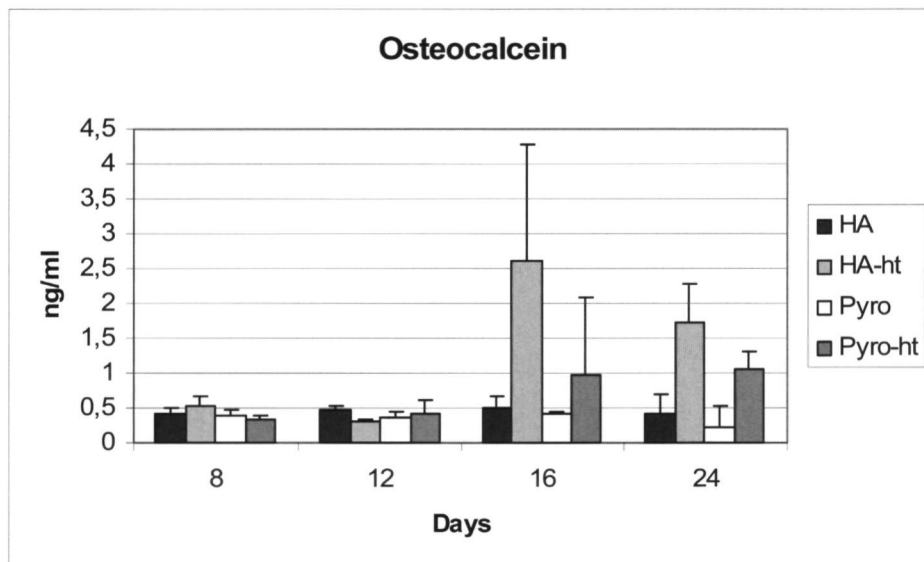


**Figure 5** Osteocalcein expression of the RBM cells on all different coating surfaces at the end of the various incubation times. Expression was normalized for protein content. Values are mean  $\pm$  SD.

### Scanning electron microscopy (SEM)

SEM confirmed the presence of cells on all four types of CaP coating for all incubation times. Nevertheless, clear differences were seen. The number of cells on both amorphous coatings was very limited (Figure 6a). Both amorphous coatings showed severe signs of dissolution as characterized by the occurrence of many surface pits and cracks. Dissolution of the amorphous HA coating could occasionally be associated with the deposition of a precipitate (Figure 6b). On the heat-treated coatings, the cells proliferated well and formed a multilayer of cells with extensive collagen fiber formation and surface mineralization in the form of globular accretions (figure 6c).

Additional EDS measurements showed that the Ca/P ratio of the amorphous HA coating decreased to  $1.61 \pm 0.02$  at 8 day of incubation and to  $1.55 \pm 0.02$  at day 16 of incubation, while the Ca/P ratio of amorphous DCPD coating increased to  $1.13 \pm 0.01$  at day 8 of incubation and  $1.32 \pm 0.01$  at day 16 of incubation. The Ca/P ratio of the heat treated DCPD coating at 8 days was found to be  $1.17 \pm 0.01$  and at 16 days  $1.25 \pm 0.02$ , while the Ca/P ratio of the heat treated HA coating decreased somewhat, i.e.  $1.95 \pm 0.05$  at day 8 and  $1.92 \pm 0.05$  at day 16.

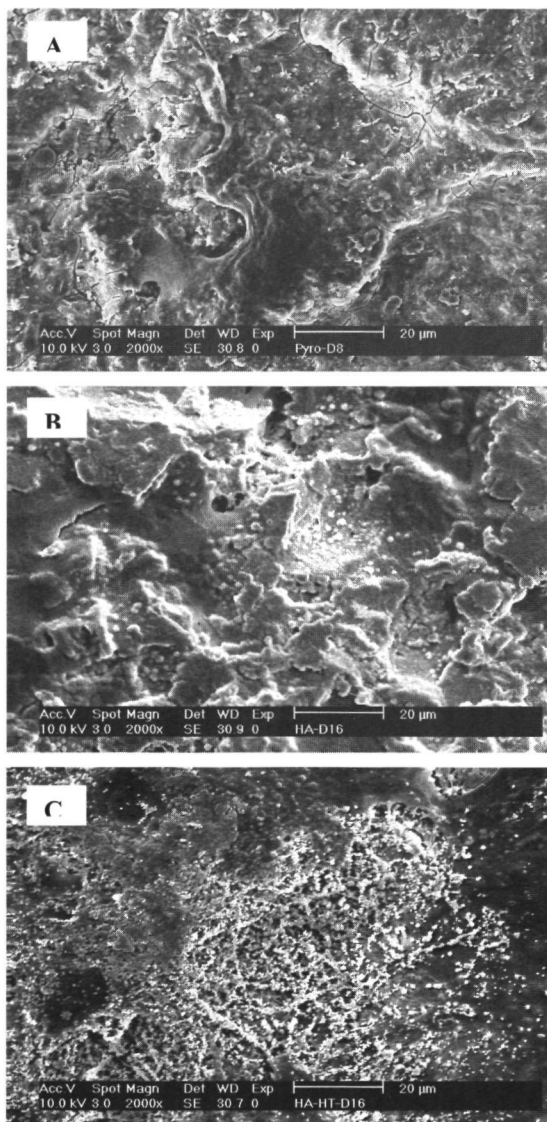


**Figure 6:** SEM micrographs showing: (A) an amorphous DCPD coating after 8 days of cell culturing, (B) an amorphous HA coating after 16 days of cell culturing, (C) an heat treated HA coating after 16 days of cell culturing.

## **Discussion and conclusions**

In this study, the growth and differentiation of bone-like cells on magnetron sputtered DCP and HA coatings were compared. The coatings were used as prepared or after receiving an additional heat treatment. Although the Ca/P ratios of the deposited coatings were found to deviate from their reported stoichiometric values, the coatings showed the XRD pattern of DCP respectively HA after heat treatment with infrared radiation [17]. Considering the rat bone marrow cell behavior, some significant differences were observed. On both amorphous DCP and HA coatings, the cells did not proliferate and differentiate at all. In contrast, bone marrow cells on the crystalline coatings showed an increase in number as well as osteogenic expression during culture. This increase in proliferation and differentiation started earlier on the crystalline HA coatings. These results corroborate with our earlier studies dealing with the behavior of bone marrow cells on magnetron sputtered CaP coatings [18].

Different theories have been presented to explain the bioactive characteristics of CaP ceramics. One hypothesis is that CaP ceramic is bioactive due to dissolution and precipitation of calcium and phosphate ions out of the surface layer resulting in the formation of a surface layer that resembles the natural bone matrix and stimulates osteogenic differentiation [19]. Nevertheless, the effect of CaP coating crystallinity and solubility on bone formation has been found to differ between different studies. For example, some studies indicated that CaP ceramics with high solubility induced more bone formation than Ca-P ceramics with a low solubility [20-22]. In addition, a number of in vitro studies showed that osteogenic differentiation of bone cell cultures is higher on amorphous CaP substrates compared to crystalline CaP substrates [23]. In contrast, other in vitro and in vivo studies reported the opposite and observed that the dissolution of CaP ceramic inhibited osteogenic differentiation and bone formation [24]. A similar observation was done in the current study, which also showed an inhibition of cell proliferation and differentiation on the amorphous HA as well as DCP coatings. SEM analysis confirmed that the amorphous substrate surfaces showed significant dissolution, whereby only for the amorphous HA coatings the dissolution resulted in the occasional deposition of a new surface precipitate. This difference can be explained by the different Ca/P ratios of both coatings. The Ca/P ratio of the amorphous DCP coating is about 0.8, resulting in the presence of a lot of  $\text{H}_2\text{PO}_4$  in the coating surface, which in addition dissolves much easier. The dissolution of the amorphous HA coating will result in a decrease of the Ca/P ratio, whereby at the same time a precipitate is formed with a lower Ca/P ratio than the original amorphous sputtered coating. Further, it has to be emphasized that dissolution of CaP coatings will result in an increase of interfacial ions [25], which may cause apoptosis of osteogenic cells and cause damage to already formed bone [26]. Besides ions, also Ca-P particles can be released from the material, which again have been shown to inhibit osteoblast function in vitro [27] and to cause inflammation and cell death in vivo [28]. Consequently, the results of this study suggest that amorphous sputtered DCP and HA coatings are not very suitable to support bone healing around medical and dental implants.



A second hypothesis to explain the bioactive behavior of CaP ceramics deals with the preferential adsorption of proteins or even the selective adhesion of specific cell populations [29]. Considering the crystalline structure of the heat treated DCPD and HA coatings and the resulting limited dissolution, our study appears to support this second hypothesis. The increase of alkaline phosphatase and osteocalcin expression during prolonged culturing proves that both crystalline coatings can have a strong influence on the mineralization process of heterogenic cell populations, like bone marrow stromal cells. Although, extrapolation of in vitro results to the in vivo situation is always complex, the results indicate that the osteogenic effect of magnetron sputtered crystalline HA coatings is even better compared with the crystalline DCPD coatings, because the level of alkaline phosphatase and osteocalcin expression, which is supposed to reflect differences in the degree of differentiation in osteoblastic cells, started to increase earlier on the crystalline HA coatings [30, 31]

In summary, we conclude that the rat bone marrow stromal cells proliferated and differentiated only on crystalline magnetron sputtered DCPD as well as HA coatings. The results seem to indicate that the crystalline HA coatings induce even an earlier osteogenic effect than the crystalline DCPD coatings. Nevertheless, it has to be emphasized that in vitro data are always difficult to extrapolate to the in vivo situation. Still, the current results warrant the further in vivo analysis of the bone healing supporting properties of magnetron sputtered crystalline DCPD and HA coatings.

## References

- 1] Barden B, Huttegger C. Failure mechanisms in total hip and knee arthroplasty. a morphologic and radiologic study. *Materialwissenschaft und Werkstofftechnik*. 1999;12:746-54.
- 2] Ryd L, Hansson U, Blunn G, Lindstrand A, Toksvig-Larsen S. Failure of partial cementation to achieve implant stability and bone ingrowth: a long-term roentgen stereophotogrammetric study of tibial components. *J Orthoped Res*. 1999;3:311-20.
- 3] Malekzadeh R, Hollinger JO, Buck D, Adams DF, McAllister BSJ. Isolation of human osteoblast-like cells and *in vitro* amplification for tissue engineering. *Periodontology*. 1998;69:1256-62
- 4] Gerstenfeld LC, Shapiro FD. Expression of bone-specific genes by hypertrophic chondrocytes: implications of the complex functions of the hypertrophic chondrocyte during endochondral bone development. *J Cell Biochem*. 1996;1:1-9
- 5] Licia NYW, Yoshinori Ishikawa, Brian RG, Kuber Sampath T, Roy EW. Effect of osteogenic protein-1 on the development and mineralization of primary cultures of avian growth plate chondrocytes: modulation by retinoic acid. *J Cell Biochem*. 1997;4:498-513.
- 6] Lecanda F, Avioli LV, Cheng, SL. Regulation of bone matrix protein expression and induction of differentiation of human osteoblasts and human bone marrow stromal cells by bone morphogenetic protein – 2. *J Cell Biochem*. 1997;67:386-98
- 7] Hanada K, Dennis JE, Caplan I. Stimulatory effects of basic fibroblast growth factor and bone morphogenetic protein – 2 on osteogenic differentiation of rat bone marrow-derived mesenchymal stem cells. *J Bone Miner Res*. 1997;12:1606-14.
- 8] Bruijn JD, Bovell YP, Blitterswijk CA. Structural arrangements at the interface between plasma sprayed calcium phosphates and bone. *Biomaterials*. 1994;15:543-50.
- 9] Yoshikawa T, Ohgushi H, Tamai S. Immediate bone forming capability of prefabricated osteogenic hydroxyapatite. *J Biomed Mater Res*. 1996;32:481-92.
- 10] Asahina I, Watanabe M, Sakurai N, Mori M, Enomoto S. Repair bone defect in primate mandible using a Bone Morphogenetic protein (BMP)-hydroxyapatite-collagen composite. *J Med Dent Sci*. 1997;44:63-70.
- 11] Ktsugi T, Yamamuro T, Nakamura T, Oka M. Transmission electron microscopy observations at the interface of bone and four types of calcium phosphate ceramics with different calcium/phosphorus molar ratios. *Biomaterials*. 1995;16:1101-7
- 12] Ducheyne P, Radin S, King L. The effect of calcium phosphate ceramic composition and structure on *in vitro* behavior. I. Dissolution, II: precipitation. *J Biomed Mater Res*. 1993;1:25-34,35-45.
- 13] Cheung HS, Story MT, McCarty DJ. Mitogenic effects of hydroxyapatite and calcium pyrophosphate dihydrate crystals on cultured mammalian cells. *Arthritis Rheum*. 1984;27:668.
- 14] Yonggang Y, Wolke JGC, Yubao L, Jansen JA. Preparation and characterization of RF magnetron sputtered calcium pyrophosphate coatings. *J Biomed Mater Res: Part A*. accepted 2005.
- 15] Yonggang Y, Wolke JGC, Yubao L, Jansen JA. Subcutaneous evaluation of RF magnetron sputtered calcium pyrophosphate and hydroxylapatite coated Ti implants. *Pers Comm*;2005.
- 16] Maniopoulos C, Sodek J, Melcher AH. Bone formation *in vitro* by stromal cells obtained from bone marrow of young adult rats. *Cell and Tiss Res*. 1998;254:317–30.
- 17] van Dijk K, Verhoeven J, Marée CMH, Habraken FHPM, Jansen JA. Study of the influence of oxygen on the composition of thin films obtained by r f sputtering from a Ca5 (PO4)3OH target. *Th Sol Films*. 1997;304:191-5.
- 18] ter Brugge, PJ, Wolke, JGC, Jansen, JA. Effect of calcium phosphate coating crystallinity and implant surface roughness on differentiation of rat bone marrow cells. *J of Biomed Mater Res*. 2002;60:70-7.
- 19] Ducheyne, P, Qui, Q. Bioactive ceramics. the effect of surface reactivity on bone formation and bone cell

- function. *Biomaterials*. 1999;20:2287-2303.
- 20]de Bruijn JD, Bovell YP, van Blitterswijk CA. Structural arrangements at the interface between plasma sprayed calcium phosphates and bone. *Biomaterials*. 1994;15:543-50
- 21]Frayssinet P, Trouillet JL, Rouquet N, Azimus E, Autefage A. Osseointegration of macroporous calcium phosphate ceramics having a different chemical composition. *Biomaterials*. 1993;14:423-9.
- 22]Kamakura S, Sasano Y, Shimizu T, Hatori K, Suzuki O, Kagayama M, Motegi K. Implanted octacalcium phosphate is more resorbable than  $\beta$ -tricalcium phosphate and hydroxyapatite. *J Biomed Mater Res*. 2002;59:29-34.
- 23]Frayssinet P, Tourenne F, Rouquet N, Conte P, Delga C, Bonel G. Comparative biological properties of HA plasma-sprayed coatings having different crystallinities. *J Mater Sci: Mater in Med*. 1994;5:11-17.
- 24]MacDonald DE, Betts F, Stranick M, Doty S, Boskey AL. Physicochemical study of plasma-sprayed hydroxyapatite-coated implants in humans. *J of Biomater Res*. 2001;54:480-90.
- 25]Ferraz MP, Fernandes MH, Santos JD, Monteiro FJ. HA and double-layer HAP2O5/CaO glass coatings: influence of chemical composition on human bone marrow cells osteoblastic behavior. *J of Mater Sci: Mater in Med*. 2001;12:629-38.
- 26]Yuan H, Yang Z, de Bruijn JD, de Groot K, Zhang X. Material-dependent bone induction by calcium phosphate ceramics: a 2,5-year study in dog. *Biomaterials*. 2001;22:2617-23.
- 27]Pioletti DP, Takei H, Lin T, van Landuyt P, Ma QJ, Kwon SY, Sung KLP. The effects of calcium phosphate cement particles on osteoblast functions. *Biomaterials*. 2000;21:1103-14
- 28]Koerten HK, van der Meulen J. Degradation of calcium phosphate ceramics. *J of Biomed Mater Res*. 1999;44:78-86.
- 29]Torensma R, ter Brugge PJ, Jansen JA, Figdor CG. Ceramic hydroxyapatite coating on titanium implants drives selective bone marrow stromal cell adhesion. *Clin Oral Impl Res*. 2003;14:569-77
- 30]Boskey AL. Current concepts of physiology and biochemistry of calcification. *Clin Orthop*. 1981;157:225-57.
- 31]Toshikatsu KH, Matshyama T, Lau W, Wergedal JE. Monolayer cultures of normal human bone cells contain multiple subpopulations of alkaline phosphatase positive cells. *Calcif Tissue Int*. 1990;47:276-83.



## **Chapter 6**

### **Subcutaneous evaluation of RF magnetron sputtered calcium pyrophosphate and hydroxylapatite coated Ti implants**

Submitted Biomaterials, 2005

Yan Yonggang, J G C Wolke, Li Yubao, J A Jansen

## Introduction

The calcium phosphate (CaP) ceramic hydroxylapatite (HA) has been used widely for bone implantological purposes [1, 2]. In view of this, many investigators have already demonstrated that HA coated implants are surrounded by more bone than uncoated ones because of the osteoconductive behavior of HA [3-8]. Also, a firm fixation in the bone tissue is obtained by the establishment of a chemical bonding at the bone–HA coating interface [9-11]. Till now, HA has been considered as the preferred material because it is the end product of the biological mineralization process during natural bone formation as well bone healing. On the other hand, several intermediate CaP phases can be discerned in the biomineralization process, which perhaps are also attractive from an implantological point of view. For example, it can be hypothesized that implants made of or provided with such early CaP phase compounds participate even more actively in the bone healing process. Hence, use has already been made of the minerals brushite ( $\text{CaHPO}_4 \cdot 2\text{H}_2\text{O}$ ), tricalcium phosphate (TCP:  $\text{Ca}_3(\text{PO}_4)_2$ ) and octacalciumphosphate (OCP:  $\text{Ca}_8(\text{HPO}_4)_2(\text{OH})_2 \cdot 5\text{H}_2\text{O}$ ). These materials show the remarkable property that they are resorbed during time after implantation with a subsequent increase in bone tissue formation. In view of this, there is also another precursor to bone apatite to which not much attention is paid as bone substitute or implant coating. This mineral phase is calcium pyrophosphate (DCPP:  $\text{Ca}_2\text{P}_2\text{O}_7$ ), a condensed phosphate which is of biological importance in calcium metabolism [14]. In bone, calcium pyrophosphate can regulate the onset of calcification and can act as a trigger mechanism to promote mineralization. It can also alter the rate of crystal growth and dissolution. In view of this suggested benefit, our current studies focus on the use of DCPP as coating material for dental and orthopedic implants.

Currently, the most applied method to deposit CaP coatings on metallic implants is plasma-spraying. However, the retention of the bond between CaP coatings and underlying metal surface is an issue of continuous discussion. To avoid this problem, use can be made of other coatings techniques, like laser ablation, electrophoretic deposition, sol-gel deposition or sputter deposition. For the current study a radio frequent (RF) magnetron sputter method was used to deposit DCPP coatings on roughened titanium substrates. The advantage of this method is that thin coatings (100 nm - 2  $\mu\text{m}$  thick) can be deposited with very high adhesion strength [15].

Besides adhesion, a relevant issue is the maintenance of the coating after implantation and the subsequent physicochemical changes that take place in the coatings after implantation. Usually, this behavior is investigated in so-called in vitro dissolution studies, where coated samples are incubated in simulated body fluid (SBF) and the resorption as well as compositional coating changes is determined after various incubation times. Unfortunately, in vitro assays cannot completely mimic the in vivo situation [16]. This is confirmed by a study in which Ca-P coated specimens were inserted into the back of rabbits [17].

Considering all the above mentioned, we hypothesize that DCPD can undergo readjustment after implantation and is a material with biological potential for the coatings of dental and orthopedic devices. In view of this, the aim of this study is to investigate the *in vivo* dissolution and compositional behavior of DCPD coated titanium discs in a subcutaneous goat model.

## **Materials and Methods**

### ***Implant preparation***

For the experiments commercially pure titanium (cpTi) discs were provided with various CaP sputter coatings. The discs measured 1.5 mm in thickness and had a diameter of 12 mm. All discs were  $\text{Al}_2\text{O}_3$ -blasted on one side ( $R_a = 1.0\text{--}1.3\ \mu\text{m}$ ), which was provided with a

- 1 Calcium pyrophosphate-coating with a thickness of  $2\ \mu\text{m}$  (DCPD), or
- 2 Hydroxyapatite coating-coating with a thickness of  $2\ \mu\text{m}$  (HA), or
- 3 Left uncoated

RF magnetron sputter coatings were made by using a commercially available RF sputter deposition system (Edwards ESM 100). The target materials were calcium pyrophosphate ( $\beta\text{-Ca}_2\text{P}_2\text{O}_7$ ) and hydroxylapatite ( $\text{Ca}_5(\text{PO}_4)_3\text{OH}$ ) granules (diameter 0.5–1.0 mm). The test specimens were mounted on a rotating and water-cooled substrate holder. The distance between target and substrate was 80 mm. Before sputtering the metal substrates were cleaned by etching for 10 min with argon ions. During deposition, the argon pressure was kept at  $5 \times 10^{-3}$  mbar and the sputter power was 400 W.

After deposition, the coated specimens were subjected to an additional infrared heat treatment (HT) for 30 sec at 550 and 650°C (Quad Ellipse Chamber, Model E4-10-P, Research Inc.).

Before implantation, the coatings were characterized by thin film X-ray diffraction (Philips, PW3710, Almelo, The Netherlands), Fourier transform infrared (FTIR, Perkin Elmer, Fremont, CA, USA) and a scanning electron microscope (SEM, Jeol 6310, Tokyo, Japan) equipped with an energy dispersive spectroscope in order to determine the coating Ca/P ratio.

### ***In vivo subcutaneous study***

Six adult male goats with a mean body weight of about 60 kg were used in this study. Before surgery blood samples of the goats were taken to ensure that the animals were CAE/CL arthritis free. The animals were housed in a stable. National guidelines for the care and use of laboratory animals were observed.

IR heated HA and DCPD coated discs were implanted subcutaneously into the dorsal region of the goats. The operation was performed under local anesthesia. The anesthesia was induced by infiltration with 2% lidocaine solution. To reduce the risk of peri-operative infection, the goats were treated according to the following doses of antibiotics:

- during the operation: Albipen<sup>®</sup> 15 %, 3 ml/50 kg s.c.;
- one day after the operation: Albipen<sup>®</sup> LA, 7.5 ml/50 kg s.c.;
- three days after the operation: Albipen<sup>®</sup> LA, 7.5 ml/50 kg s.c.

Four implantation periods were used: 1 week, 4 weeks, 8 weeks, and 12 weeks. Paravertebrally, on either side of the vertebral column four surgical areas were used as recipient sites (alternately the left or right flank and caudal or frontal). The various recipient sites (each recipient site represented one implantation time) as well as materials in each recipient area were randomized according to a split plot design to exclude the effect of implantation location and individual differences. In four surgical sessions, the implants were placed subcutaneously into the back. Before surgery, the skin was shaved, washed, and disinfected with iodine. During each surgical session, three longitudinal incisions of about 1.5 cm were made parallel to the spinal column in the specific recipient site. Lateral to these incisions, small subcutaneous pockets were created by blunt dissection with scissors. The implants were inserted into these pockets and the wounds closed using Vicryl 3–0 intracutaneously. Each goat received 12 discs, six in the left and six at the right side of the spinal column. In total 72 discs were implanted, i.e. 24 infrared heated HA, 24 infrared heated DCPD coatings and 24 control Ti discs.

#### ***Physicochemical and histological analysis***

At the end of the 12 week period of the experiment, a longitudinal incision was made on both sides of the vertebral column. Then, the implants were exposed and retrieved including their surrounding fibrous tissue capsule. After removal, the implants were stored in alcohol water and transported to the laboratory. Subsequently, half of the retrieved specimens were used for physicochemical characterization and half for histological analysis.

For physicochemical characterization of the coatings after implantation, discs were removed out of the surrounding fibrous tissue capsule. The characterization consisted of thin film X-ray diffraction and scanning electron microscopy including energy dispersive spectroscopy.

For the histological observation, the specimens were fixed in formaldehyde 4%, dehydrated in serial ethanol solutions and embedded in methylmethacrylate (MMA). After polymerization in MMA thin (10 µm) non-decalcified sections were prepared with the Leiden-Microtome Cutting System (Biomaterial Research Group, Leiden University, The Netherlands), stained with basic fuchsin and methylene blue, and studied with a light microscope. Photomicrographs were taken of the tissue–implant interfaces for each histological section. At least two histological sections were evaluated of each material.



## Results

### *Implant surface characterization before implantation*

#### X-ray diffraction

The XRD patterns of the as-sputtered coatings showed an amorphous structure with no clear peaks (Figure 1). Infrared heat-treatment at 550°C changed the amorphous sputtered HA coatings into a crystalline apatite structure with reflections 002, 211, 112, 202, resp. 25.9°, 31.9°, 32.4° and 34.0° in 2-Theta, comparative with the XRD pattern of HA powder (JCPDS #09-0432). In contrast, the sputtered amorphous pyrophosphate coating required an annealing temperature of 650°C to alter into crystalline beta-calcium pyrophosphate structure with reflections lines 201, 202, 008 and 212, which correspond to peaks at 26.6°, 27.7°, 29.5° and 30.7° in 2-Theta (JCPDS#09-0346).

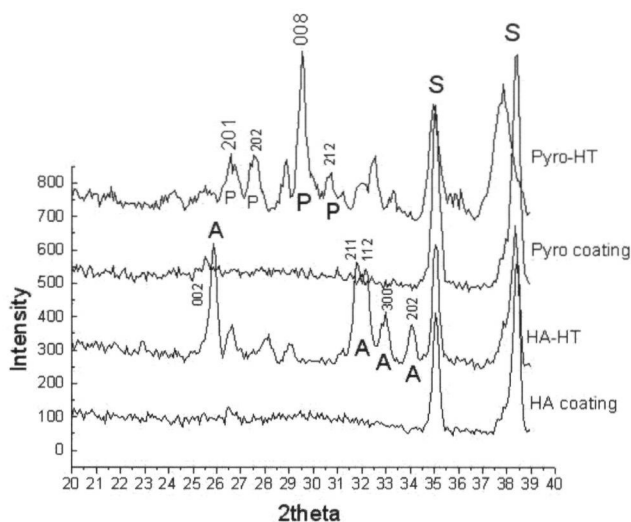


**Figure 1:** XRD patterns of the sputtered CaP coatings. The numbers indicate the major reflection lines for HA and dicalcium pyrophosphate. (A: apatite, P: pyrophosphate and S: titanium substrate)

#### Fourier transform infrared spectroscopy

FTIR measurements showed for all the amorphous coatings two clusters of bands from 900-1150 and from 550-600  $\text{cm}^{-1}$  attributed to the major absorption modes associated with the presence of phosphate (Figure 2). Heat treatment of the amorphous HA coatings resulted in the appearance of the hydroxyl band at 630  $\text{cm}^{-1}$ , characteristic for hydroxylapatite and the appearance of

various P-O bands at a wavelength of 587, 630, 965, 1009, 1083  $\text{cm}^{-1}$  (Figure 2). Heat treatment of the sputtered amorphous pyrophosphate coatings resulted in the appearance of various P-O bonds at the wavelength around 1202, 1163, 1125, 1095, 1081, 993, 957, 644, 608, and 522  $\text{cm}^{-1}$ , which are characteristic for the beta-calcium pyrophosphate structure (Figure 2).

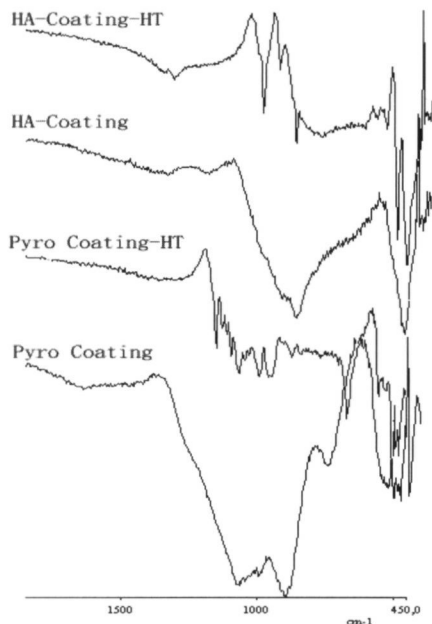


**Figure 2:** FTIR spectra of the various CaP coatings before and after infrared heat treatment (Y axis is in transmittance).

### **Scanning electron microscopy**

SEM examination of the sputtered coatings showed an excellent coverage of the substrate surface. Heat treatment was found to have no evident effect on the HA as well as pyrophosphate coating morphology (Figure3).

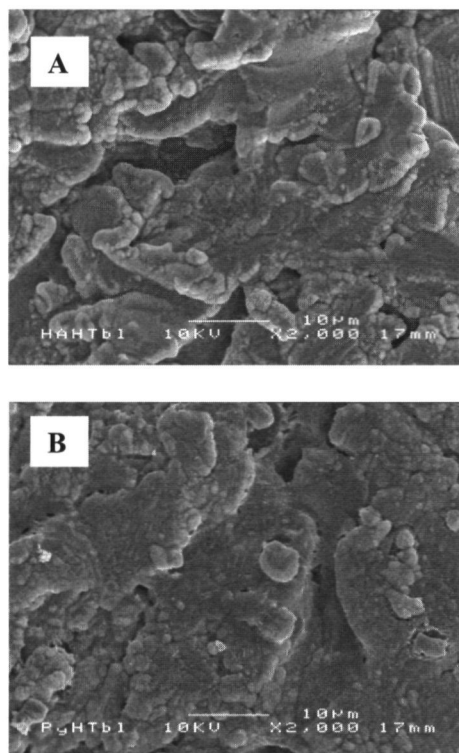


**Figure 3** SEM pictures of RF sputtered HA and DCPD coatings after infrared heat treatment; A = IR heated HA coating, B = IR heated calcium pyrophosphate coating.

### **Energy dispersive spectroscopy**

EDS analysis revealed that Ca/P ratio of amorphous as well as crystalline HA- and DCPD coatings varied between respectively 1.9-2.0 and 0.76-0.8.

### ***In vivo evaluation***

#### **Coating surface changes measured by XRD**

Figure 4 and 5 show the XRD patterns of the sputtered coating surfaces after 2, 4, 8 and 12 weeks implantation in the goat. The peaks around  $25.9^\circ$ ,  $26.6^\circ$ ,  $31-33^\circ$  in the XRD of infrared heated HA coatings showed a very limited decrease during the 12 weeks implantation time, which indicates a stable behavior of these coatings during implantation in an *in vivo* environment. In contrast, the XRD patterns of the infrared heated DCPD coated discs showed significant changes during implantation. Additional peaks appeared and some peaks intensified around  $25.9^\circ$  and  $31-33^\circ$ , which indicates the formation of an apatite and TCP precipitate on the coated surface. Especially, the appearance of TCP and apatite peaks corresponding to  $25.9^\circ$ ,  $31^\circ$ ,  $31.9^\circ$ ,  $32.4^\circ$  and  $34.5^\circ$  and the decrease of peak intensity around  $29.7^\circ$  for the 12 week specimens showed the change of DCPD into TCP and apatite in a biological environment (Figure 5).

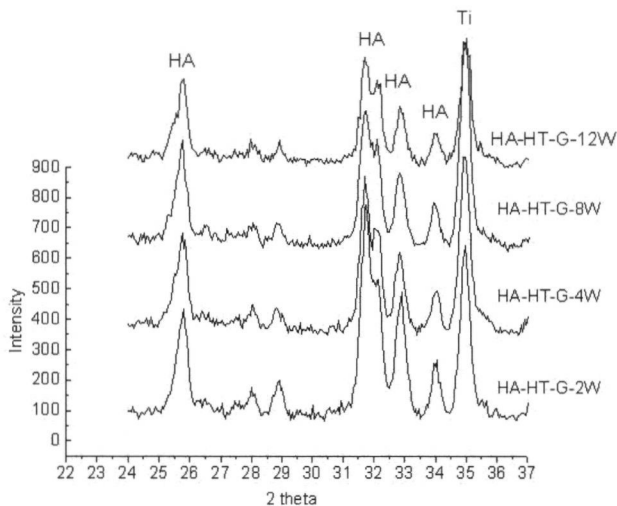


**Figure 4** XRD patterns of infrared heated HA coating after implantation for 2 to 12 weeks in the goats.

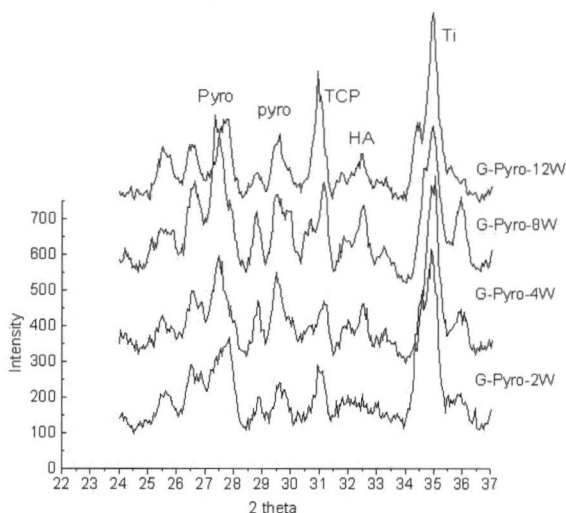


**Figure 5** XRD patterns of infrared heated DCP coating after implantation for 2 weeks to 12 weeks in the goats.

#### **Coating surface changes measured by SEM and EDS analysis**

Scanning electron microscopic (SEM) evaluation revealed that the removal of the implants out of their surrounding capsule had still left in the maintenance of some tissue debris. The implants were locally still covered by a tenacious layer of collagen fibers (Figure 6A). Nevertheless, this did not prevent a proper analysis. As demonstrated by SEM, after 12 weeks of implantation both the infrared heat-treated HA and DCP coating were maintained (Figure 6B and 6C). This was confirmed by EDS analysis (Table 1). EDS examination revealed that the Ca/P ratio of the DCP coating changed from 0.8 to 1.52, while the Ca/P ratio of the HA coatings remained stable during the 12 weeks of implantation.

**Table 1:** Ca/P measurements of DCP and HA coatings after subcutaneous implantation.

Implantation time	DCPP (Ca/P ratio)	HA (Ca/P ratio)
2 weeks	1.30 ± 0.01	1.88 ± 0.02
4 weeks	1.47 ± 0.09	1.85 ± 0.01
8 weeks	1.52 ± 0.04	1.86 ± 0.02
12 weeks	1.52 ± 0.04	1.85 ± 0.01

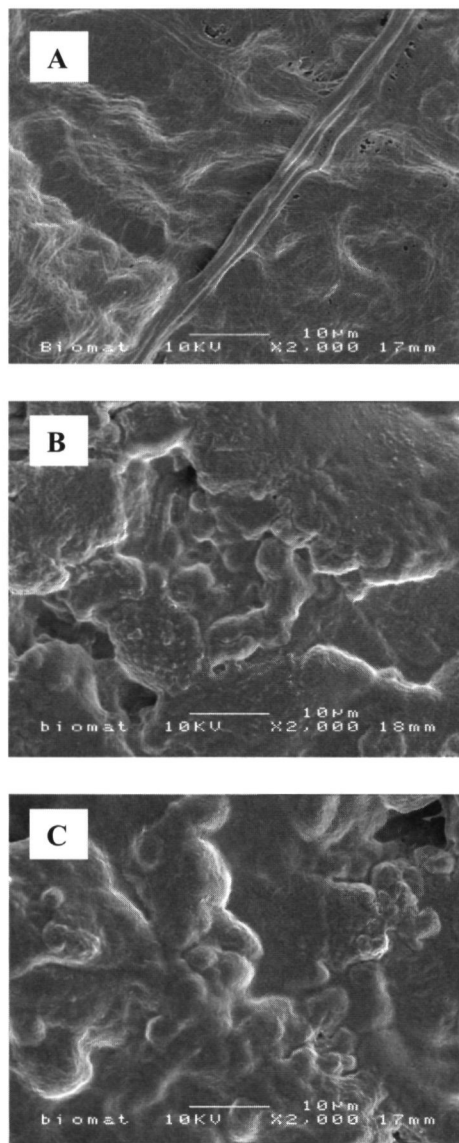


**Figure 6** SEM photographs of HA and DCP coating surface after subcutaneous implantation: A = HA coating after 2 weeks of implantation, B = HA coatings after 12 weeks of implantation and C = DCP coatings after 12 weeks of implantation.

### **Histological analysis**

Light microscopical evaluation of the specimens retrieved for histological analysis showed a biocompatible tissue behavior of both coatings and non-coated control specimens at all implantation times. Already at two weeks of implantation, both the heat-treated HA, DCPD coated and control Ti discs were surrounded by a thin (10-20 cells thick) fibrous tissue capsule (Figure 7A). During time, the capsule became denser, but did not increase in thickness. The capsular tissue was almost completely free of inflammatory cells. At the interface, a close contact existed between the fibrous capsule and the coating surfaces. In general, the interfacial response at all implantation times was characterized by the absence of inflammatory cells (Figure 7B).

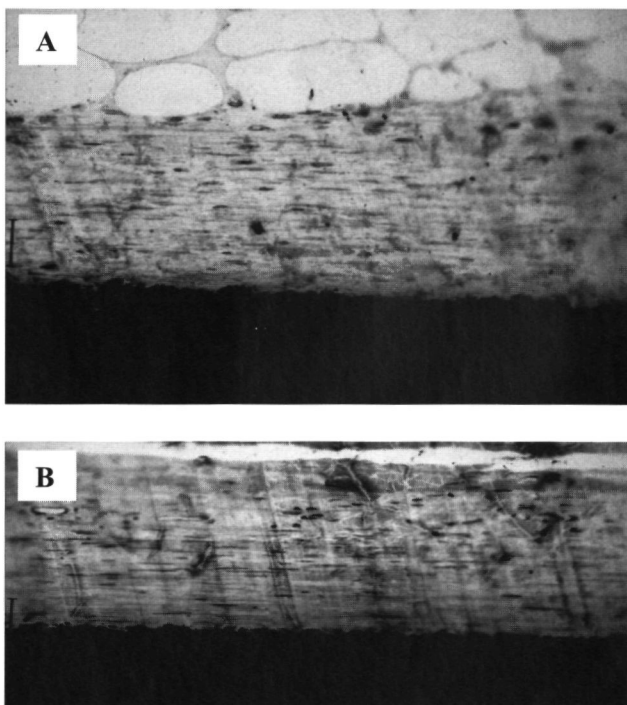


**Figure 7** Light micrographs of histological sections of HA and DCPD coated discs after subcutaneous implantation: A = DCPD coated disc; already two weeks after implantation, the disc is surrounded by a thin fibrous capsule that is in close contact with the coated surface (original magnification = 400x), B = HA coated disc; 12 weeks after implantation the fibrous capsule has densified and inflammatory cells are absent at the capsule-coating interface (original magnification = 400x).

## Discussion and Conclusion

The aim of the current study was to learn more about the dissolution and compositional behavior of thin heat-treated HA and DCPD coatings under *in vivo* conditions. Evidently, the results confirmed again the effectivity of our model for this kind of analyses. The heat-treated HA coatings were found to be stable during 12 week implantation in the subcutaneous tissue of goats. No structural or compositional changes were observed. This in contrast to the heat-treated DCPD coatings, which changed during time into apatite and TCP, which could be linked with a change in Ca/P ratio from 0.8 to 1.52. Further, both coatings were observed to evoke a biocompatible behavior characterized by the lack of a serious inflammatory response. Referring to implantation studies with plasma-sprayed TCP coatings [18] where during the initial weeks of implantation a significant increase in the number of inflammatory cells was seen, this suggests that the conformational change of the DCPD coatings is related to a gradual increase in the local concentration of calcium and phosphorus due to surface dissolution and precipitation. However, we have to emphasize that more research is required to the associated coating surface phenomena to support this suggestion. Further for the *in vivo* coating characterization, no use was made of FTIR. This was done, because the coatings were found to be coated with a very persistent organic layer, consisting amongst others of NH<sub>2</sub>-groups, which prevented a proper analysis of the coatings. SEM examination confirmed the presence of this organic layer that also could not be removed without serious damage to the coated film.

The X-ray diffractograms and EDS measurements revealed a gradual conformational change of the DCPD coatings into apatite and TCP in the subcutaneous tissue. This corroborates with the existing theory about the stability of calcium phosphate salts in a biological environment [19]. Under physiological conditions, calcium phosphate compounds are in a state of equilibrium with the formation of hydroxylapatite as the preferred, most stable phase. This is also the reason that all calcium phosphate ceramics are considered to be biocompatible besides the occurrence of differences in solubility and dissolution rate into biological fluids. The resistance against dissolution can further be affected by thermal post-treatment. For example, transforming amorphous HA coatings thermally into a more stable phase, is a standard procedure to avoid fast coating degradation [20]. A similar observation was done in the current study, rapid infrared radiation appeared to be an effective way to improve the crystallinity of the deposited coatings. Consequently, the peaks in the XRD pattern of the HA coatings showed a very limited, but still gradual decrease during the 12 week implantation time. This indicates that bioadsorption of the coating is possible, but only at a very low dissolution rate. A similar finding was done in an earlier subcutaneous study to the dissolution behavior of sputtered CaP coatings in rabbits [17, 21]. Then, a 0.1  $\mu\text{m}$  thick heat-treated HA coating deposited on roughened titanium discs was found to degrade completely within 8 weeks of implantation, while 1 and 4  $\mu\text{m}$  thick coatings



were maintained till 12 weeks of implantation. It can be assumed that finally the same will happen with the heat-treated DCPD coatings, i.e. during the transformation of the DCPD in apatite and TCP dissolution will occur resulting at the end in complete loss of the coating. Of course in a bony environment, at the same time an interfacial bonding zone will develop between the implant surface and surrounding bone [22, 23].

Considering the above mentioned, the reason for the choice of an *in vivo* test was that the dissolution behavior of CaP biomaterials implanted *in vivo* can be completely different compared with classical *in vitro* tests. This is due to the fact that the *in vivo* environment is composed of a complex array of various constituents, in particular macromolecules, which can all interact with CaP compounds. Such a condition can never be completely copied in an *in vitro* model. In view of this, it is even possible that CaP coated implants show different behavior in different tissues, like bone, muscle and subcutaneous tissue. For example, it is well known that all these tissues differ in composition and complexity and that difference in concentrations and availability of proteins, relevant for the dissolution and subsequent bonding zone development, occurs [24].

The light microscopical evaluation confirmed also the biocompatibility of both the HA and DCPD coatings. The interfacial response was characterized by a close contact between the fibrous capsule and coated implant surface with hardly any inflammatory response. The capsule is the consequence of the surgical trauma and the subsequent installation of foreign body. Nevertheless, the interfacial response is much better compared to a lot of polymeric implant materials. Evidently, this is caused by the biocompatible behavior of both titanium and CaP materials. In addition, a very limited surface roughness seems to have no additional negative effect on the final tissue response, which agrees with a previous study [21]. It can be supposed that movement in the flank of a goat is still very restricted or that the very confined surface roughness results in an improved subcutaneous anchorage of the coated discs, which can explain why the surface roughness did not result in an increase of inflammatory cells.

Our final goal is to use the DCPD coatings for bone implants. Currently, only very limited information is available, which indicates that both *in vitro* and *in vivo*, synthetic dicalcium pyrophosphate supports bone tissue formation [13, 25, 26]. In a recent *in vitro* study, we also observed that DCPD coatings are able to increase the proliferation and differentiation of osteoblast-like cells [27]. However, the mechanism of the underlying process and the exact benefit of DCPD coatings have to be proven. Further, care has to be taken of the fact that the precise structure of synthetic CaP compounds can differ very considerably of the natural material [28]. Starting material and processing route are very important parameters for the finally prepared product. How this interferes with the aimed tissue response is yet unclear.

On basis of the results, we conclude that 2  $\mu\text{m}$  thick infrared heat-treated, RF magnetron

sputtered HA and DCPD coatings are of sufficient thickness to withstand dissolution during 12 weeks of implantation in a subcutaneous location in goats. In addition, both coatings showed a biocompatible tissue behavior characterized by the formation of a thin fibrous tissue capsule and the absence of an inflammatory response. Further, infrared heat-treated DCPD coatings revealed a gradual compositional change into apatite and TCP. Of course, the conclusive beneficial effect of DCPD coatings has to be proven in a bone implantation study.

## References

- 1] Rosen HM. Porous, block hydroxyapatite as an interpositional bone graft substitute in orthognathic surgery. *Plast Reconstr Surg*. 1989;83:985-90.
- 2] Hes J, de Man K. Use of blocks of hydroxylapatite for secondary reconstruction of the orbital floor *Int J Int Maxillofac Surg*. 1990;19 275-78.
- 3] Klein CPAT, Patka P, Wolke JGC, De Groot K. Plasma sprayed coating of tetracalcium phosphate, hydroxylapatite and alpha TCP on titanium alloy an interphase study *J Biomed Mater Res*. 1991;25:53-65
- 4] Martin Lind, Søren Overgaard, Cody Bunger and Kjeld Søballe. Improved bone anchorage of hydroxyapatite coated implants compared with tricalcium-phosphate coated implants in trabecular bone in dogs. *Biomaterials* 1999;9:803-8.
- 5] Sanden B, Olerud C, Larsson S Hydroxyapatite coating enhances fixation of loaded pedicle screws A mechanical *in vivo* study in sheep *Eur Spine J*. 2001;10 334-9
- 6] Sanden B, Olerud C, Johansson C, Larsson S Improved bone screw interface with hydroxyapatite coating An *in vivo* study of loaded pedicle screws in sheep *Spine* 2001;26:2673-8
- 7] Fini M, Giavaresi G, Greggi T, Martini L, Nicoli Aldini N, Parisini P, Giardino R. Biological assessment of the bone-screw interface after insertion of uncoated and hydroxyapatite-coated pedicular screws in the osteopenic sheep *J Biomed Mater Res* 2003, 66A 17683
- 8] Lee TM, Wang BC, Yang YC, Chang E, Yang CY. Comparison of plasma-sprayed hydroxyapatite coatings and hydroxyapatite/tricalcium phosphate composite coatings *In vivo* study *J Biomed Mater Res* 2001;55:360-7
- 9] Chen QZ, Wong CT, Lu WW, Cheung KMC, Leong JCY, Luk KDK. Strengthening mechanisms of bone bonding to crystalline hydroxyapatite *in vivo* *Biomaterials*. 2004;25 4243-54.
- 10] Porter AE, Taak P, Hobbs LW, Coathup MJ, Blunn GW and Spector M. Bone bonding to hydroxyapatite and titanium surfaces on femoral stems retrieved from human subjects at autopsy, *Biomaterials*. 2004;21.5199-208.
- 11] Weichang X, Shunyan T, Xuanyong L, XueBin Z and Chuanxian D *In vivo* evaluation of plasma sprayed hydroxyapatite coatings having different crystallinity. *Biomaterials*. 2004;3:415-21.
- 12] Langstaff S, Sayer M, Smith TJN and Pugh SM. Resorbable bioceramics based on stabilized calcium phosphates. Part II: evaluation of biological response, *Biomaterials*. 2001;22:135-50
- 13] Sun JS, Tsuang YH, Liao CJ, Liu HC, Hang YS, Lin FH. The effects of calcium phosphate particles on the growth of osteoblasts, *Journal of Biomedical Materials Research*. 1997;37:324-34
- 14] Cheung HS, Story MT, McCarty DJ Mitogenic effects of hydroxyapatite and calcium pyrophosphate dihydrate crystals on cultured mammalian cells *Arthritis Rheum*. 1984;27 668-74.
- 15] van Dijk K, Gupta V, Yu AK, Jansen JA Measurement and control of interface strength of RF magnetron-sputtered Ca-PO coatings on Ti-6Al-4V substrates using a laser spallation technique. *J Biomed Mater Res*. 1998;41:624-32.
- 16] Klein CPAT, Patka P, van der Lubbe HBM, Wolke JGC, de Groot K. Plasma-sprayed coatings of tetracalciumphosphate, hydroxyapatite, and  $\alpha$ -TCP on titanium alloy An interface study. *J Biomed Mater Res*. 1991;25:53-65.
- 17] Wolke JGC, Groot Kd, Jansen JA. *In vivo* dissolution behavior of various RF magnetron sputtered Ca-P coatings *J Biomed Mater Res* 1998;39 524-30.
- 18] Dhert WJA, Klein CPAT, Jansen JA, van der Velde EA, Vriesde RC, Rozing PM, de Groot K A histological and histomorphometrical investigation of fluorapatite, magnesiumwhitlockite, and hydroxylapatite

- plasma-sprayed coatings in goats. *J Biomed Mater Res.* 1993;27:127-38
- 19] Ravaglioli A, Krajewski A. Materials for surgical use, in: *Bioceramics*. Chapman, Hall (eds). London, 1992;100-197
- 20] Lu YP, Song YZ, Zhu RF, Li MS, Lei TQ. Factors influencing phase compositions and structure of plasma sprayed hydroxyapatite coatings during heat treatment, *applied surface. Science.* 2003;206:345-54
- 21] Wolke JGC, van der Waerden JPCM, Schaecken H, Jansen JA. In vivo dissolution behavior of various RF magnetron sputtered Ca-P coatings on roughened titanium implants. *Biomaterials* 2003;24:2623-9
- 22] Hanawa T, Ota M. Characterization of surface film formed on titanium in electrolyte using XPS. *App Surf Sci* 1992;55:269-76.
- 23] Hulshoff JEG, van Dijk K, de Ruijter JE, Rietveld FJR, Ginsel LA, Jansen JA. Interfacial phenomena: an in vitro study to the effect of calcium phosphate (Ca-P) ceramic on bone formation. *J Biomed Mater Res* 1998;40:464-74.
- 24] Combes C, Rey C. Adsorption of proteins and calcium phosphate materials bioactivity. *Biomaterials* 2002;23: 2817-23.
- 25] Lin FH, Lin CC, Lu CM, Liu HC, Sun JS, Wang CY. Mechanical properties and histological evaluation of sintered  $\beta$ - $\text{Ca}_2\text{P}_2\text{O}_7$  with  $\text{Na}_4\text{P}_2\text{O}_7 \cdot 10\text{H}_2\text{O}$  addition. *Biomaterials* 1995;16:793-802
- 26] Sun JS, Huang YC, Tsuang YH, Chen LT, Lin FH. Sintered dicalcium pyrophosphate increases bone mass in ovariectomized rats. *J Biomed Mater Res* 2002;59:246-53.
- 27] Yan Y, Wolke JGC, de Ruijter JE, Li Y, Jansen JA. Growth behaviour of Rat Bone Marrow (RBM) cells on RF magnetron sputtered hydroxyapatite and dicalcium pyrophosphate coatings, Submitted. *J Biomed Mater Res* 2005.
- 28] Murugan R, Ramakrishna S. Crystallographic study of hydroxyapatite bioceramics derived from various sources. *Crystal Growth and Design.* 2005;5:111-112.

## **Chapter 7**

### **Thin Hydroxyapatite film formation on the surface of polyamide-6 and nano-HA/ polyamide-6 composite by RF magnetron sputtering deposition**

Submitted: J Mat. Sc: Mat. Med, 2005

Yonggang Yan, J. G.C Wolke, Li Yubao, J.A. Jansen

## Introduction

Hydrothermally synthesized, nanograde, needle-shaped apatite crystal (nanoapatite) is similar to bone apatite in morphology, crystal structure, composition and crystallinity, and could probably improve biological performance of calcium phosphate biomaterials [1-4]. But most calcium phosphate ceramics are brittle and fracture easily when used for load bearing implants. In order to enhance the toughness of calcium phosphate biomaterials, this ceramic is applied as coating on mechanical strong titanium implant materials [5-7]. There are many ways to make this kind of coatings of which plasma spraying is nowadays the most widely used technique to apply such coatings [8, 9]. However, this method suffers from some severe drawbacks (such as a limited adherence to the substrate, the large thickness of the coating and the non-thickness uniformity) [10]. Another limitation of plasma spraying is the high temperature that may decompose or destroy polymers, so that it cannot be applied to deposit CaP coatings on polymeric biomaterials. Therefore other techniques to prepare thin, strong and dense coatings have been investigated [10-16]. Among these techniques RF magnetron sputter deposition is a promising way to get a thin, adherent, and dense calcium phosphate coatings and can also be used for the coating of polymers [17-21].

Another way to avoid the brittle poor property of CaP bioceramic is to make HA/polymer composites. The combination of bioactive HA and tough polymer may result in a new load-bearing bioactive material with good mechanical and biological properties [18-25]. At present, most HA/Polymer composites are prepared through mixing HA powder and polymers and their subsequent extrusion, which makes it difficult to make composites with good homogeneity and high bioactivity. Preparation of apatite/polymer composites in solution and co-polymerization would be more helpful than mechanically mixing with clogged powders [26-29]. Since the HA component in the composite is usually lower than 50% in weight (when the HA content is too high, the composite becomes brittle) [30, 31], the composite may not be as bioactive as pure HA. To develop more bioactive and strong biomaterials, we suggest to deposit a HA coating on the polymer and the HA/polymer composite surface in order to improve the bioactivity of these materials similar to what is done on the surface of metals

Therefore, the objective of this study is to deposit thin HA films on the surfaces of polyamide-6 (PA6) and nano-HA /PA-6 composite (NHA/PA-6) using a RF magnetron sputter deposition method in order to obtain biomaterials with increased bioactivity.

## **Materials and Methods**

### ***Target materials***

Hydroxyapatite (HA) granules were used as target material. Further, Polyamide-6 (PA-6) with a molecular weight of 18000 (weight average molecular mass) (Asahi Chemical Co. Ltd, Japan) was used.

Nanohydroxyapatite/Polyamide-6 composite (NHA/PA-6) was prepared by a solution approach as described before [21-22]. The nano-HA in the composite was about 40 wt%.

Substrates for coating deposition were prepared by injecting PA-6 at 250°C and nanohydroxyapatite/PA-6 composites at 265°C respectively through an extruder and then cut to 10x10x1mm discs.

### ***Sputtering***

RF magnetron sputter coating was performed using a commercially available RF sputter deposition system (Edwards ESM 100). The target material was HA. The substrates, PA-6 and NHA/PA-6, were attached to a water-cooled specimen holder using silver-paint. The specimen holder was continuously rotated. The process pressure was  $5 \times 10^{-3}$  mbar, the sputter power was 300w and the sputter time was 6 hours, resulting in a coating with a thickness of about 2  $\mu\text{m}$ . Subsequently, a part of the sputtered samples was heated at 140°C in water steam for 6 hours.

### ***Coating characterization***

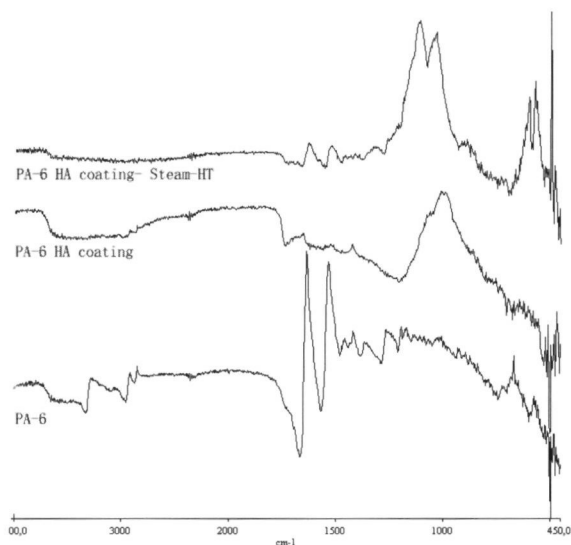
The crystallographic structure of the deposited HA films and precipitates on the coating surface were determined by thin film X-ray diffraction (XRD) using a Philips X-Ray Diffractometer (PW3710), using  $\text{CuK}\alpha$ -radiation. The infrared spectra of the films on the substrates were obtained by reflection Fourier transmission infrared spectroscopy (FTIR) (Perkin-Elmer 850). The appearance and the uniformity of the coating were examined with a scanning electron microscope (Philips SEM-525) with an energy disperse spectroscopy (EDS) x-ray detector. Information about the elemental compositions of the coated specimens was obtained by both EDS analysis and X-ray probe scanning (XPS, XSAM 800). Atomic force microscopy (AFM) was done with a SPA 400 Instrument (SIS Co. Lt.).

## Results

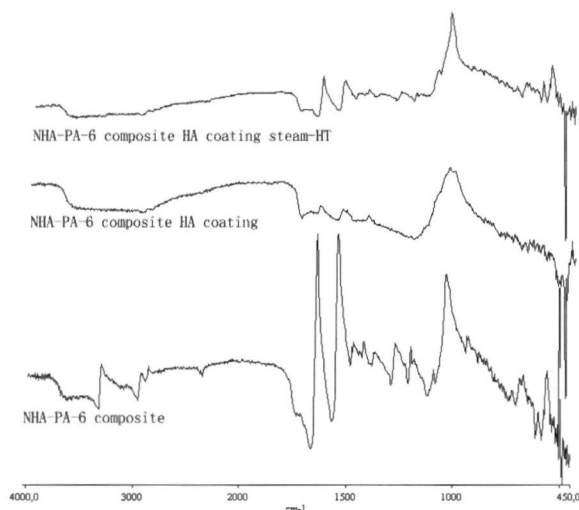
### *Changes in the structure of the PA-6 and NHA/PA-6 composite surface*

Figure 1a shows the IR spectra of PA-6, sputtered PA-6, and sputtered PA-6 after heat treatment at 140°C in water steam. Figure 1b shows the IR spectra of NHA/PA-6 and its sputtered samples, respectively. The peak at 3301  $\text{cm}^{-1}$  in PA-6 and in NHA/PA-6 composite belongs to the N-H bond. The stretching vibration of N-H and C=O in PA-6 could be observed at 3423  $\text{cm}^{-1}$  and 1641  $\text{cm}^{-1}$  in both PA-6 and NHA/PA-6 composite. Comparison of IR spectra of original PA-6 and NHA/PA-6 composite with those of sputtered samples revealed that the peaks at 3301  $\text{cm}^{-1}$  and 3423  $\text{cm}^{-1}$  disappeared in both PA-6 and NHA/PA-6 composite, while the peaks around 1641  $\text{cm}^{-1}$  became very weak for both PA-6 and its nano HA composite after sputtering. A broad big peak around 1000  $\text{cm}^{-1}$  was present for the sputtered PA-6 sample and the peaks around 1000  $\text{cm}^{-1}$  in NHA/PA-6 became rounded. After heating at 140°C in water steam, the peaks around 1000  $\text{cm}^{-1}$  became sharp and did split. Also, a peak at 630  $\text{cm}^{-1}$  became stronger after heating at 140°C in water steam, indicating that the amorphous HA coating changed into a crystalline structure.

**A**





**B**

**Figure 1:** FTIR spectra of PA-6 and NHA/PA-6 composite before and after sputtering (A) PA-6 and (B) NHA/PA-6

### ***Ca, P and O binding energy changes in the NHA/PA-6 composite surface***

Table 1 lists the binding energy of the Ca, P and O in original HA (hydroxyapatite powder), PA-6, NHA/PA-6 composite, sputtered samples and sputtered samples heated at 140°C in water steam. The results show that the binding energy of Ca, P and O differs before and after sputtering. The binding energy of O in NHA/PA-6 composite was 531.8 eV, higher than that of O in original HA with 0.3 eV; the binding energies of Ca in NHA/PA-6 composite were 351.5 and 347.6, also higher than those of the original HA with 0.6 and 0.2 eV. The binding energy of P was also 0.1 eV higher than the original binding energy. These findings can be explained by the affinity between  $\text{Ca}^{2+}$ , hydroxyl (-OH),  $\text{PO}_4^{3-}$  in apatite and carboxyl (-COOH) in the copolymer. In view of this, there appears to be some combination between HA and Poly amide-6, indicating that the composite has a stable interface.

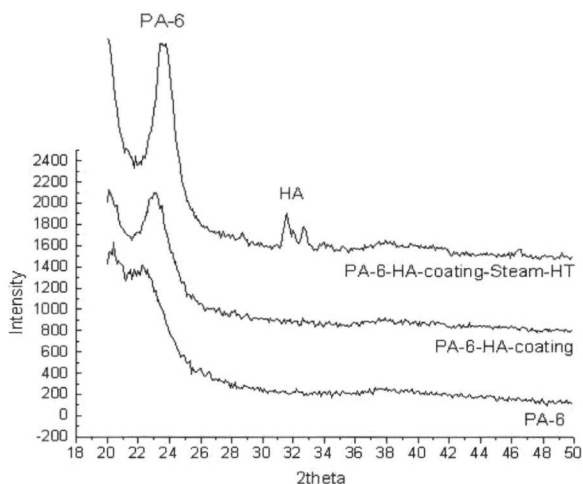
Comparison of the binding energy of Ca, O, and P in sputtered PA-6, sputtered NHA/PA-6 composite and heated samples in water steam with those of the original HA showed that the binding energy of Ca, O, and P in sputtered PA-6 and sputtered NHA/PA-6 composite was very close to those in original HA. This means that the coating kept the HA properties after sputtering and after heated at 140°C in water steam.

**Table 1** Binding energy changes in Ca, P after sputtering on NHA/PA-6 composite

Binding energy(ev)	Ca <sub>2p</sub>	P <sub>2p</sub>	O <sub>1s</sub>	N <sub>2p</sub>
HA (original)	350.9 347.4	133.5	531.5	-----
PA-6 Blank	---- ----	-----	532.0	399.8
NHA/PA-6 composite Blank	351.5 347.6	133.6	531.8	399.8
PA-6-RF	350.9 347.3	133.6	531.3	399.5
PA-6-RF-HT	350.8 347.2	133.3	531.3	399.5
NHA/PA-6-RF	350.9 347.3	133.6	531.3	399.5
NHA/PA-6-RF-HT	350.8 347.2	133.3	531.3	399.5

### *Changes in surface composition of PA-6 and NHA/PA-6 composite*

Figure 2 shows the XRD patterns of PA-6, sputtered PA-6, and sputtered PA-6 after heat treatment at 140°C in water steam. Figure 3 depicts the XRD patterns of NHA/PA-6 composite and its sputtered samples, respectively. The peaks at 21° and 23.5° in 2 $\theta$  can be assigned to the PA-6 substrate. These peaks show no big changes in the XRD before and after sputtering of both PA-6 and NHA/PA-6 composite. After heating of the sputter coated PA-6 samples at 140°C in water steam, peaks at 25.9°, 31.9°, 32.4° and 34.0° 2 $\theta$  appeared (reflections 002, 211, 112, 202), indicating HA crystal formation on the PA-6 surface. A similar phenomenon occurred at the NHA/PA-6 composite specimens. Evidently, after heating the sputtered coatings showed the same typical HA crystal structure as the XRD patterns of HA coatings on a titanium surface after heat treatment [16].

**Figure 2** XRD patterns of PA-6, sputtered PA-6 and sputtered PA-6 heated at 140°C in water steam

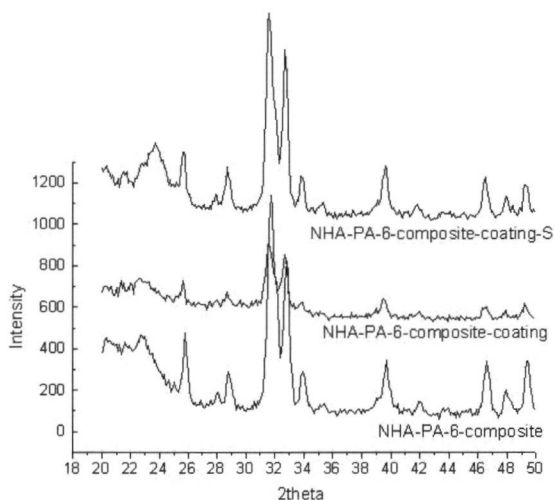


**Figure 3:** XRD patterns of NHA/PA-6 composite, sputtered NHA/PA-6 and sputtered NHA/PA-6 heated at 140°C in water steam

#### ***Ca-P content and Ca/P ratio changes of the PA-6 surface and NHA/PA6 composite surface***

Table 2 shows the Ca/P ratio and HA content on the surface of the PA-6 and NHA/PA-6 composite before and after sputtering as measured by EDS. These figures show that little Ca and P were present on the original PA-6 surface. The Ca and P content on the original NHA/PA-6 composite surface was 25.78 % and 11.27 %, respectively. After sputtering, the Ca and P content on the surface of PA-6 increased to 42.55 % and 17.66 %, and for the NHA/PA-6 composite to 31.10a% and 14.61 % respectively. After heating at 140°C in water steam, the Ca and P content changed very little. The Ca/P ratio of the as-prepared NHA/PA-6 composite surface was 1.77 and decreased after sputtering to 1.64. The Ca/P ratios of the coated specimens changed very limited after heating at 140°C in water steam, indicating that the original composition and properties of both polymers were maintained.

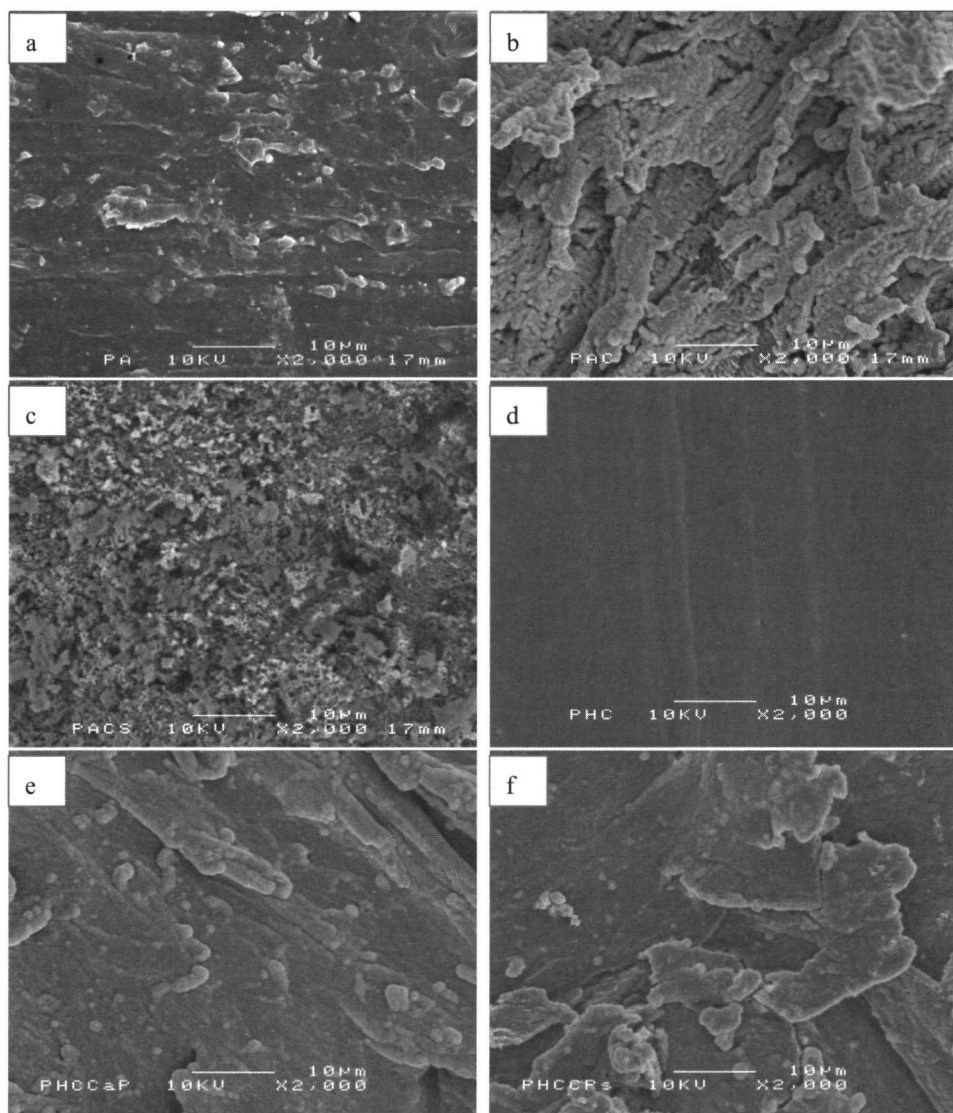
#### ***Morphology of the surface of the coated PA-6 and NHA/PA-6 composites***

Figure 4 shows the SEM micrographs of PA-6, sputtered PA-6, and sputtered PA-6 after heat treatment at 140°C in water steam. Figure 4 shows also the SEM pictures of NHA/PA-6 composite and its sputtered samples. The results show that after sputtering the surfaces of both PA-6 and NHA/PA-6 composite were covered with dense HA films. The HA film looked homogenous. After heating at 140°C in water steam a uniform layer of crystals was formed, this covered the surfaces of both PA-6 and NHA/PA-6 composites. Figure 5 depicts the AFM macrographs of the uncoated NHA/PA-6 composite, sputtered NHA/PA-6

composite and sputtered sample after heating 140°C in water steam. A lot of small particles covered the original composite surface (Figure 5a). Additional small particles appeared on the surface after sputtering and the surface looked blurred because of the amorphous coating deposition (Figure 5b). After heat treatment the crystals became clearly visible (Figure 5c). The diameter of the particles was about 30~50 nm and their length was about 50~70nm. This indicated that the HA crystals in the coating had the same morphology as those in the original composite, i.e. they maintained their nanograde character.

**Table 2** Calcium and Phosphate content and Ca/P ratio on the surface of PA-6 and NHA/PA-6 composite measured by EDS

Items	Ca (wt%)	P (wt %)	Ca/P (At %)
PA-6 blank	---	---	---
PA-6-RF	42.55	17.66	1.86
PA-6-RF-HT	42.45	17.72	1.85
NHA/PA-6 composite	25.78	11.27	1.77
NHA/PA-6 composite-RF	31.10	14.61	1.64
NHA/PA-6 composite-RF-HT	33.23	14.16	1.64



**Figure 6:** SEM macrograph of PA-6/HA compsite surface after RF sputtering. (a) PA-6 surface, (b) sputtered PA-6, (c) sputtered PA-6 heated at 140°C in water steam, (d) NHA/PA-6 composite, (e) sputtered NHA/PA-6 composite and (f) sputtered NHA/PA-6 composite heated at 140°C in water steam

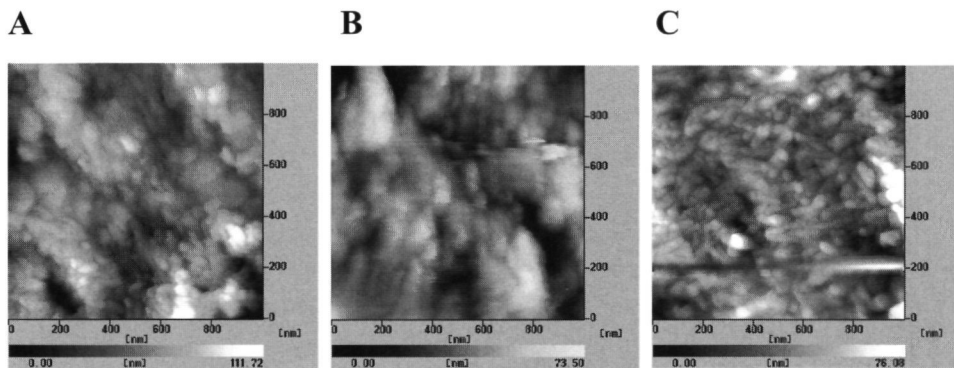


**Figure 5:** AFM micrograph of (A) NHA/PA-6 composite, (B) NHA/PA-6/HA composite after sputtering and (C) NHA/PA-6/HA composite after a steam heat treatment.

## Discussion

After implantation in the bone, implants directly contact with the body fluid. Precipitation, dissolution and exchange of ions occur immediately on the surface of the implants. The bioactivity of an implanted material is determined by the surface composition and activity of osteoblast-like cells is dependent on the crystallinity and phase composition of the CaP-coated surfaces [23, 24]. Although PA is used as medical device, like for sutures, it is not bioactive. On the other hand, nano HA/PA showed a good bioactivity and biocompatibility, but it becomes brittle when the HA content in the composite is too high [30, 31]. Consequently, the deposition of an additional HA coating on the PA and PA composite surface can provide bioactivity, while the mechanical properties of the polymers are maintained.

In the present research, we applied the RF magnetron sputter deposition technique to modify the surfaces of the PA-6 and NHA/PA-6 composite. The obtained results were found to be promising. Usually CaP coatings deposited on the substrates are amorphous or contain amorphous phases and need post annealing to get improved crystallinity. The crystallization of amorphous Ca-P coating can occur only above a certain temperature (i.e. 500°C) [25]. However, heat treatment at a high temperature destroys the polymer. Therefore, a lower heat treatment temperature is essential for HA coatings on polymers. Hontsu et al [26, 27] investigated the crystallization of CaP coatings on polymeric substrates (PTFE, PI, PDMS, and PET) by performing a long anneal (10 hours) just below the melting temperature of the substrates. On PTFE and PI, partially crystalline coatings were obtained by annealing at 320°C and 360°C, respectively. However, on PDMS and PET, the coating remained amorphous, after an annealing at 240°C and 260°C. Evidently, decreasing the heat treatment temperature is very important for CaP coatings on polymeric substrates. In the current study,

we used steam heating to change the crystallinity of amorphous HA coatings on PA-6 and NHA/PA-6 composite surface at a low temperature of 140°C. The FTIR peaks at 3301  $\text{cm}^{-1}$  and 3423  $\text{cm}^{-1}$  disappeared in both PA-6 and NHA/PA-6 composite after sputtering, which confirmed the deposition of HA on both PA-6 and NHA/PA-6 composite surface. The peak around 1000  $\text{cm}^{-1}$  (PO group) was split up after heat treatment at 140°C in water steam on both PA-6 and NHA/PA-6 composite surfaces. The XRD patterns indicated that the HA coatings on both substrates were amorphous and turned into a crystalline phase after heating at 140°C in water steam. Comparison of XRD curve of before and after sputtering showed that the PA-6 and NHA/PA-6 material maintained the original crystal structure.

Besides, it is generally supposed that an amorphous coating dissolves faster than a crystalline coating, i.e. crystallinity is the dominant factor for the dissolution of the HA coating. However, it has to be noticed that also some studies found little difference in dissolution between amorphous and crystalline coatings or even opposite results were obtained [28]. Further, the Ca and P content measurements and the Ca/P ratio changes indicated that the HA content on the NHA/PA-6 surfaces was much higher than in the NHA/PA-6 composite, because the HA content in the substrates decreased from the surface to the inside till a stable level was reached. From this point of the view, the coated NHA/PA-6 composite can be considered as a gradient bioactive biomaterial.

The SEM and AFM pictures illustrated that the coating was homogeneously deposited and that the size of the HA crystals was less than 50 nm. Consequently, the sputtered HA coatings on the NHA/PA-6 are a type of nano-HA coatings. This is similar as natural bone, which also can be considered as nano-apatitic [29]. Natural bone is an organic-inorganic hybrid material made of organic collagen and inorganic apatite crystals with a characteristic structure that leads to specific mechanical properties, such as a high fatigue toughness and high flexibility [30]. In view of this, the nano-HA coating-nano-HA/PA-6 composite system developed in the present study imitates the bone structure. Therefore, the nano-HA coating-PA-6 and nano-HA coating-NHA/PA-6 composite system as prepared by RF sputtering might be suitable for clinical application as potential bone replacement material and bone fixation material.

## **Conclusions**

A new kind of inorganic-organic biomaterials (HA thin film-PA-6 and HA coating-nano-HA/Polyamide-6 composite) were successfully developed using RF magnetron sputtering.

Sputtered HA coatings on both the PA-6 and nano-HA/PA-6 composite are homogenous and amorphous. The amorphous HA film can change into a fine crystalline structure when heated at 140°C in water steam. The crystal structure of the sputtered HA coatings on both PA-6 and NHA/PA-6 composite shows a typical HA structure. Therefore, water steam heat treatment is

a promising method to alter amorphous HA into crystalline on the polymer surface

The binding energy of Ca, P and O of HA in the HA coating on the composites surface was more like that of the original HA powder. The diameter of the HA particles in the deposited coating was about 40nm. The Ca/P ratio was 1.64 after RF sputtering, close to that of the stoichiometric HA, but different compared with the HA particles in the original composites.

The prepared inorganic-organic and inorganic-organic/inorganic composites show a structure similar to natural bone and can have a promising potential for use as bone implant and as scaffold material in tissue engineering.



## References

- 1] Groot K. Bioceramics consisting of calcium phosphate salts. *Biomaterials*. 1980;1:47-50
- 2] Yubao L, Groot K, Wijn J. Morphology and composition of nanograde calcium phosphate needle-like crystal formed by simple hydrothermal treatment. *J Mater Sci: Mater in Med*. 1994;5:326-31.
- 3] Yubao L, de Wijn J, Klein CPAT, van der Meer, Groot K. Preparation and characterization of nanograde osteoapatite-like rod crystals. *J Mater Sci.: Mater in Med*. 1994;5:252-5.
- 4] Hulbert SF, Bokros JC, Hench LL, Wilson J, Heimke G. P. Vincenzini. High Tech. Ceramics: Ceramics in clinical applications, past, present and future: 1986;Milan:189-213.
- 5] Groot K, Geesink R, Klein CPAT, Serelien P. Plasma sprayed coatings of hydroxyapatite. *J Biomed Mater Res*. 1987; 21:1375-81.
- 6] Barthell HL, Archuleta TA, Kossowsky R. Ion beam deposition of calcium hydroxyapatite. *Mater Res Soc Sym Proc*. 1989;110:709.
- 7] Oguchi H, Ishikawa K, Ojima S, Hirayama Y, Seto K, Eguchi G. Evaluation of a high velocity flames spraying technique for hydroxyapatite. *Biomaterials*. 1992;13:471-7.
- 8] Ducheyene P, Radin S, Heughebaert M, Heughebaert JC. Calcium phosphate ceramic coatings on porous titanium: effect of structure and composition on electrophoretic deposition, vacuum sintering and in vitro dissolution. *Biomaterials*. 1990;11:244-54.
- 9] Rajiv K, Singh F, Qian F, Nagabushnam V, Dammodaran R, Moudgil BM. Excimer laser deposition of hydroxyapatite thin films. *Biomaterials*. 1994;15:522-8.
- 10] Cotell CM, Chrisey DB, Grabowski KS, Sprague JA. Pulsed laser deposition of hydroxyapatite thin films on Ti-6Al-4V. *J Appl Biomater*. 1992;8:87-93.
- 11] Yoshinari M, Ohtsuka Y, Dérand T. Thin hydroxyapatite coating produced by ion beam dynamic mixing method. *Biomaterials*. 1994;15:529-35
- 12] Wolke JGC, de Bleeck-Hogervorst JMA, Dhert WJA, Klein CPAT, de Groot K. Studies on thermal spraying of apatite bioceramics. *J Therm Spray Techn*. 1992;1:79-...
- 13] Jansen JA, Wolke JGC, Swann S, van der Waerden JPCM, de Groot K. Application of magnetron sputtering for producing ceramic coatings on implant materials. *Clin Oral Impl Res*. 1993;4:28-34.
- 14] van Dijk K, Schaeken HG, Wolke JGC, Jansen JA. Influence of annealing temperature on RF magnetron sputtered calcium phosphate coatings. *Biomaterials*. 1996;17:405-10.
- 15] van Dijk K, Schaeken HG, Wolke JGC, Maree CHM, Habraken FHPM, Verhoeven J, Jansen JA. Influence of discharge power level on the properties of hydroxyapatite films deposited on Ti6Al4V with RF magnetron sputtering. *J Biomed Mat Res*. 1995;29:269-76.
- 16] Yoshinari M, Hayakawa T, Wolke JGC, Nemoto K, Jansen JA. Influence of rapid heating with infrared radiation on RF magnetron-sputtered calcium phosphate coatings. *J Biomed Mater Res*. 1997;37:60-7.
- 17] Ozeki K, Yuhta T, Fukui Y. A functionally graded titanium/ hydroxyapatite film obtained by sputtering. *J Mater Sci: Mater in Med*. 2002;13:253-64.
- 18] Bonfield W. Biomaterials and biomechanics: hydroxyapatite reinforced polyethylene composites for bone

- replacement. Ducheyne P, van der Perre G, Aubert AE. Elsevier Science Publishers BV Amsterdam 1984.345-51.
- 19]van Blitterswijk CA Bone-bonding biomaterials: interfacial reaction leading to Bone-bonding with PEO/PBT copolymer. Ducheyne P et al : 1992, Reed Healthcare Communications: 13
- 20]Huang M, Feng J, Wang J, Zhang X, Li Y, Yan Y. Synthesis and characterization of nano-HA/PA66 composites. J of Mat Sci: Mater in Med. 2003;14:655-60.
- 21]Yan Y, Yubao L, et al. Preparation and characterization of nano-HA/PA66 composites. Pl Industr. 2000,3:38- .
- 22]Kisugi T, Yamamuro T, Nakamura T, Oka M. Transmission electron microscopy observations at the interface of bone and four types of calcium phosphate ceramics with different calcium/ phosphorus molar ratios Biomaterials 1995;16:1101-7.
- 23]Ducheyne P, Radin S, King L. The effect of calcium phosphate ceramic composition and structure on in vitro behavior. I. dissolution J Biomed Mater Res. 1993;27:25-34.
- 24]Luo ZS, Cui, Li WZ. Low-temperature crystallization of calcium phosphate coatings synthesized by ion-beam-assisted deposition. J Biomed Mater Res. 1999;46:80-6.
- 25]Hontsu S, Nakamori M, Tabata H, Ishii J, Kawai T. Pulsed laser deposition of bioceramic hydroxyapatite thin films on polymer materials. Jpn J Appl Phys. 1996;2 L1208-10.
- 26]Hontsu S, Nakamori M, Tabata H, Ishii J, Matsumoto T, Kawai T. Formation of hydroxyapatite thin films on surface-modified polytetrafluoroethylene substrates. Jpn J Appl Phys. 1998;2:L116971.
- 27]Maxian SH, Zawadsky JP, Dunn MG. *In vitro* evaluation of amorphous calcium phosphate and poorly crystallized hydroxyapatite coatings on titanium implants. J Biomed Mater Res. 1993;2791.111-17.
- 28]Miyazaki T, Ohtsuki C, Akioka Y, Tanihara M. Apatite deposition on polyamide films contain carboxyl group in a biomimetic solution. J of Mat Sci: Mat in Med 2003;14:569-74.
- 29]Shi D, Jiang G, Bauer J. The effect of structural characteristics on the in vitro bioactivity of hydroxyapatite. J. Biomed Mater Res. 2002,63B.71-8

## **Chapter 8**

### **Summary and final remarks**

Considering the chemical composition, structure, and response to the biological environment, calcium phosphate ceramics have been proven to show an outstanding behavior in orthopedic and dental applications, especially for the healing of bone defects and replacement of lost teeth as well as damaged joints. CaP ceramics provide a more rapid fixation and stronger bonding with the host bone as well as increased uniform bone in-growth and/or on-growth. On the other hand, they revealed apparent limitations in the load bearing bone repair and fixation, because of their brittle and easily fatigue nature. Therefore, our research was focused on a coating technology to develop CaP coatings on mechanically strong metallic substrates. In our studies, we used mainly titanium as substrate material because of its tissue biocompatible and mechanical properties.

Calcium phosphate ceramics are materials that contain Ca and P. However, they can vary in chemical composition, structure, crystallinity and morphological state. Further, they can alter into each other under specific physico-chemical or biological conditions. Also, the manufacturing methods can affect the final properties of the prepared CaP compound. Usually, most CaP materials are considered to be biocompatible and to support bone formation, except monocalcium phosphate (MCP,  $\text{Ca}(\text{H}_2\text{PO}_4)_2$ ), which is too acidic to support the cell growth. HA is considered to be the end product of bone formation and thereby the main ingredient of mature bone. However, other CaP ceramics, like CHA (carbonated hydroxyapatite), DCPD (dicalcium pyrophosphate) and OCP (octa calcium phosphate) are also involved in the biological process of bone formation. During the development of HA, degradation and transformation of the various CaP phases occurs. To learn more about this process, we focused for our studies on the behavior of DCPD and HA. As post heat treatments have a strong influence on the properties of a CaP ceramic, like the crystallinity, phase composition and morphology, and even controls their final response in the biological environment of these materials, we used different post heat treatments in order to obtain RF magnetron sputtered CaP coatings with different characteristics.

So, in the **chapter 1** we give a general review of the background about bone, calcium phosphate ceramics, coatings, heat treatment, surface characteristic and biocompatibility.

In **chapter 2**, calcium pyrophosphate and hydroxylapatite coatings were successfully prepared by RF magnetron sputtering deposition. The results showed that all the sputtered coatings were amorphous and changed into a crystal structure after IR-radiation. The temperature for the crystallisation of the amorphous coatings is lower for the hydroxylapatite coating (550°C), as compared to the calcium pyrophosphate coating (650°C). All sputtered amorphous coatings were instable in SBF and dissolved partially within 4 of incubation. The heat-treated coatings appeared to be stable after incubation. These results showed that magnetron sputtering of calcium pyrophosphate coating is a promising method for forming a biocompatible ceramic coating.

To improve the properties and to control the composition of the CaP coatings and thereby to get the most favourable biocompatible and variable response, Ca-P coatings with different Ca/P ratio and composition were successfully prepared by RF magnetron sputtering deposition.

In **chapter 3** the production of mixtures of hydroxylapatite and calcium pyrophosphate coatings on titanium substrates were investigated. All the as-sputtered coatings were amorphous and after IR-irradiation the coatings altered into a crystalline phase. The crystallization temperature of amorphous pyrophosphate coating is higher as compared to amorphous hydroxylapatite coating. The obtained coatings had a Ca/P ratio that varied from 0.55 to 2.10 and different phase compositions or mixtures of apatite, beta-pyrophosphate and beta-tricalciumphosphate structures were formed. Evidently, the phase compositions of the sputtered coatings are determined not only by the discharge power ratio of the hydroxylapatite and dicalcium pyrophosphate targets but also by the annealing temperature. Post heat treatment at 750°C resulted in an increase of thickness of the TiO<sub>2</sub> layer.

In **chapter 4**, the different post heat treatment methods were compared. These surfaces were left as-prepared (amorphous HA coating; A-HA, amorphous dicalcium pyrophosphate coating; A-DCPP) or heat-treated with: infrared at 550°C (I-HA) or at 650°C (I-DCPP), and water steam at 140°C (S-HA and S-DCPP). The results showed that all the sputtered coatings were amorphous and both infrared and water steam heat treatment changed the amorphous phase into the crystalline phase. All the sputtered amorphous coatings were instable in SBF and dissolved almost completely within 4 weeks of incubation. In contrast, the heat-treated coatings appeared to be present after incubation, resulting in the formation of a carbonated apatite precipitate on both I-HA and S-HA coating surface, while on the I-DCPP and S-DCPP coatings a TCP phase was formed.

The Ca/P ratio of the A-HA, I-HA, S-HA, A-DCPP, I-DCPP and S-DCPP coatings changed respectively from 1.98-1.12, 2.01-1.76, 1.91-1.68, 0.76-1.23, 0.76-1.26 and 1.62-1.55 after 4 weeks of incubation in SBF.

No matter how preferable the materials are in the physico-chemical properties and in the SBF, the final evaluation of the materials has to be occur in the biological environment.

Consequently, the aim of the study in **chapter 5** was to evaluate the osteogenic properties of magnetron sputtered dicalcium pyrophosphate (DCPP) and hydroxylapatite (HA) coatings. Therefore, DCPP and HA coatings were deposited on grit-blasted titanium discs. Results demonstrated that the cells did not proliferate and differentiate on all amorphous coatings. SEM revealed that the amorphous coatings showed significant dissolution. On the crystalline DCPP and HA coatings an increase in DNA and alkaline phosphatase activity was seen

starting at day 8 of incubation Osteocalcin expression on the crystalline coatings started to increase at day 16 of incubation SEM showed that the growth and differentiation of the cells was associated with extensive collagen fiber formation and surface mineralization in the form of globular accretions Further, statistical analysis of the obtained data revealed that proliferation and differentiation of the rat bone marrow stromal cells started significantly earlier on the crystalline HA coatings than on the crystalline DCPD coatings These results demonstrate that the rat bone marrow stromal cells proliferated and differentiated only on crystalline magnetron sputtered DCPD as well as HA coatings, which warrants the further *in vivo* analysis of the bone healing supporting properties of these coatings

In **chapter 6** the *in vivo* behavior of infrared heated RF magnetron sputtered hydroxylapatite (HA) and calcium pyrophosphate (DCPD) coated titanium discs was investigated The coated discs were implanted subcutaneously in the back of six goats for 2, 4, 8 and 12 weeks The result showed that the heat-treated HA coatings showed a stable behavior, i.e. no changes in the XRD pattern were observed during implantation Also, no dissolution of the coating was observed by SEM EDS revealed that the Ca/P ratio of the HA coatings remained stable during the 12 weeks of implantation On the other hand, the heat-treated DCPD coatings showed a compositional change into apatite and tricalcium phosphate (TCP) during implantation This was confirmed by the SEM and EDS analysis The Ca/P ratio of the DCPD coatings changed from 0.8 to 1.52 after 12 weeks of incubation Finally, light microscopical analysis showed that both the heat-treated HA and DCPD coatings showed no adverse tissue response All discs became surrounded during time by a thin, dense fibrous tissue capsule with the very sparse presence of inflammatory cells On basis of these observations, it can be concluded that 2  $\mu$ m thick infrared heat-treated, RF magnetron sputtered HA and DCPD coatings are of sufficient thickness to withstand dissolution during 12 weeks of implantation in a subcutaneous location in goats In addition, both coatings showed a biocompatible tissue behavior characterized by the formation of a thin fibrous tissue capsule and the absence of an inflammatory response Further, infrared heat-treated DCPD coatings revealed a gradual compositional change into apatite and TCP

To enlarge the application of RF magnetron sputtering method and steam heating heat treatment, we applied this system to the polymer surface In **chapter 7** HA ceramics were developed as coatings on the surfaces of both the PA-6 and nano-HA/PA-6 composite by RF magnetron sputtering The results showed that a thin homogenous amorphous dense HA coating formed on the surface of both the PA-6 and nano-HA/PA-6 composite after sputtering, and turned into fine crystal when heated at 140°C 0.4MPa in water steam The Ca, P contents on the surface of both the polyamide-6 and nano-HA/polyamide-6 composite strongly increased after sputtering, to 42.55wt%, 17.66wt% and 37.70wt%(25.78), 20.93wt%(11.27),

respectively. The Ca/P ratio was 1.86 after RF sputtering, different from that of in the NHA/PA-6 composites, 1.77. The crystal structure of the sputtered coatings on both PA-6 and NHA/PA-6 composite had a typical HA structure. The micrographs showed the HA coating consisted of small particles on nano-grade with the diameter about 40 nm. The binding energy of Ca, P and O in the coating on the composites surface was similar to the original HA in the composites. In conclusion, the structure of the inorganic-organic and inorganic-organic/inorganic composites was comparable with natural bone, which can make them more bioactive and bone biocompatible. Also the RF magnetron sputtering deposition and water steam heat treatment method can be applied for the modification of other polymer and polymer composite surfaces.

### Final remarks

On basis of the obtained results we could conclude that magnetron sputtering is an excellent method for forming DCPD coatings onto metallic and polymeric substrates. Using rf magnetron sputtering it is possible to deposit thin, dense, homogenous and well adhering CaP coatings. All the as-sputtered coatings are amorphous and dissolve in simulated body fluid (SBF). Heat treatment below 650° C did not result in crystallization of amorphous DCPD coatings. Under these conditions only the amorphous HA coating transformed into a crystalline apatite structure. However, after heat treatment at temperature of 650° C, the amorphous DCPD coating changed into a crystalline  $\beta$ -Ca<sub>2</sub>P<sub>2</sub>O<sub>7</sub> structure. All heat-treated sputter coatings were observed to be stable and no dissolution or precipitate deposition was seen after incubation in SBF. On the other hand, a disadvantage of IR-radiation is an increase in the thickness of the TiO<sub>2</sub> layer. Nevertheless, this increase is not considered to be unfavorable for the long-term bone response (chapter 2 and 3). During the production of mixtures of hydroxylapatite and calcium pyrophosphate coatings, we found that the Ca/P ratio of the coatings varied from 0.55 to 2.0. Further, different phase compositions or mixtures of apatite, beta-pyrophosphate and beta-tricalciumphosphate structures were formed. The phase compositions of the sputtered coatings are determined not only by the discharge power ratio of the hydroxylapatite and dicalcium pyrophosphate target, but also by the annealing temperature.

In this thesis, different crystallization procedures were used to crystallize the amorphous coatings. The most used heat treatment is heating in a furnace at high temperature (e.g., above 600°C) in air. This heat treatment can reduce the adhesive strength of a sputtered CaP coating to the underlying substrate surface and can even result in the buckling of the coating at the surface. Also it is known, that with increasing temperature of the heat treatment, the purity of the HA phase in the coating decreases. We decided to heat the coatings either with infrared at high temperature (500-700°C) for a very short time (30 seconds) or water steam at a lower temperature for a long time (140°C). Infrared heat treatment induced no changes in the

coating morphology, while steam heating resulted in the deposition of a CaP precipitate on the coated surface. Further, after incubation in SBF these heat-treated coatings appeared to be present, resulting in the formation of a carbonated apatite precipitate on both infrared and steam heated HA coating surface, while on the DCPD coatings a TCP phase was formed (chapter 4)

The growth and differentiation of bone-like cells on magnetron sputtered DCPD and HA coatings were compared. On the infrared heated HA coatings, the cells proliferated well and formed a multilayer of cells with extensive collagen fiber formation and surface mineralization in the form of globular accretions, while on the steam treated HA surfaces, the cell proliferation was combined with the deposition of very fine mineralization particles. The same was observed for the steam heated DCPD coatings, although the number of cells appeared to be somewhat less. On the infrared heated DCPD surface a multilayer of cells was observed, but the deposition of calcified globuli was very limited (chapter 4 and 5)

In addition, an *in vivo* experiment of DCPD coatings showed a biocompatible tissue behavior characterized by the formation of a thin fibrous tissue capsule and the absence of an inflammatory response. Further, infrared heat-treated DCPD coatings revealed a gradual compositional change into apatite and TCP. Of course, the conclusive beneficial effect of DCPD coatings has to be proven in a bone implantation study.

### **Future research**

The results of this study lead to the following recommendation for future research.

First, our knowledge about how bone formation on calcium phosphate ceramics occurs, is still at best rudimentary. This lack of knowledge hampers the safe application and further development of biomaterials eliciting predictable and controlled bone responses as required by their application. Therefore, the mechanism of the underlying process and the exact benefit of DCPD coatings have to be proven. Further, care has to be taken of the fact that the precise structure of synthetic CaP compounds can differ considerably of the natural material. Starting material and processing route are very important parameters for the finally prepared product. How this interferes with the aimed tissue response is yet unclear. Therefore, in depth physicochemical analysis has to be focused at the coating/biological tissue interface. In this way, information will be provided about the mechanism involved in the dissolution of calcium ions from the coating and the relation of this  $\text{Ca}^{2+}$  dissolution to apatite and tricalcium phosphate deposition and extracellular matrix maturation. For example, studies can be performed to examine the influence of coating parameters on the behavior of extracellular proteins and the subsequent bone formation process.

Secondly, heat treatment in steam is introduced as a suitable method to improve the crystallinity of the as-deposited coatings. This application increases the heating time and can have a great influence on the morphology and interfacial properties of the coating surface.



However, more insight of steam heating has to be obtained on the final changes of the calcium phosphate coatings during this treatment. These experiments have not only to involve the structural changes of the coating. Also, final adhesion strength of the coating to underlying substrate needs more attention, because this can seriously hamper the clinical application of CaP coated medical and dental implants.



## **Chapter 9**

### **Samenvatting**

Wanneer we de chemische samenstelling, structuur en de biologische eigenschappen van calciumfosfaat keramiek in ogenschouw nemen, blijken deze materialen uitstekend toepasbaar voor de vervaardiging van orthopedische en tandheelkundige implantaten, gebruikt bij het herstel van botdefecten en ter vervanging van verloren tanden. Calciumfosfaat (CaP) keramiek veroorzaakt een snelle fixatie en sterkere binding tussen implantaat en het bot en verhoogt een gelijkmatige bot ingroei. Helaas zijn de mechanische eigenschappen van calciumfosfaat keramiek slecht. Het keramiek is vrij bros en breukgevoelig, dit beperkt de toepasbaarheid van dit materiaal in belaste situaties. Daarom richt ons onderzoek zich op de ontwikkeling van CaP coatings aangebracht op sterke metalen substraten. In onze studies gebruiken wij titaan substraten vanwege de goede biocompatibele en mechanische eigenschappen van dit materiaal. Calciumfosfaat keramieken zijn Ca en P bevattende materialen, die kunnen verschillen in chemische samenstelling, structuur, kristalliniteit en morfologie. Verder is het mogelijk om onder bepaalde fysisch-chemische en biologische omstandigheden een overgang te krijgen van de ene in een ander calciumfosfaat fase. Ook beïnvloedt de productie methode de eigenschappen van het materiaal. Over het algemeen zijn CaP materialen biocompatibel en betrokken bij de botvorming, een uitzondering hierop is monocalciumfosfaat (MCP;  $\text{Ca}(\text{H}_2\text{PO}_4)_2$ ), dit materiaal is te zuur om celgroei te bevorderen.

Hydroxyapatiet (HA) is het hoofdbestanddeel van bot. Andere CaP keramieken, zoals CHA (carbonaat hydroxyapatiet), DCPD (dicalcium pyrofosfaat) and OCP (octa calcium fosfaat) spelen echter ook een rol in het biologische proces met betrekking tot de bot vorming. Tijdens de vorming van HA, vinden degradatie en transformatie van verschillende CaP fases plaats. Om dit proces beter te begrijpen, onderzochten wij de rol van DCPD en HA. Uit de literatuur blijkt dat een hittebehandeling achteraf de fysisch-chemische eigenschappen van CaP keramiek sterk kunnen beïnvloeden. Verder heeft deze nabehandeling ook effect op de uiteindelijke reactie van dit materiaal in een biologische omgeving. In onze studies maken wij gebruik van verschillende hittebehandelingen achteraf om de RF magnetron gesputterde CaP coatings met verschillende eigenschappen te verkrijgen.

In **hoofdstuk 1** geven we een algemeen overzicht met betrekking tot de achtergrond van bot, calciumfosfaat keramiek, coatings, hitte behandelingen, morfologie en biocompatibiliteit.

In **hoofdstuk 2** werd gebruik gemaakt van RF magnetron sputter techniek om calcium pyrofosfaat en hydroxylapatiet coatings aan te brengen op metalen substraten. X-ray diffractie (XRD) liet zien dat infrarood (IR) hittebehandeling de amorfe structuur van geputterde coatings veranderde in een kristallijne structuur. De temperatuur van de kristallisatie van amorfe coatings is lager voor hydroxylapatiet coatings ( $550^\circ\text{C}$ ), in vergelijking met de calcium pyrofaat coatings ( $650^\circ\text{C}$ ). Scanning elektronen microscopie

(SEM) en energie dispersieve spectrometrie (EDS) toonden aan dat de gesputterde coatings een uniforme structuur hadden met een Ca/P verhouding van 0.55-2.0. Het oplosgedrag van deze calciumfosfaat coatings werd bepaald in een zoutoplossing gelijkend op weefselvocht (simulated body fluid (SBF)). Alle amorfe coatings waren instabiel en losten gedeeltelijk op na 4 weken incubatie. Daarentegen bleek dat alle hittebehandelde coatings stabiel waren onder deze testcondities. Op basis van deze bevindingen, werd geconcludeerd dat RF magnetron sputteren van calcium pyrofosfaat coating een veelbelovende techniek is om biocompatibele coatings te vervaardigen.

In **hoofdstuk 3** werden mengsels van hydroxylapatiet en calcium pyrofosfaat coatings op titanium substraten onderzocht. De CaP coatings werden geproduceerd met verschillende sputtercondities en hierbij werd het sputtervermogen gevarieerd. Alle gesputterde coatings waren amorf. Na een IR hitte behandeling veranderde de amorfe structuur in een kristallijne structuur. De kristallisatie temperatuur van amorfe pyrofosfaat coatings was hoger in vergelijking met amorfe HA coatings. De verkregen coatings hadden een Ca/P ratio van 0.55-2.10 en lieten verschillende fases zien, bestaande uit mengsels van apatiet, beta-pyrofosfaat en beta-tricalciumfosfaat. Hieruit bleek dat de fase samenstelling niet alleen bepaald werd door het sputtervermogen, maar ook door de hitte-behandeling.

In **hoofdstuk 4** werden verschillende hitte nabehandelingen van DCPD en HA coatings met elkaar vergeleken. De onderzochte coatings waren zoals gesputterd (amorphe HA coating, A-HA, amorfe dicalcium pyrofosfaat coating, A-DCPD), IR hitte-behandeld bij 550°C (I-HA) of bij 650°C (I-DCPD), en stoom behandeld bij 140°C (S-HA and S-DCPD). De resultaten lieten zien dat alle gesputterde coatings een amorfe structuur hadden en alle hitte-behandelde coatings een kristallijne structuur. Uit het oplosgedrag in SBF bleek dat de onverhitte coatings instabiel waren en bijna volledig oplosten na 4 weken incubatie. Daarentegen bleven alle hitte-behandelde coatings in stand. Infrarood onderzoek (FTIR) toonde de vorming van een carbonaatapatiet fase op de I-HA and S-HA coating oppervlak, terwijl op de I-DCPD en S-DCPD coatings een TCP fase was gevormd.

De Ca/P ratio van de A-HA, I-HA, S-HA, A-DCPD, I-DCPD and S-DCPD coatings veranderde respectievelijk van 1.98-1.12, 2.01-1.76, 1.91-1.68, 0.76-1.23, 0.76-1.26 en 1.62-1.55 na 4 weken incuberen in SBF.

De biocompatibiliteit van de coatings werd met behulp van celweek experimenten bepaald. Hieruit bleek dat de gesputterde coatings biocompatibel zijn. Op basis van deze bevindingen werd geconcludeerd dat verschillende hitte-behandelingen de morfologie van gesputterde HA en DCPD coatings veranderde, waarbij een combinatie van kristalliniteit en specifieke fase samenstelling (Ca/P ratio) een groot effect had op de *in vitro* bioactiviteit van gesputterde CaP coatings.

Het doel van het onderzoek in **hoofdstuk 5** was om de osteogene eigenschappen van RF magnetron gesputterde dicalcium pyrofosfaat (DCPP) en hydroxyapatiet (HA) coatings te evalueren. Daarvoor werd het effect van DCPP en HA coatings bestudeerd, met betrekking tot de groei en differentiatie van osteoblast-achtige cellen. Uit de resultaten bleek dat de osteoblast-achtige cellen niet groeien en differentieren op de amorfe coatings. SEM liet zien dat de amorfe coatings duidelijk oplosten. De kristallijne DCPP en HA coatings lieten een toename zien van de DNA en alkalische fosfatase activiteit van af dag 8. De osteocalcine expressie nam toe vanaf dag 16. SEM liet zien dat de groei en differentiatie van de cellen samenging met extensieve vorming van collageen fibers en mineralisatie. Verder, lieten statische analyses zien dat de groei en differentiatie van de osteoblast-achtige cellen significant eerder begon op de kristallijne HA coatings dan op de kristallijne DCPP coatings. Hieruit werd geconcludeerd dat osteoblast-achtige cellen groeien en differentieren op kristallijn magnetron gesputterde DCPP en HA coatings en dit resultaat rechtvaardigt verdere *in vivo* onderzoek naar de bot eigenschappen van deze coatings tijdens botgenezing.

In **hoofdstuk 6** wordt een *in vivo* experiment beschreven, waarin schijfjes met RF magnetron gesputterde hydroxyapatiet (HA) and calcium pyrofosfaat (DCPP) coatings onderhuids in de rug van geiten werden geïmplant. De laagdikte bedroeg 20  $\mu\text{m}$ . Alle gesputterde coatings werden IR hitte-behandeld, HA (550°C) en DCPP (650°C). De gecoate schijfjes werden ingebracht gedurende 2, 4, 8 and 12 weken. SEM liet zien dat de gesputterde HA coatings na 12 weken implantatie nog grotendeels aanwezig waren. Verder werd met behulp van XRD aangetoond dat de coatings niet waren opgelost. EDS metingen toonde aan dat de Ca/P ratio van de HA coatings niet veranderde na 12 weken implantatie. Daarentegen transformeerde hitte-behandelde DCPP coatings in een apatiet- en een tricalciumfosfaat fase gedurende 12 weken implantatie. Verder veranderde de Ca/P ratio van 0.8 naar 1.52. Uit de histologische waarnemingen bleek dat alle implantaten omgeven waren met een dun, dicht fibreus kapsel met af en toe de aanwezigheid van enkele ontstekings cellen. Uit deze bevindingen kan geconcludeerd worden dat *in vivo* een 20  $\mu\text{m}$  dikke gesputterde IR hitte-behandelde HA en DCPP coating voldoende laagdikte heeft met betrekking tot oplos- en bioactieve eigenschappen.

In **hoofdstuk 7** werden dunne gesputterde HA coatings op polyamide-6 (PA-6) en een nano HA/Polyamide-6 (NHA/PA-6) composiet aangebracht. SEM onderzoek toonde aan dat de gesputterde coatings de polymeren homogeen bedekte. Verder toonde XRD aan dat de gecoate laag een amorfe structuur had. Met een stoom behandeling veranderde de amorfe structuur in een kristallijne HA structuur. EDS liet zien dat de verkregen coating een Ca/P ratio had van 1.64.

Hieruit werd geconcludeerd dat RF magnetron sputtering een geschikte methode is om dunne

coatings op polymeren aan te brengen en een stoom hitte-behandeling een geschikte techniek is om amorf HA te kristalliseren.

In **hoofdstuk 8** zijn de belangrijkste conclusies van dit proefschrift samengevat en werden suggesties gegeven voor verder onderzoek.

## Acknowledgements

The work forming this thesis was performed at Department of Periodontology and Biomaterials of the Radboud University Medical Center Nijmegen and supported by a grant of the China exchange program of the Royal Academy of Art and Sciences under the supervision of the WHO Collaborating Center of the College of Dental Sciences of the Radboud University Medical Center Nijmegen. I gratefully acknowledge the generosity of these institutions to give me a chance to do research and to use their facilities without any limitation. Although it is impossible to mention everyone who helped and supported me during stay in Nijmegen, each individual will hold a special place in my memory.

In particular, I am grateful to Professor John Jansen and Dr. Joop Wolke, for their careful scientific training, extensive supervision, and edificatory enlightenment during all my studies in the Netherlands. They did not only give me the scientific training, but also enlarged and widened my scope in other fields. This will be beneficial for my future career.

Sincerely, I would also like to express my thanks to all members of the biomaterials group who contributed to this thesis, for their continuous support, stimulating scientific discussions, trust and encouragement. I give special thanks to Anja de Ruijter for her help in the cell culture studies. I also give thanks to Olga Reijnders, who arranged my study and daily life in the Netherlands.

I also give my thanks to my classmates and friends of in the department, their friendly help ensured my smooth finish of the research. Frank, Marijke, Anne, Natasja, Juliette, Jacky, Nelleke, Sander, Wouter, Walter, Jeroen, Manal, Weibo, Esther, Dennis, Li, Peter thank you very much.

My sincere acknowledgements are also for Professor Li Yubao, my advisor in China, who encouraged me to go to The Netherlands and who helped me in my work and life.

Finally I give my acknowledgement to my family. I am grateful to my father, Yan Chengmao, and my Mother, Xu Caiqin, for their love during my youth and for all their support. I am especially grateful to my elder brother Yan Bo, for his self-offering love to me and constant support during my study and work. Unfortunately, he passed away too early, but I miss and remember him forever. I also give my thanks to my younger brother Yan Kailun, for his careful care of my parents and for his constant support.



## Curriculum vitae

Yonggang Yan, born December 22, 1967, Shaanxi, China

### Education:

Primary school, high school and teach college in Shaanxi, China

Sept 1990-Jul 1993 Sichuan University, Chengdu, China

July 1993 Master degree in polymer science, China

Sept 2000-Feb 2002 Sichuan University, Chengdu, China

Feb 2002-Oct 2002 University medical center, Department of biomaterials , Raboud  
University Nijmegen Medical Center, the Netherlands PhD Student

Nov 2002-Jul 2003 Sichuan University, Chengdu, China

Jul 2003 PhD degree in Materials Engineering biomedical composites, China

Dec 2003-May 2005 University medical center, Department of biomaterials , Raboud  
University Nijmegen Medical Center, the Netherlands PhD Student

June 2005-Nov 2005 Sichuan University, Chengdu, China

Dec 2005-date University medical center, Department of biomaterials, Raboud University  
Nijmegen Medical Center, the Netherlands PhD Student

### Professional Experience:

1987-1990 Middle school Teacher in chemistry Shaanxi China

1993-2001 Analytical and testing center, Sichuan University, Chengdu, China, assistant  
professor, associate professor polymer materials and composite

2002-date study in UMCN, Raboud University Nijmegen Medical Center Research in  
Biomaterials



